SHRP R06D Round 7 IAP
Evaluation of 3D Radar

Final Report

Agreement No. BE291

Prepared by

Infrasense, Inc.

October 30, 2018

Table of Contents

List of Figures

List of Tables

Summary

The overall objective of the SHRP2 R06D IAP program has been to thoroughly assess the utility of 3D-Radar system as applicable to FDOT transportation network elements, with the ultimate goal to determine if this type of equipment would be beneficial to the needs of FDOT. This objective has been achieved by conducting tests on roadway sections representing various pavement conditions of interest, and by analyzing the data to determine whether and how effectively these conditions could be revealed. The testing objectives included identification and quantification of: damage within the asphalt pavement due to moisture infiltration and other effects; deterioration and depth of cover in bridge decks; pavement substructure types and thickness of the various layers; dowel bars in concrete pavement and the depth and alignment of the dowel bars; voids over culverts, piles, and sink holes; and voids under concrete pavement.

The testing was carried out in two stages. The first stage included 10 sites and focused on obtaining an initial understanding of the equipment and its operation, the data collection process, the type of data produced, and the data analysis procedures. Data analysis for stage 1 data was primarily visual and qualitative. The second stage used the knowledge of the stage 1 experience at 8 additional sites to refine the data collection equipment and process, and to delve more deeply into the analysis of data from the various applications. The analysis of stage 2 data incorporated a greater emphasis on quantitative evaluation with condition maps and estimated quantities. In both stages there has been some comparison of 3D Radar results with those obtained by FDOT using its current GPR system.

The results documented in this report describe the capabilities and limitations of the 3D Radar system as applied to the evaluation of the 18 sites. Section 2 describes the equipment setup and implementation, and how it evolved from stage 1 to stage 2. Section 3 describes each test site, along with the detection objective based on available data provided by FDOT. Section 4 describes how the 3D Radar data was collected and analyzed at each site. Samples of data are presented for each site, along with the methods and results of data analysis.

1. Project Background and Objectives

As a part of Agreement BE291, Infrasense carried out a preliminary review of the capabilities and deployments of the latest 3D-Radar system. Available antenna types were reviewed, including ground-coupled and air-coupled systems. The review considered different available antenna types, vehicle requirements for deployment, special mounting requirements, lane coverage achieved with each pass of the equipment, methods for combining data from multiple passes, available data collection rates vs. vehicle speed, data transfer, and currently available post-processing capabilities. The antenna model 1821DX was selected to be used under this program. The "18" indicates that the antenna is 1.8 meters wide, and the "21" indicates that there are 21 transmit-receive pairs spaced laterally along the 1.8-meter length at 7.5 cm apart. Infrasense examined capabilities of the 3D-Radar system for a broad range of applications.

Considering the FDOT requirements, a set of test sites was identified for employed system evaluation and its capabilities for detecting delamination and stripping, including data collection protocol, post-processing, data analysis, and data interpretation workflow. In addition to delamination and stripping, the performance of 3D-Radar system was evaluated for the following applications:

a. Detection of voids under concrete pavement
b. Evaluation of dowel bar alignment
c. Evaluation of density variations in new asphalt pavement
d. Quality assurance of new bridge deck construction
e. Identification and quantification of delaminations in older bridge decks
f. Detection of voids over culverts, piles, and sink holes

Prior to the data collection, a detailed test plan was developed for each of the test sites. Test plans considered length and relative location of each site, coverage limits, particular lane(s) to be tested, required types of conditions to be identified, and type of ground truth to be utilized. Established data collection protocol was accounted for scan rates, antenna positioning, file documentation, and QA of the collected data. A testing schedule was established, and arrangements for rental of the 3D-Radar equipment were made ahead of the execution of Task 4 (Implement Test Plan); plans were examined by FDOT to ensure that all the elements of the test plan will be carried out in coordination with the local districts with regard to site access and availability of support and ground truth information. Testing was carried out in two stages. Stage one focused on easily accessible sites that had well-documented built-in conditions, where delamination and stripping have either been created or were known to exist. Those areas served as an initial screening on the equipment operation and data generation. A particular emphasis in stage 1 was on the FDOT Heavy Vehicle Simulator (HVS) sites, which are available at FDOT's State Materials Office (SMO) Research facility in Gainesville. Stage 2 focused more on covering the full matrix of conditions highlighted in the test plan, with more of an emphasis on operational issues under realistic highway testing conditions. Documentation of the field data collection program, including a description of the equipment used, the data that was obtained, the methods and procedures utilized for data analysis, and the correlation with ground truth were provided.

In order to meet the data processing and interpretation requirements, algorithms were identified and tested; their performance and accuracy were verified and documented. A specification for software required to extract the relevant information from the processed data was established, taking into consideration the outcomes of previous work, R06D research project, and specifications for any further processing, analysis, and interpretation. Significant software enhancements were proposed to account for the evaluation of asphalt delamination.

"Examiner" software, provided by 3D Radar, enables users to easily process, analyze and inspect data from 3D-Radar ground penetrating radar systems. It converts the frequency domain data into the time domain data; provides b-scan, c-scan, and cross line views of the time domain data; automatically aligns the pavement surface in the time domain data to occur at a fixed time; applies background removal to eliminate unwanted fixed reflections from the antenna, the vehicle or mounting arrangement; allows the user to "stitch" together multiple parallel files into a single file representative of the region being surveyed; and allows the user to track interfaces such as the boundaries between pavement layers. The tracing can be carried out on individual as well as stitched layers.

In order to implement quantitative analysis beyond the Examiner visualization, Infrasense has developed post-processing software called “ExploreGPR”. ExploreGPR uses the data generated by Examiner to make calculations of layer properties, layer thickness, amplitude of layer interface reflections, and reflection activity between multiple layers. The results generated by ExploreGPR are tabular and can be readily input into plotting programs to show contour plots of thickness and deterioration conditions within a bridge deck or pavement. At present, the software provides extraction of the amplitudes of interfaces traced using Examiner; another available function is "activity analysis" that can be performed for any selected depth interval between two boundary levels within the GPR data. The outcomes of the activity analysis were correlated with available ground truth, and a good relationship between areas of high activity and the presence of delamination and stripping was observed.

Final results were presented in tabular format showing stations and ranges where particular conditions have been detected; contour maps showing delineated regions of potential damage, spatial distribution of thickness values, and reflection activity index distribution; color-coded reflection activity plots; GPR cross-sections showing the identified defects and/or features of tested structure composition; charts and plots showing the 3D-Radar measured asphalt thickness; plots, demonstrating the distribution of measured.

2. Equipment Setup and Calibration

The equipment used for the Stage 1 data collection was a combination of 3D-Radar GPR system, including the step frequency GeoScope system with DX1821 antenna and survey vehicle, borrowed from MnDOT as it shown in Figure 1. Due to concern about the influence of the vehicle reflection on the GPR data, there was an attempt to extend the antenna brackets for an additional foot beyond the original position midway through the testing. This action resulted in a small reduction in the vehicle effect, but not significant enough to improve the processing of the data. The equipment used for Stage 2 the data collection was the same 3D-Radar system mounted to the FDOT GPR survey vehicle, as it shown in Figure 2. In this case, due to concern about the influence of the vehicle reflection on the GPR data, the antenna was positioned on a mounting system, designed similarly to one used by TxDOT/TTI for their 3D-Radar testing to extend the antenna as far as possible from the vehicle in an effort to minimize problem.

Figure 1: 3D-Radar test vehicle employed for Stage 1 data collection.

Figure 2: 3D-Radar test vehicle employed for Stage 2 data collection.

GPS data was collected using a Trimble AgGPS 262 (Stage 1) and SPS985 (Stage 2) receivers in conjunction with OmniStar HP positioning service provided by Infrasense. Trimble specifications indicate that this system provides <10 cm positioning accuracy. Testing showed that this combination produced a high degree of accuracy and excellent alignment of parallel lines of data when the receiver was receiving good quality GPS data. However, there were conditions encountered that degraded the GPS signal, under which GPS alignment between parallel lines of data were poor.

Setup, checkout, and calibration procedures were performed prior to the data collection. The survey crew checked the system functionality by doing multiple lines of data, checking the DMI functionality, testing the GPS antenna performance, performing the whole workflow of data collection routine, and examining the appearance of collected data to ensure that 3D-Radar system works properly. 3D-Radar Examiner software was used in-field to process test data on site for data quality verification. Typical calibration for air-launch antenna system was also performed on SMO testing site, including an air-test (direct coupling) and a static metal plate test. It should be noted that at the time of this writing, there is no software available to automatically incorporate this calibration data into the data analysis. Despite the presently existing software limitation, calibration, as a process of data adjustment, was manually performed for certain applications to calculate dielectrics values as required.

Prior to data collection, a series of short tests were conducted to ensure that system was functioning properly and getting reliable GPS readings. The proper system operation and consistency of the generated results were confirmed with this testing.

The following data processing settings were used with 3D-Radar's Examiner software to convert 3D GPR data from frequency to time domain for further interpretation:

1) Interference suppression (10 dB);
2) Automatic Ground Alignment (typically surface at 3 ns.) to align the traces at the air-to-pavement interface;
3) Selective inverse discrete Fourier transform (DFT) on the data using default settings;
4) Automatic scaling of the data (default settings);
5) Background removal using high pass filter (starting at depth of 0.5 ns below the surface).

Throughout the data analysis, Examiner was used to visualize the data using b-scans and c-scans (or "depth slices"), and for geolocation of the data. The use of Examiner included:

1) Geospatial layout of multiple data files collected on a particular structure of length of roadway.
2) Stitching together of the individual survey lines to form a complete 3D image of the entire driving lane.
3) Checking of the radar distance measurements against the known length and MP locations;
4) Identification of features (testing trenches, repeating cracks patterns, coreholes, etc.) that appear as dielectric discontinuities in the GPR data;
5) Tracking pavement layers for further analysis.

3. Description Test Sites

The sites tested, along with the objective of the testing, are shown in Table 1. Fieldwork was carried out on February 13-16 (Stage 1), and November 13-16 (Stage 2), 2017. The following sections describe the known conditions at each of the test sites in further detail, along with the results of the 3D-Radar data analysis. Known conditions were determined from reports provided by FDOT, and these reports are referenced in the following sections. It should be noted that 3D-Radar data for Test Site 1.2 were collected, but the task was excluded from the survey list due to the insufficient information on existing pavement condition to conduct an evaluation. Site 1.5 was not available at the time of the survey due to position of HVS units and Site 1.6 was removed from the scope of work.

Table 1: Summary of test sites for Stages 1 and 2 testing.

Stage	Task	Description	County	BMP | EMP	Construction	Detection objective
1	1	I-10, EB & WB	Duval	0-8.989	Composite	Stripping and delamination
1	2	I-95, NB & SB	St. Johns	26.4-34.86	Asphalt	Delamination
1	3	I-75, NB & SB	Alachua	14.5-27.5	Asphalt	Subsidence
1	4	SMO, Lanes 3-6	Alachua		Asphalt	Density, bonding, segregation
1	7	SR 20, EB	Alachua	5.0-6.0	Asphalt	Thickness
1	8	SR 5/US 1, NB & SB	St. Johns	17.0-17.29	Concrete	Distress/voids
1	9	SR 18, EB	Putnam	3.2-3.55	Asphalt	Distress issues
1	10	SR 100, EB & WB	Putnam	7.0-8.0	Asphalt	Monitor piles
1	11	Pablo Creek Bridge	Duval	10.36-11.23	RCC bridge deck	Condition, cover
1	12	Waldo Rd, SB	Alachua	4.25-5.73	Asphalt	Subsidence at drains
2	1	SR22	Gulf	5.42-12.14	Asphalt	Stripping and Delamination
2	2	SR77	Washington	26.22-29.83	Asphalt	Stripping and Delamination
2	3	I10	Santa Rosa	24.52-29.83	Asphalt	Subsurface Investigation
2	4	S R75/US 231	Bay	0.87-11.97	Asphalt surface layer over the concrete base	Thickness, detection of concrete base
2	5	SR 5/US 1	Volusia	9.6-11.46	Concrete roadway	Dowel bar detection and alignment evaluation
2	6	SR816	Broward	2.23-2.32	Precast, prestressed deck	Deterioration Mapping
2	7	SR A1A Blue Heron bridge	Palm Beach	0.41-0.79	Reinforced Bridge Deck	Deterioration Mapping
2	8	SR A1A North bridge over ICWW	St. Lucie	0.33-0.72	Reinforced Bridge Deck	Deterioration Mapping

The following sections describe the known conditions at each of the test sites in further detail, along with the results of the 3D-Radar data analysis. Known conditions were determined from reports provided by FDOT, and these reports are referenced in the following sections.

Site 1.1: I-10 – Project # 424634-1-52-01 / Roadway ID #: 72270000; (MP 0.000 – MP 8.989), Duval County – Evaluation of stripping and delaminations

The test section of I-10 is a four-lane highway comprised of divided eastbound and westbound travel lanes located in Duval County, Florida. The tested sections consist of full-depth HMA pavement material. Figure 3 displays schematic design of tested roadway. Signs of surface distresses that were observed at various

locations over a 9 miles-long segment of I-10 have been considered as evidence of unexposed subsurface damage (Figure 4). Seven core samples were acquired at these locations to better understand the source of the damage and to reveal premature pavement deficiencies (five core samples along the right side of eastbound pavement section R2; two core samples along the right side of westbound pavement section L2). Table 2 summarizes the core length, number of pieces, and bond conditions between layers of bituminous mix (BM) material. Transverse and longitudinal cracks are observed in the outside wheel path of the outside lane as it is shown in Figure 4.

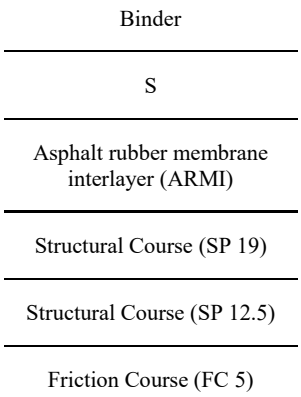

Figure 3: Diagram showing the pavement cross section. Not to scale.

Table 2: Core information summary.

Core Number	Mile Post	Lane	Wheel Path	Core Length	Base Type	Crack				Rut Depth (inches)
						Depth	Type	Class	Extent	
1	0.123	R2	OWP	7.6	LR	7.6	C	II	M	0.53
2	6.163	R2	OWP	6.6	LR	---	---	---	---	0.18
3	6.170	R2	OWP	6.7	LR	6.7	C	II	M	0.18
4	6.268	R2	OWP	6.3	LR	6.3	C	II	M	0.18
5	6.355	R2	OWP	7.1	LR	---	---	---	---	0.20
6	6.424	L2	OWP	7.2	LR	---	---	---	---	---
7	5.869	L2	OWP	7.9	LR	7.9	C	II	M	---

Core data in this area has showed a total asphalt thickness of approximately 7 in. It is believed that stripping and deteriorating most probably occur between the SP 19 mix and ARMI layers or between the SP 12.5 and the SP 19 mixes. It should be noted that core information is indicative of pavement condition at an isolated extraction point only and does not represent the quality of the whole tested areas. The goal

of carrying out the 3D GPR survey has been to see if data collected with 3D-Radar system can be used to non-destructively identify the locations and extent of stripping and delaminations.

Figure 4: Photographs of eastbound pavement section R2 in proximity of core #1 extraction point at MP 0.123 (left); eastbound pavement section R2 in proximity of core #3 extraction point at MP 6.170 (center), eastbound pavement section R2 in proximity of core #4 extraction point at MP 6.268 (right).

Site 1.2: I-95 – I-95 NB and SB, St. John's County, MP 26.4-34.86, Pavement Delamination

Data was collected at this site in the high-speed lane, but supporting documentation describing the pavement conditions of interest was not available, and no further analysis was carried out at this site.

Site 1.3: I-75 – Project # 428803/4-1-52-01 / Roadway ID #: 26260000; (MP 14.5 – MP 27.5), Alachua County – Pavement Subsidence

In 2016 FDOT carried out a study on I-75 to investigate subsurface conditions associated with pavement subsidence. The investigation focused on areas from MP 14.5 to 17.2 (Site 1) and MP 25.2 to 28.3 (Site 2). Preliminary investigations were conducted in the travel lanes using FDOT's air launched GPR. Pre-storm testing was conducted in September 2016 and post-storm testing was conducted in October 2016. Preliminary locations were identified for follow-up with a 400 MHz ground-coupled GPR. The purpose of the 3D GPR survey was to see if the findings using the FDOT GPR system could be replicated with the 3D-Radar system.

Site 1.4: State Material Office (SMO) Asphalt Test Tracks - Flexible Test Lanes 3, 4, and 5 - Interlayer bonding research, density, and segregation study

The Florida DOT State Materials Office (SMO) maintains a pavement test facility in which pavement sections of prescribed design are constructed and being tested. One of the primary forms of testing on these sections is Accelerated Pavement Testing (APT) using a Heavy Vehicle Simulator (HVS). The HVS is a specially equipped tractor-trailer vehicle that applies repeated tire loading to a small patch of pavement (20 x 2.5 feet). Sections of the SMO test pavements have recently been placed with artificially induced defects, including density variations, segregation, and debonding between the asphalt layers. These sections are shown in Figure 5 below. The pavement cross section is shown in Figure 6. The purpose of the evaluation has been to determine the ability of the 3D-Radar system to detect the conditions embedded into these pavement sections.

Lane 3 – Delamination. To illustrate an interlayer delamination of an asphalt pavement, the first 150 feet of this lane was built with no tack between the surface 1.5-inch thick lift and the lift below, but rather a thin sand layer (no bonding).

Figure 5: SMO Facility showing lanes 3, 4, and 5 with embedded defects.

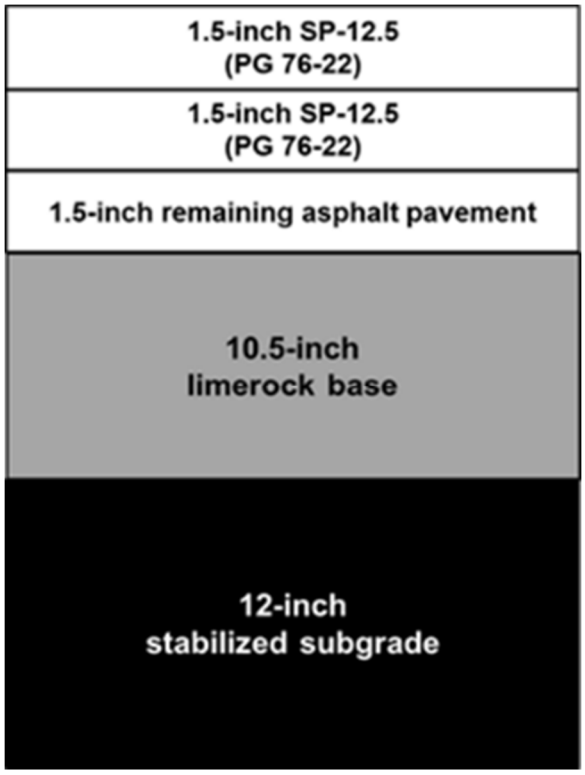

Figure 6: Pavement cross section for lanes 3, 4, and 5. Not to scale.

Lane 4 – Density. This lane was tested with the HVS at 6 various locations within the first 150 feet, and consequently density variations are expected due to the local compaction. HVS testing locations are shown in Figure 7.

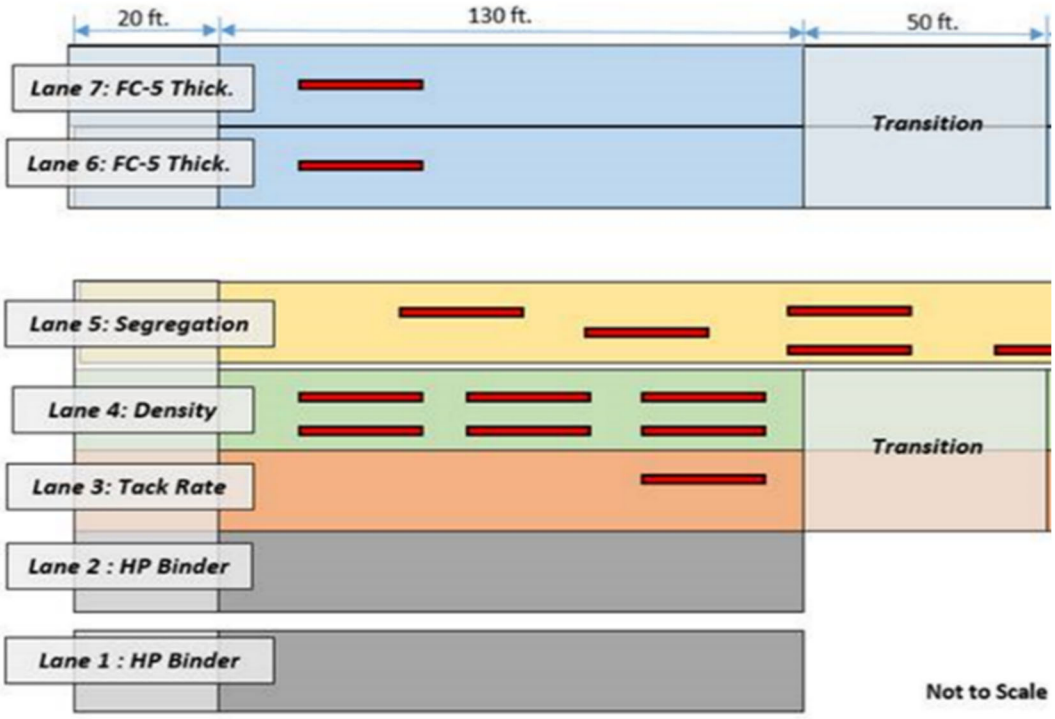

Figure 7: HVS Testing Pattern.

Lane 5 – Segregation. To generate localized areas of segregation on the test lane, end of load segregation was simulated. The paver wings were dumped to send coarser mix into the paver at end of each truck load. The tarps were removed from the truck loads upon arrival at the site to increase potential for segregation. Also, the screed heater on the paver was cycled on and off during construction. These techniques were effective in generating localized segregation. The temperature profile measured during paving using an infrared thermal imaging camera confirmed the presence of segregation, as shown in the Figure 8. Circled area shows denoted temperature zone.

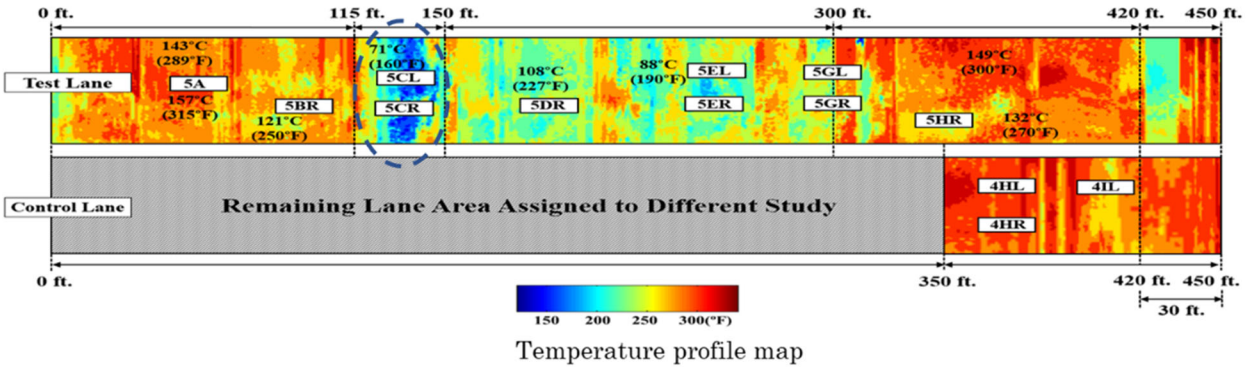

Figure 8: Contour map showing spatial distribution of surface temperature values over the Lane 5.

Site 1.7: SR 20 – Project # 430565-3-52-01 / Roadway ID #: 26080000; (MP 5.000 – MP 6.000), Alachua County – Thickness Evaluation

SR 20 consists of a four-lane divided roadway in the east and westbound direction. It is located in Alachua County. This paved roadway comprised of multiple layers of asphalt material of varying thicknesses and a 12-inch limerock base. The goal of carrying out the 3D GPR survey has been to confirm that data collected with 3D-Radar system can be used to perform pavement thickness evaluation.

Site 1.8: SR 5 (US-1) – Project # 436168-1-32-01 & 436169-1-32-01 Roadway ID #: 78010000; (MP 16.120 – MP 18.692), St. Johns County – Distress and void detection

SR 5 (US-1) consists of two northbound travel lanes, two southbound lanes, and a center turn lane. It is located between the intersection of SR 207 in the south and the St. Augustine City Gates in St. Johns County. This roadway comprised of rigid (concrete) pavement and isolated areas of asphalt pavement. It is understood that a section of this roadway between the intersections of Saragossa and Orange Streets are supported by timber piles, and that the northbound and southbound lanes in this area have undergone severe differential settlement with respect to one another. The amount of settlement observed was greater in the southbound direction as evidenced by the presence of an asphalt leveling course. Several areas along this roadway were reported to experience severe pavement distresses and potential voids. An evaluation of the area is presented in a March 2016 report [3] prepared by Environmental and Geotechnical Specialists, Inc. (EGS). The report presents cases of observed surface distress, results of GPR surveys, and borings. The GPR survey consisted of 14 survey lines, each carried out at walking speed, with combined 800 and 1600 MHz antennas. The report concluded that:

a. The predominant concrete thickness is 8-10 inches;
b. The pavement thickness (asphalt plus concrete) in the timber pile area ranges from 11-36 inches, with the increased thickness due to the use of asphalt to level the sagging concrete pavement;
c. Subsurface anomalies associated with "loose" to "very loose" subsoils were detected.

The goals of carrying out the 3D GPR survey haves been to confirm the findings of a previous extensive low-speed survey and reveal any construction information that was not previously reported.

Site 1.9: SR 18 – Project # 207973-2-52-01; Roadway ID #: 28040000; (MP 3.464 – MP 3.596), Bradford County – Evaluation of Pavement Distress

SR 18 from milepost 2.184 to 7.608 was reconstructed in September 2008. The project consisted of milling 1 1/2" of the existing asphalt and placing a 1 1/2" layer of Superpave FC-12.5 mix containing ARB-5 asphalt binder. Some areas required an overbuild layer for correction of cross slope. The contractor used a Superpave SP-12.5 mix for the overbuild. The project included a three-year Value-Added Asphalt Pavement (VAAP) warranty. At the end of the three-year warranty period, pavement distresses, which resulted in low ride ratings (Ride number below 3.5) at various locations, were observed and pavement sections were experiencing cracks and ripples. The State Materials Office (SMO) conducted an evaluation

in 2010 to investigate the causes of these distresses. The evaluation included FWD, GPR, and laboratory testing on field cores.

Although the pavement distresses were observed at several locations throughout the length of the entire project, SMO's investigation was limited to a representative section. A control section located adjacent to the distressed section was also tested for relative comparison purposes. As depicted in Figure 3, the distressed section limits are between milepost 3.434 and 3.517 and the control section limits are between milepost 3.517 and 3.596.

The FWD analysis concluded that the stiffness of the entire pavement system significantly decreases at higher temperatures in the distressed section when compared to the control section. However, the stiffness of the embankment is generally independent of temperature changes. Based on these variations, it can be concluded that either the asphalt and base layers (or either one individually) could be susceptible to environmental conditions like temperature changes.

With respect to the laboratory test results, the overbuild layer in the distressed section did have a moisture content of 1.5%, which is significantly higher than the other dense graded asphalt layers tested from this project. Additionally, the subgrade layer in the distressed section had slightly higher moisture content than the subgrade layer in the control section. None of the other laboratory tests performed indicate a problem with the asphalt mixture in either the control or distressed sections.

There is no definitive explanation as to the cause of the distresses observed on-SR 18. One possible theory being proposed by the asphalt contractor is that the problem is due to underlying moisture that is being wicked up by the sand bituminous road mix (SBRM) layer and is being trapped by the upper dense graded asphalt layers. Excessive vapor pressure due to high pavement temperatures is then causing the observed stresses. Furthermore, edge widening that occurred in during this construction project has placed a deep asphalt layer at the outside edge of the pavement preventing moisture from escaping laterally. Results of this pavement investigation have not been able to confirm or deny this proposed theory. The goal of carrying out the 3D GPR survey has been to provide evidence that moisture infiltration is the primary cause of observed damage.

Site 1.10: SR 100 – Project 213940-1-52-01; Roadway ID #: 76110000; (~MP 7.800), Putnam County – Monitoring of piles

SR 100 is a two-lanes roadway consisting of asphalt concrete. Due to a peat layer, approximately 5 feet thick and located 6 feet below the pavement surface, segment of SR 100 in Putnam County had experienced significant settlement between mileposts 7 and 8 that has resulted in the placement of more than 12 inches of asphalt. The average thickness of the surrounding asphalt is only 5 inches. In 2007, a pavement rehabilitation project was completed. Grout columns were placed along the westbound travel lane to transfer embankment support through the peat layer and minimize future settlement. Two test areas were also strengthened with a high-strength geocomposite Stress Absorbing Membrane (SAM) also known as PavePrep. According to the 2010 report [4], no soil modification was provided for the eastbound lane.

In 2011, a 3722 ft.-long test section was constructed between mileposts 7.109 and 7.815 in both eastbound and westbound lanes. Test area was straightened with Soil Stabilized Columns (SSC) and

PavePrep. Following the test section, a 1050 ft.-long control section without SSC and SAM was constructed between mileposts 7.815 and 8.099.

Several field tests were performed in test area to characterize the subsurface including the standard penetration tests (SPT) to evaluate the depth and thickness of the peat strata, quantify the relative consistency of the natural soils, and measure the water table depth, ground penetrating radar (GPR) to estimate the asphalt layer thickness, falling weight deflectometer (FWD) to indicate the stiffness of the embankment and elevation measurements to assess settlement of the roadway, and elevation measurements to assess settlement of the roadway.

GPR data were used to determine the thickness of asphalt layer which appeared to be 11.7 - 14.2 and 13.2 – 14.6 inches for the eastbound and westbound lanes respectively.

The 2010 report [4] describing results of FWD testing performed within two years interval reveals more than a 20% greater reduction in strength in the westbound lane as compared to the eastbound lane. Average increase of embankment stiffness for the section with grout columns was approximately 45%. Sites with SAM showed moderate improvement in deflection and modulus compared to the sites with no PavePrep installed (49% vs 35%). The 2013 report [5] concluded that deflection response of asphalt and base layers tend to fluctuate with temperature. The results also demonstrated lower deflections and higher embankment moduli measured over the test section with installed SSC and SAM. Also, treated test section provided higher stiffness to the overall pavement system when compared to the non-treated control section.

Elevation measurements taken from the westbound test area in the time between 3/27/08 and 9/2/10 showed minor settlement of approximately 0.001 inch developed after the installation of grout columns indicating approximate 50% reduction of settlement when compared to the control section. The control section showed approximately twice the settlement measured from the test section with maximum observed average settlement of 0.41 inch observed in the inner wheel patch [3, 4]. In spite of the fact that SSC and SAM improved the pavement stiffness, uneven settlement was observed between the grout columns and the surrounding soil. Figure 9 displays the photograph taken during the section rehabilitation fieldwork.

Figure 9: SSC installation grid layout on SR 100 (left); roadway surface after the milling (right) [5].

The FDOT document entitled “Final solution for SR 100” [6] concluded:

- >2006: up to 21 inches of asphalt over the thick layer of highly organic soil (muck/peat) containing up to 96% of organics at depth from 3 to 18 ft.;

- 2006: 2.5 ft. grid pattern of grout columns in combination with Stress Absorbing Material (SAM) placed between two layers of structural asphalt at four test sections;
- 2007: grout columns were installed and observed at 4 locations as a test sections for the monitoring purposes;
- 2010: Soil Stabilization Columns (SSC) were installed with the placement of pre-production load test columns, followed by the production columns between September 9, 2010 and January 19, 2011;
- 2011: installation of production SSC – a total of 12,376 SSC installed within 34 X 3,270 ft. roadway section on a 3 X 3.5 ft. grid pattern; pavement surface was milled 6 inches below existing grade for the placement of the SAM. After milled surface was cleaned and all pavement cracks were sealed, 1-inch leveling course was placed and compacted. SAM layer was then placed over the leveling course to cover the entire width of the road (travel lanes and paved shoulders). Asphalt overlay was then placed on top of the SAM to the final grade of the pavement.

The goal of carrying out the 3D GPR survey has been to see if any detail of the pavement structure can be revealed that would explain region strength reduction.

Site 1.11: Pablo Creek Bridge – (Bridge# 720509) – SR 202 Roadway ID #: 72292000; (~MP 10.358 – MP 11.228), Duval County – Condition, cover

The bridge # 720509 (Pablo Creek Bridge) consists of four divided lanes and inside/outside shoulders and is located on SR 202 over the Intracoastal Waterway in the east part of Butler Blvd in Jacksonville, Duval County. The bridge deck comprised of reinforced cement concrete (RCC) deck with thickness of 9 inches. Length of the bridge measures about 4,594 feet long, from approximate MP 10.358 – MP 11.228. The bridge is 42 feet wide. An evaluation of bridge deck is presented in a 2015 report prepared by Florida Department of Transportation. The report included results of ground penetrating radar measurements of the depth of concrete cover over the top layer rebar in the eastbound direction. The GPR survey consisted of 4 survey lines with 4 2.0 GHz air-launched antennas. The report [6] concluded that:

- The GPR data shows that the average cover depth to the top layer rebar is 2.49 inches and 2.32 inches in the left and right driving sides respectively, and for the merge lane is 2.93 inches. The predominant concrete cover calculated for the whole bridge is fairly uniform with indicated average depth to the top layer rebar of 2.58 inches in the travel lanes and 2.65 inches in the shoulder lanes.
- The minimum and maximum cover depth to rebar in the travel lanes is 1.01 inches and 4.78 inches, respectively. The minimum cover depth to the top layer rebar is about 1.01 and 0.47 inches for the travel and shoulder lanes respectively. The maximum cover depth to the top layer rebar is about 4.78 and 5.56 inches for the travel and shoulder lanes respectively.

Figure 10 shows the contour map of the concrete cover depths to the rebar generated from an analysis of the GPR data [6]. The goal of carrying out the 3D GPR survey has been to compare the concrete cover data with that generated by the FDOT survey

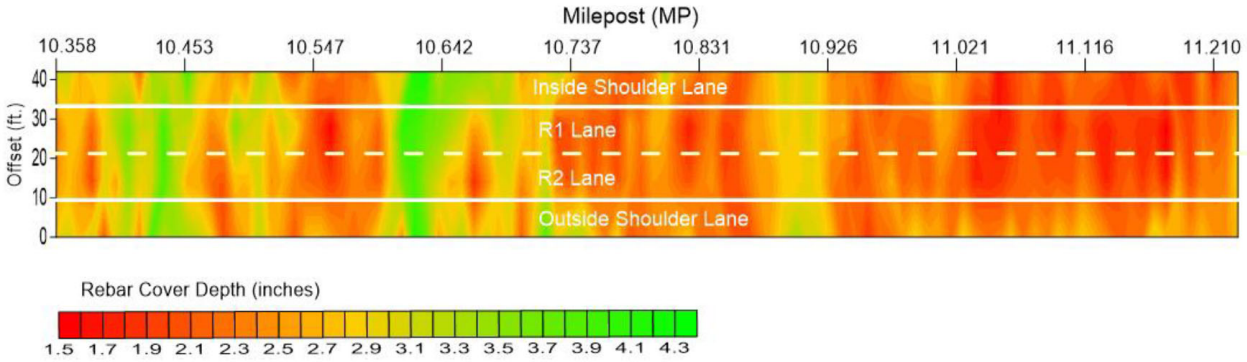

Figure 10: Contour map showing concrete cover depth to rebar (2 GHz air-launched GPR data, FDOT). Not to scale.

Site 1.12: Waldo Road (SR 24) – Roadway ID #: 26050000; (~MP 4.150 – MP 5.733), Alachua County – detection objective – voids over culverts

The test section is located on SR 24/Northeast Waldo Road in Alachua County and consists of three lanes (divided northbound and southbound travel lanes with an isolated center turn). Over the years, the roadway has experienced depressions at drainage inlet locations. FDOT conducted 400 MHz GPR survey near the approximate MP 5.753 where the pavement depression was noticed over the southbound lanes [7]. A series of longitudinal and transverse tests revealed potential voids and shifting soils locations and depths in southbound lanes. No potential pavement voids were located in the northbound lanes. It was decided that depressions were presumably caused by a previous Jack and Bore performed under the road. The center of depression was cut out to reveal the underneath cavity. A similar GPR survey was conducted between the MP 4.15 and 5.6 over the four patched areas to investigate the potential voids beneath the surface and evaluate the extent of pavement depression, delineate potential voids beneath the roadway, and determine the edge and depth of the underground utilities. [8]. The survey revealed the presence of potential voids, shifting soils, and utility pipes.

The goal of carrying out the 3D GPR survey has been to see if this system can replicate the assessment of the 400 MHz survey more quickly and without the inconvenience and cost of traffic disruption and lane closures.

Site 2.1 and 2.2 SR 22 – Project # 41641-1-52-01 / Roadway ID #: 51030000; (MP 5.418 – MP 12.136), Gulf County and SR 77 – Project # 424625-1-52-01 / Roadway ID #: 61080000; (MP 26.217 – MP 29.826), Washington County – Detection of stripping and delamination

SR 22 and SR 77 are rural two-lane highways with a 12-foot lane and 5-foot shoulder in each direction. SR 22 runs east- west and is located near Wewahitchka in Gulf County and SR 77 runs north-south and is located near Chipley in Washington county. Both roadways have asphalt pavements and have been reported to experience severe ride issues related to ripples or "worms". The overall objective of this task was to investigate the cause of the premature failure associated with the rippling or "worms". [9]. Roadway worms (distortions) are a type of pavement distress that manifests itself as a series of blisters

or small ripples appearing on AC pavement surface. They may occur on thin AC overlays over existing AC and PCC and on new AC pavement surfaces, typically transverse to the direction of travel between and outside the wheel paths. These are believed to be caused by underlying moisture or other gas-producing substances existing at layers interfaces within the body of AC pavements, typically situated below a thin surface layer. Substantial heating of the trapped substance results in its expansion in volume and migration of the vapor product to the surface, causing rises and buckles. Formed blisters/ripples are typically reduced in swell size with a temperature reduction or flattened out by upcoming traffic. AC blisters may cause severe consequences and may result in development of other distresses such corrugation, shoving, slippage cracking, and tensile cracking. Surface manifestations of road worms can vary from small bubbles to major bulges measuring several feet; they may occur in isolated spots, or they may be evenly distributed over the pavement surface. The intensity level of road worm imperfections determines whether the pavement's performance characteristics have been affected. The goal of carrying out the 3D GPR survey has been to see if data collected with 3D Radar system can be used to non-destructively identify the locations and extent of stripping, delamination, and "road worms" phenomena.

Site 2.3. Interstate 10 – Project # 432736-1-52-01 / Roadway ID #: 58002000; (MP 24.520 – MP 26.300), Santa Rosa County - Subsurface Investigation

This test section of I-10 is a four-lane highway comprised of divided eastbound and westbound lanes located in Santa Rosa County. On July 13, 2017, performed milling to remove a 1-inch temporary over-build patch and the existing structural asphalt surface in the eastbound outside lane (R2 lane) from Station 1253+25 to 1255+07. The surface was discovered to have been rutted and upheaved for more than 2.5" between wheel paths (see Figure 11). The upheaved area was cored in two locations resulting in the core holes filling with a clay-type white slurry. After removal of the slurry from one of the core holes, it filled back up again after 1 hour. The initial damage to existing structural course was discovered July 5, 2017 and the subsequent temporary over-build patch was placed July 7, 2017. The objective of this Task is to investigate the pavement depression and upheaval between this section and to understand the nature, source, and extent of the problem.

After a milling procedure was performed on July 13, 2017, the surface was discovered to have been rutted and upheaved between wheel paths more than 2.5". The upheaved area was cored in two locations resulting in the core holes filling with a clay-type white slurry of unidentified nature.

Figure 11: Observed rutting over the test section on I-10.

Figure 12 shows the exposed slurry-type material in the milled pavement section in proximity of MP 25.71 where the extensive rut and upheaval were reported. The extent of upheaved area was identified, and repair actions were taken: milling was performed over the full length of the area, including the development of additional 20 feet long "stepped" areas before and after the milled section. A core was cut after milling, directly over a wet spot, but no specific findings were provided that could assist in determining a cause. The repair area was thoroughly cleaned and dried with a power broom and a heavy coat of tack applied. The tack was inspected closely after breaking to make sure there is no more moisture/slurry material observed to push up through the tack. The goal of carrying out the 3D GPR survey has been to see if 3D GPR can be used to non-destructively identify the extent of observed pavement upheaval and high rut area where the repair actions were taken.

Figure 12: Examples of unidentified clay-type slurry, revealed after the milling procedure.

Site 2.4: SR 75/US 231, Panama City, Bay County, Composite (asphalt + concrete*) Roadway Section – Confirm the nature and extent of the underlying pavement layers

This test section of I-10 is a four lanes highway comprised of divided eastbound and westbound lanes located in Washington County. District 3 had several edge drains installed along the pavement edge with outfall pipes situated at specified locations of I-10. These drains were designed to carry runoff/moisture from the rubberized concrete or limerock base layer to protect the pavement structure. The test section located in Bay County, from south of Pipeline Road to south of Penny Road. This section of roadway was initially selected to identify areas of "concrete" below a thick asphalt layer. After review of the data and discussion with district personnel, it became clear that the roadway has a “cemented" (represented by sand-asphalt hot mix) base layer and an asphaltic surface layer with a reported thickness of greater than 3.5 inches. The goal of carrying out the 3D GPR survey has been to confirm the nature of and extent of the underlying pavement layers.

Site 2.5: SR 5 (Whitetopping Project) – Roadway ID #: 79010000; (~MP 9.600 – MP 11.458), Volusia County - Dowel bar alignment and voids detection under concrete pavement

This test section is a two-lane southbound roadway between Dayton Beach and Titusville, FL. It is a 1.85-mile long (from MP 9.598 to MP 11.456), built of rigid pavement (whitetopping) and made up of segments of varying thickness. Below the concrete is a 1-inch asphalt layer supported by 8.5-inch limerock base on top of stabilized subgrade. This roadway is part of an experiment project and has been in service for 28 years. This project is composed of three sections according to concrete slab thickness of 6-inch, 7 inch and 8 inches. The first three subsections in each of the major sections include joints with special dowel configuration consisting of 3 dowels in each wheel path spaced at 12 inches on centers and 12 inches from the pavement edge. The remaining three subsections in each primary section include joints with standard 12-dowel configuration spaced at 12 inches on the centers and 6 inches from the pavement edge. There are four undoweled joints in each primary section. The undoweled joints are located in the last four slabs between the special and standard dowel subsections. There is a controlled section (subsection 0) that comprised of 7-inch-thick concrete pavement with joint spacing of 14 ft. All the joints for the control sections were doweled using the standard 12- dowel configuration. Figure 13 shows the transition at the south end between the regular and test roadway sections.

Figure 13: Transition from south end of the test section to the regular roadway on SR 5 in proximity of MP 9.6.

Figure 14 displays schematic design of tested roadway. The purpose of the 3D GPR survey was to confirm the ability of 3D Radar system to evaluate the presence and alignment of dowel bars.

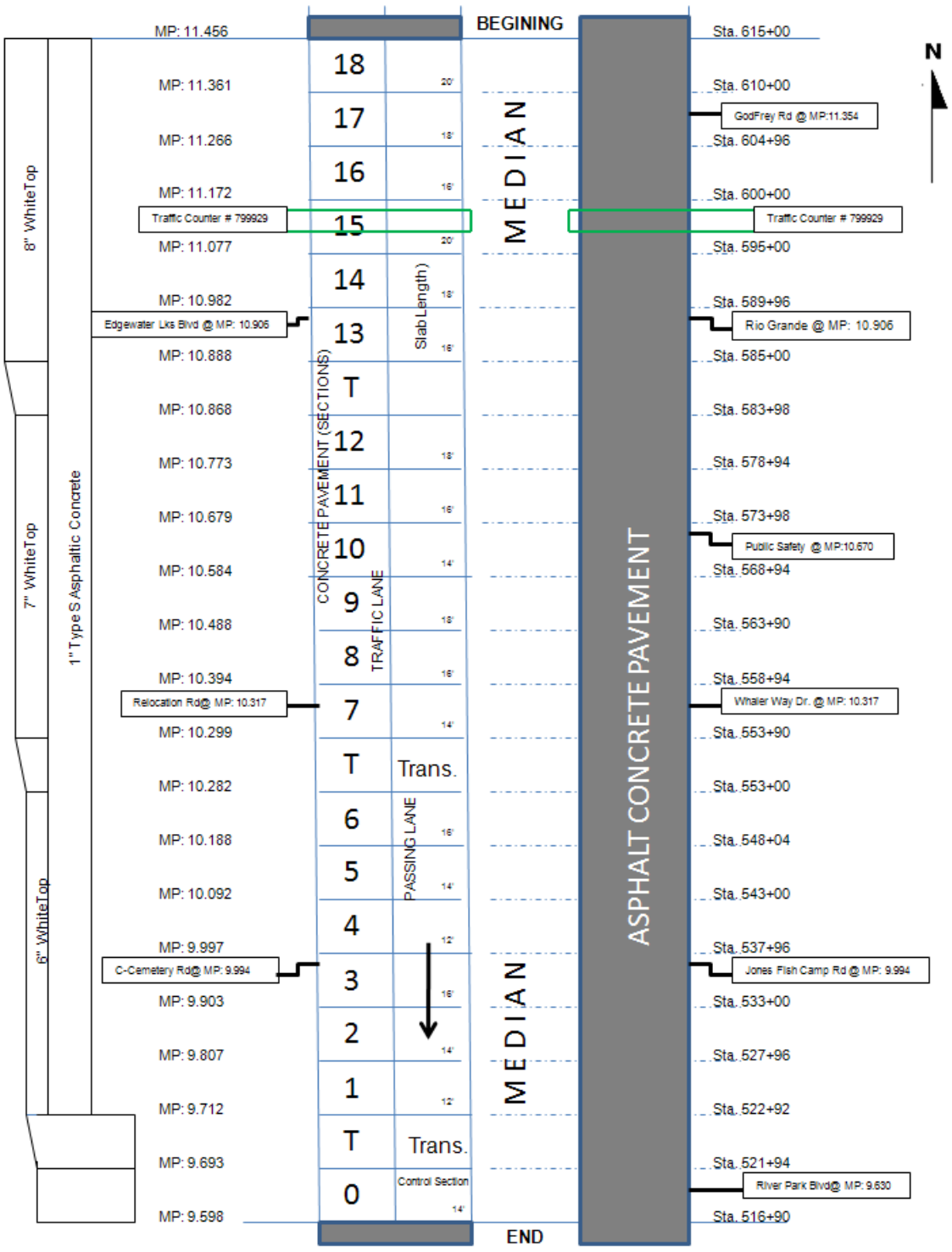

Figure 14: Schematic drawing of test section design. Not to scale [11].

Sites 2.6-2.8 – Bridge Decks

2.6: SR 816 (W. Oakland Park Blvd) Roadway ID #: 86090000; (~MP 2.263 – MP 2.323), Broward County - Bridge Deck Delamination Mapping

2.7: SR A1A (Blue Heron Blvd.) Blue Heron Bridge – Roadway ID #: 93080000; (~MP 0.414 – MP 0.788), Palm Beach County - Bridge Deck delamination/deterioration mapping

2.8: SR A1A/ North Causeway (Shorewinds Dr.) North Bridge over ICWW – Roadway ID #: 94060000; (~MP 0.330 – MP 0.719), St. Lucie County - Bridge Deck Delamination/deterioration mapping

Bridge # 860245 was built in 1978 and consists of three lanes and a pedestrian walkway in each of the westbound and eastbound directions. It is located on SR 816 (westbound Oakland Park Blvd) and spans over the SR 91 Florida's Turnpike highway one mile west of SR 7 in Oakland Park, Broward County. The bridge deck comprised of four spans made of prestressed concrete. The length of the bridge is 329.4 feet, from approximate MP 2.236 to MP 2.323, with width from curb to curb of 49.9 feet. Figure 15 and Figure 16 display the overall bridge condition observed from the survey vehicle.

Figure 15: General view of Broward bridge deck. Westbound lane, right side. Camera pointing west.

Figure 16: General view of Broward bridge deck. Eastbound lane, right side. Camera pointing east.

Bridge # 930269 (Blue Heron Bridge) was built in 1976 and consists of four lanes and two pedestrian walkways in westbound and eastbound directions. It is located on SR A1A (Florida State Road A1A). The

bridge spans over the Intracoastal Waterway in approximately 0.5 miles east of US 1 in Palm Beach, Florida. The bridge deck comprised of nineteen spans made of concrete precast panels. The length of the bridge is 1975.8 feet, from approximate MP 0.414 to MP 0.788, with width from curb to curb of 95.5 feet. Figure 17 and Figure 18 display the overall bridge condition observed from the survey vehicle.

Figure 17: General view of Blue Heron Bridge. Westbound lane, right side. Camera pointing West.

Figure 18: General view of Blue Heron Bridge. Eastbound lane, left side. Camera pointing East.

Bridge # 940045 is a movable (bascule) bridge that was built in 1963 and consists of two lanes, one in each of the westbound and eastbound directions, and one pedestrian walkway. It is located on SR A1A (Florida State Road A1A, N Causeway). The bridge spans over the Intracoastal Waterway connecting the barrier island to the mainland in approximately 200' East of US 1 (SR 5) in Fort Pierce, Florida. The bridge deck comprised of 43 spans made of cast-in-place concrete. The main span is a 103-foot-long double-leaf bascule flanked by two 45-foot, 2¾-inch rolled steel beam spans. The whole length of the bridge is 2054.6. feet, from approximate MP 0.33. to MP 0.719, with width from curb to curb of 37.7 feet. Figure 19 and Figure 20 display the overall bridge condition observed from the survey vehicle. It should be noted that signs of moderate deterioration can be visually observed over the westbound lane, while the eastbound lane cover appears to be in better condition.

The goals of carrying out the 3D GPR survey have been to map the distribution of deterioration and the depth of rebar.

Figure 19: General view of St. Lucie bridge deck. Camera pointing West. Vehicle positioned ~50 ft. to the west from the bascule span.

Figure 20: General view of St. Lucie bridge deck. Camera pointing West. Vehicle positioned ~450 ft. to the west from the bascule span.

4. Description of the Testing and Data Analysis

Data was collected in two stages. Stage 1 was the week of February 13, 2017 and the second stage was the week of November 13, 2017. Unless otherwise stated, all data was collected at normal driving speed. In Stage 1 the3D Radar data was collected using the FHWA van provided by MnDOT (see Figure 1). In Stage 2 the data was collected using the FDOT GPR vehicle with a special mounting configured for the 3D Radar antenna (Figure 2). The following describes the data collection and analysis for each test site.

Site 1.1: Interstate 10 – Project # 424634-1-52-01 / Roadway ID #: 72270000; (MP 0.000 – MP 8.989), Duval County – Evaluation of stripping and delaminations

The 3D-Radar survey was carried out on February 16, 2017. Four lines of data were collected, two each in the westbound and eastbound driving lanes. The western limit was MP 0 (Nassau County Line) and the eastern limit was MP 8.989 (West of SR 23) on I-10 in Duval County.

The goal of carrying out the survey has been to see if data collected with 3D-Radar system can be used to non-destructively identify the locations and extent of stripping and delaminations. 3D-Radar data was examined in proximity to core extraction locations for deviations of the pavement material dielectric value and presence of strong internal reflectors appearing at variable depths which are not normally seen within intact pavement layers and typically indicative of near-surface stripping. Figure 21 displays segment of 3D-Radar data showing prominent interfaces associated with bridge deck, AC, and base.

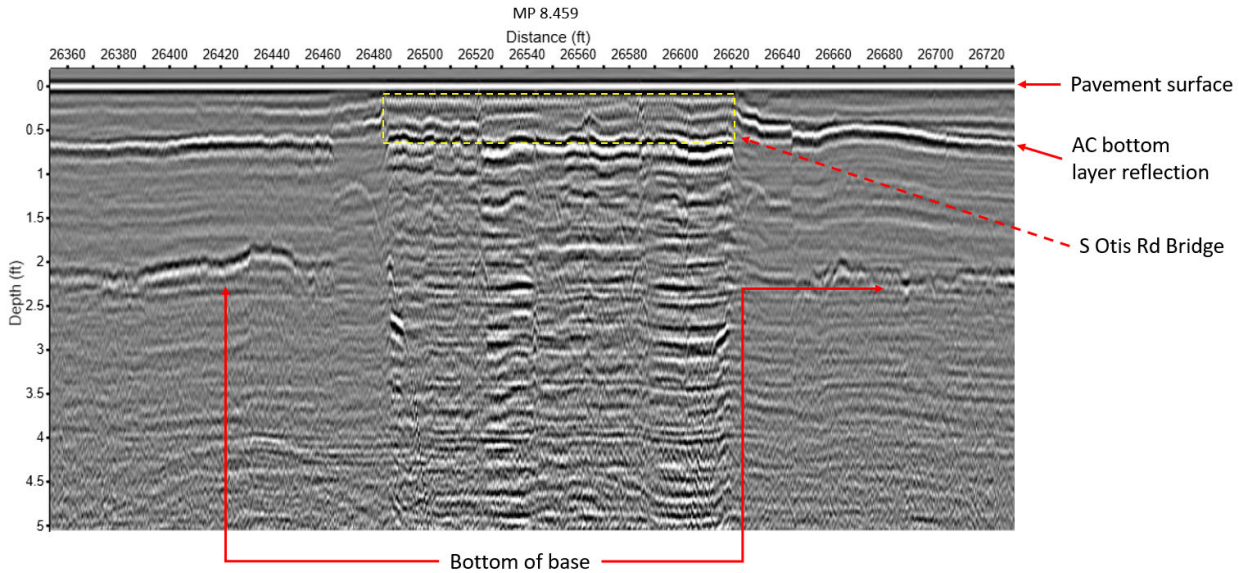

Figure 21: Cross-section of 3D-Radar data, showing the identified layers within the pavement.

Available core control data were used to constrain and verify the reliability of the interpretations of the 3D-Radar data. Figure 22-27 show the core locations superimposed over the 3D-Radar data. Figure 22 represents 3D-Radar data collected in proximity of core #1 extraction point (MP 0.123, R2), where the roadway depression was noted. Core extraction revealed evidences of cracking below the pavement layer. Reflection activity spot related to the observed damage can be clearly recognized on 3D-Radar data. Figure 22b displays corresponding GPR C-scan obtained from depth of 0.4 inches. Figure 22c and Figure

22d exhibit GPR C-scans obtained from depths of 3.23 inches and 4.26 inches, where signs of potential stripping development can be recognized. Orange frames indicate areas with potential raveling/stripping developed within the pavement material. Additional layer reflectors observed between the surface and base reflection can be indicative of broken bond between the bitumen and aggregate leaving a lower density material layer within the asphalt. The dielectric properties of stripped HMA can be affected by the presence of moisture content and/or air voids; stripping development can be also accounted to the incompatible aggregate and asphalt binder, reduced adhesion, and/or the impact of moisture content separating the asphalt binder from the aggregate.

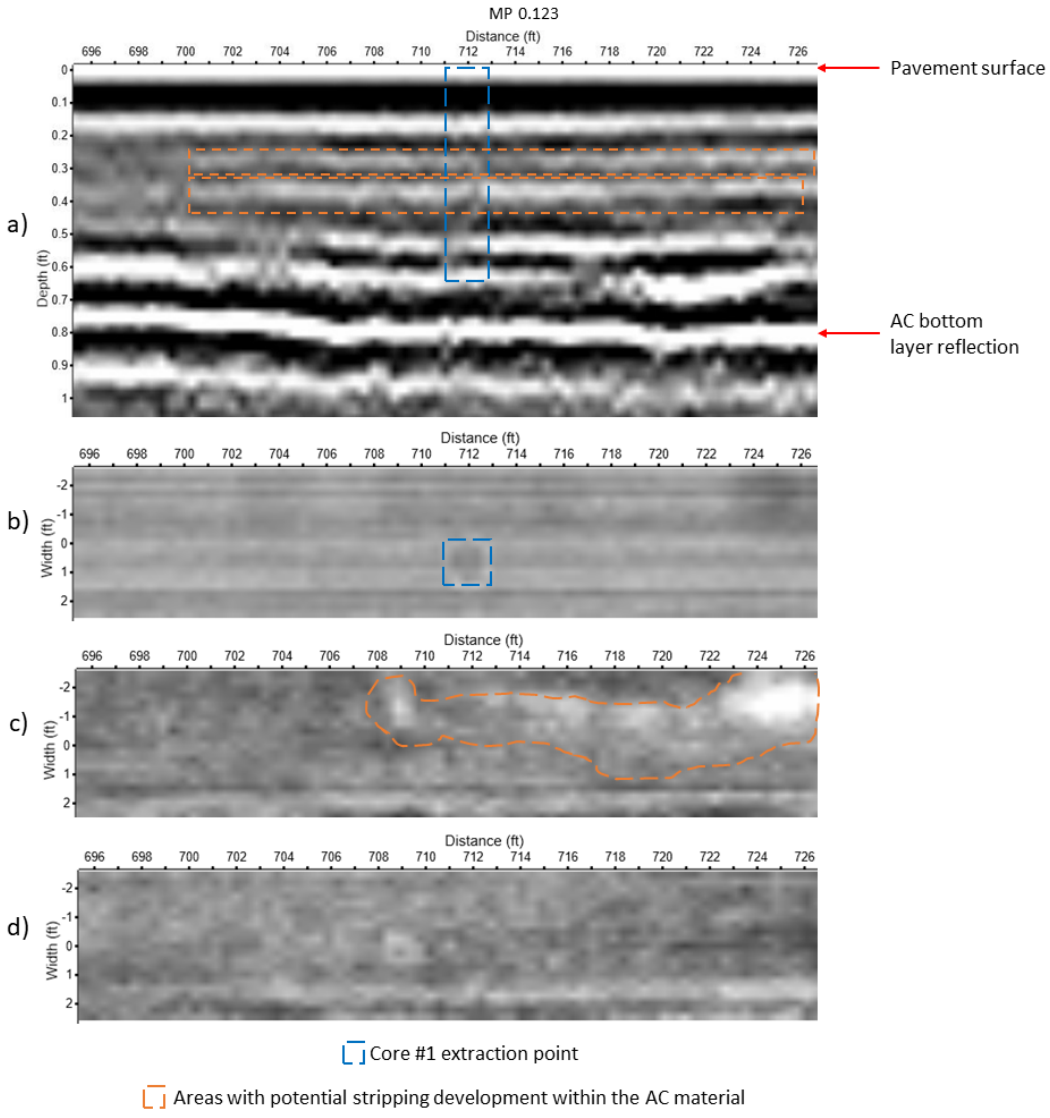

Figure 22: 3D-Radar cross-section in proximity of the core #1 extraction point (a); I-10 reflection at the depth of 0.48 inches. (b); I-10 reflection at the depth of 3.23 inches (c); I-10 reflection at the depth of 4.26 inches (d).

Figure 23 represents 3D-Radar data collected in proximity of cores #2 and #3 extraction points (MP 6.163 and MP 6.170, R2). Core #2 showed no damage, which corresponds well with very low reflection activity

noted in 3D-Radar data. Core #3 that was extracted in proximity of the area, where the roadway depression and signs of limerock dust bleeding through the asphalt were noted, revealed evidences of Class II C type cracking below the pavement layer.

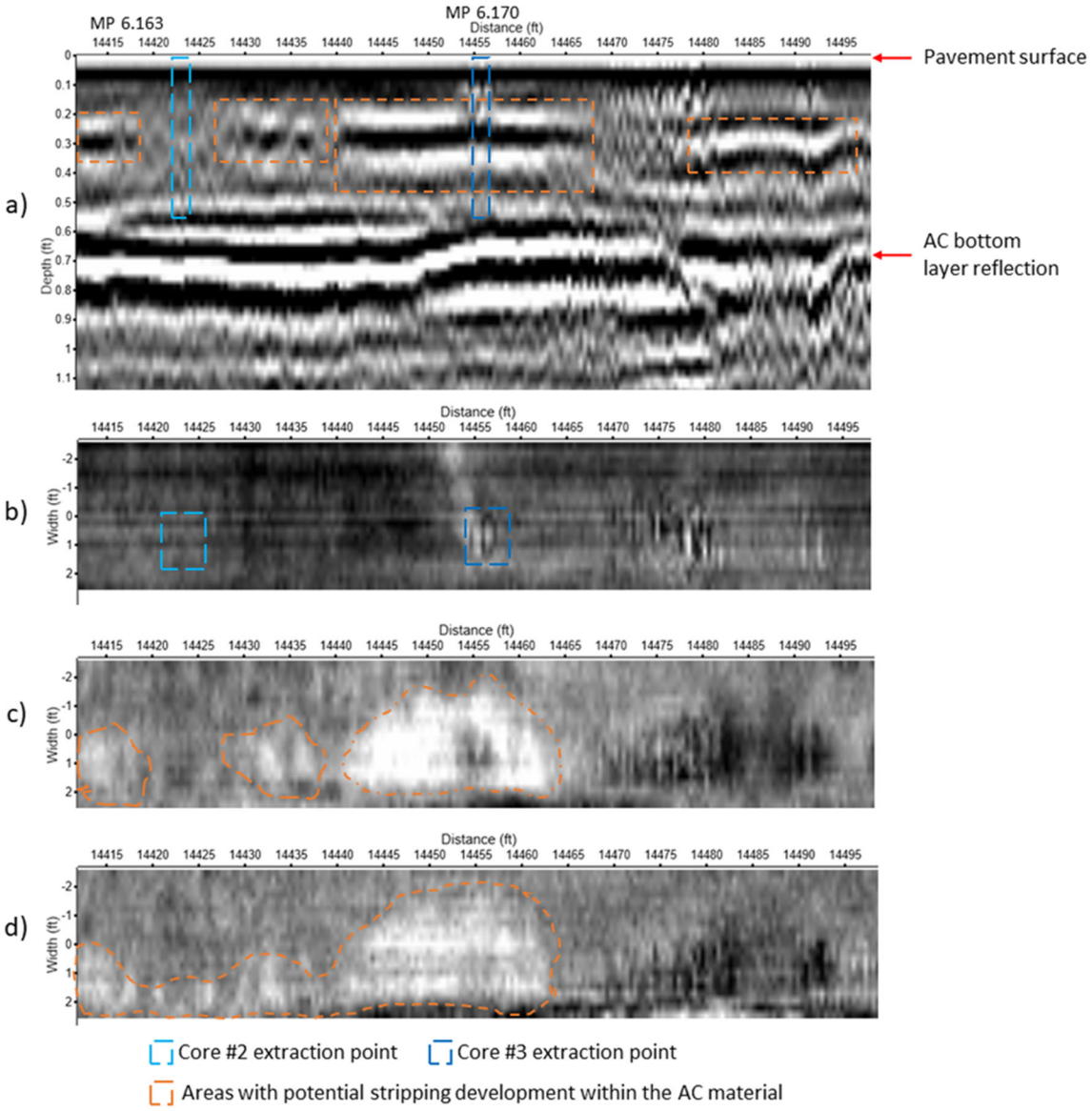

Figure 23: 3D-Radar cross-section in proximity of the cores #2 and #3 extraction points (a); I-10 reflection at the depth of 1.44 inches (b); I-10 reflection at the depth of 2.71 inches (c); I-10 reflection at the depth of 4.51 inches (d).

Figure 23b displays corresponding GPR C-scan obtained from depth of 1.44 inches. Figure 23c and Figure 23d exhibit GPR C-scans obtained from depths of 2.71 inches and 4.51 inches, where signs of potential stripping development can be recognized. Moderate reflection activity can be observed over the core #3 extraction point on corresponding 3D-Radar data. Orange frames indicate areas with potential raveling/stripping developed within the pavement material.

Figure 24 represents 3D-Radar data collected in proximity of core #4 extraction point (MP 6.268, R2). Core #4 that was extracted in proximity of the area, where the roadway depression and signs of limerock dust bleeding through the asphalt were noted, revealed evidences of cracking below the pavement layer. Core showed moderate damage which correlates well with observed reflection activity spots in Figure 24c. Figure 24b and Figure 24c exhibit corresponding GPR C-scans obtained from depth of 2.4 inches and 3.48 inches, respectively. High reflection activity can be observed over the core #4 extraction point on corresponding 3D-Radar data. Orange frames indicate areas with potential stripping developed within the pavement material.

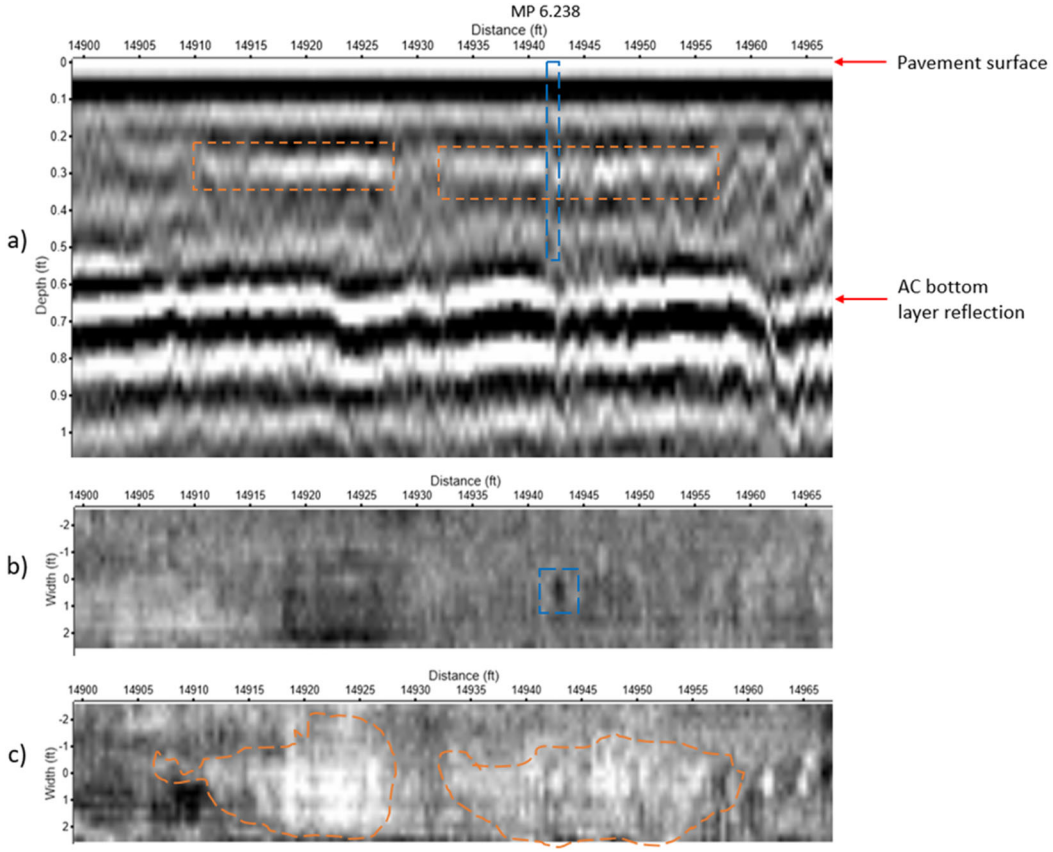

Figure 24: 3D-Radar cross-section through the core #4 extraction point (a); I-10 reflection at the depth of 2.4 inches (b); I-10 reflection at the depth of 3.48 inches (c).

Figure 25 represents 3D-Radar data collected in proximity of core #5 extraction point (MP 6.355, R2). Core #5 showed no damage; however, some reflection activity can be observed within the asphalt layer at depth of approximately 3.6 inches. Figure 25a display the GPR B-scan with corresponding GPR C-scans obtained from depth of 1.94 inches (25b) and 3.6 inches (25c), respectively. Orange frames indicate areas with potential stripping developed within the pavement material.

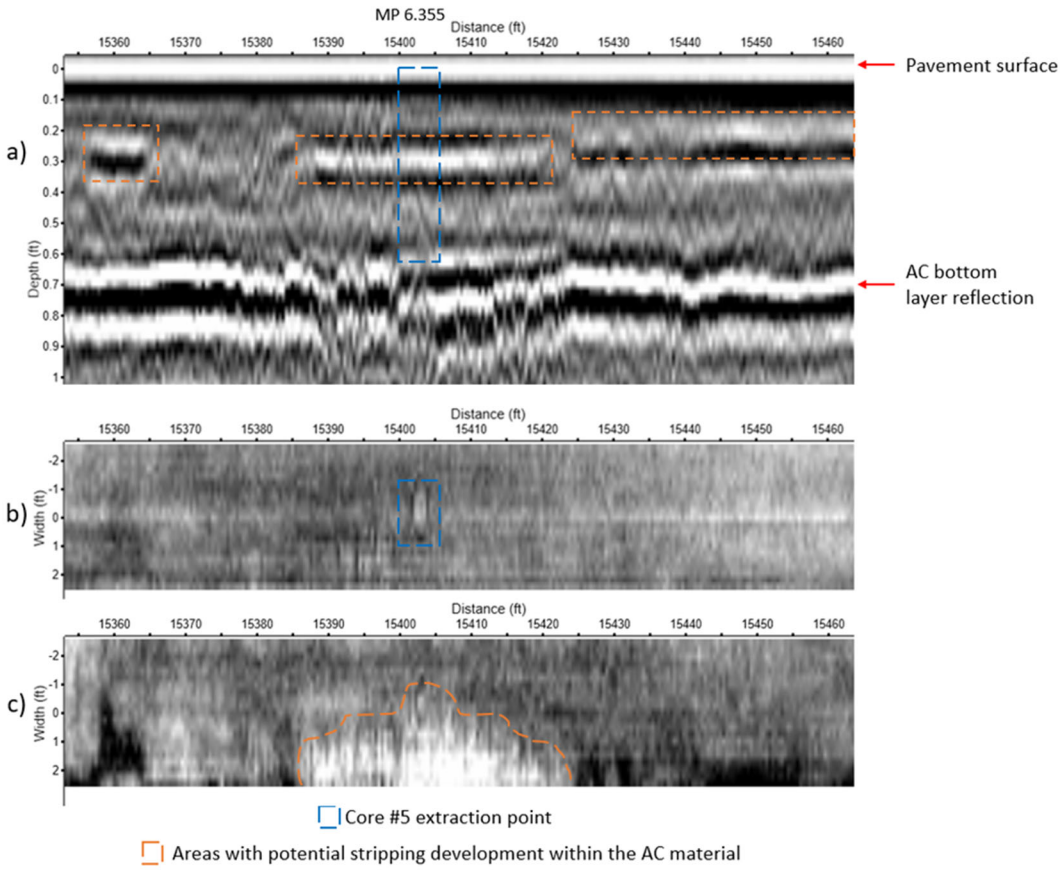

Figure 25: 3D-Radar cross-section through the core #5 extraction point (a); I-10 reflection at the depth of 1.9 inches (b); I-10 reflection at the depth of 3.6 inches (c).

Figure 26 represents 3D-Radar data collected in proximity of core #6 extraction point (MP 6.424, L2), where the roadway depression and bleeding asphalt were noted. Core showed no damage which correlates well with very minor interlayer reflection activity. Corresponding GPR C-scans obtained from depths of 1.68 inches and 4.5 inches are shown in Figure 26b and Figure 26c, respectively. Orange frames indicate areas with potential stripping developed within the pavement material. Green dashed line delineates the location of reported fuel damage. It should be noted that a strong internal reflector, that varies in depth, can be indicative of severe stripping and cannot be accounted for horizontal interface along the asphalt material layer boundary. Another thing to note – reflection obtained at the depth of 4.5 inches does not reveal any features that can be associated with existing stripping.

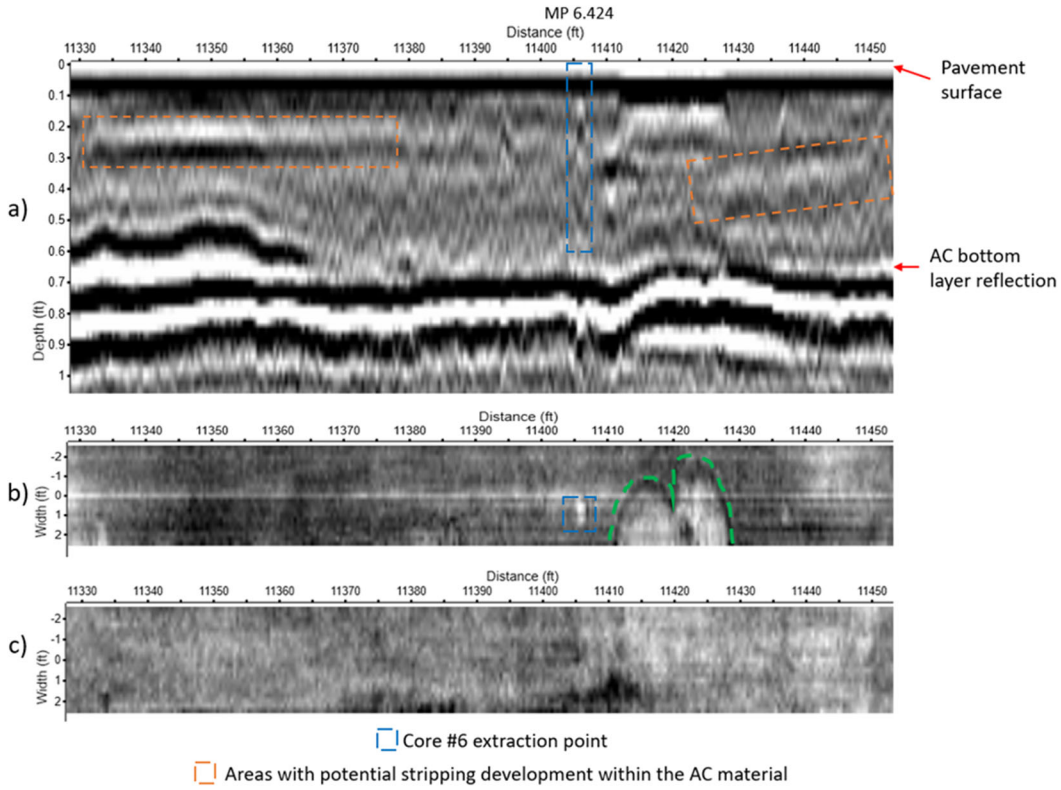

Figure 26: 3D-Radar cross-section through the core #6 extraction point (a); I-10 reflection at the depth of 1.68 inches (b); I-10 reflection at the depth of 4.51 inches (c). Green dashed line delineates the location of reported fuel damage.

Figure 27 represents 3D-Radar data collected in proximity of core #7 extraction point (MP 5.869, L2). Core #7 revealed evidences of cracking below the pavement layer. Corresponding GPR C-scans obtained from depth of 2.9 inches and 3.6 inches are shown in Figure 27b and Figure 27c, respectively. Orange frames indicate areas with potential stripping developed within the pavement material.

3D GPR survey results were examined in proximity to core locations for deviations of dielectric values and presence of internal reflectors at variable depths which are not normally seen within intact pavement layers and can be indicative of stripping. Anomalous interlayer activity was identified and reported as potential stripping development within the pavement material.

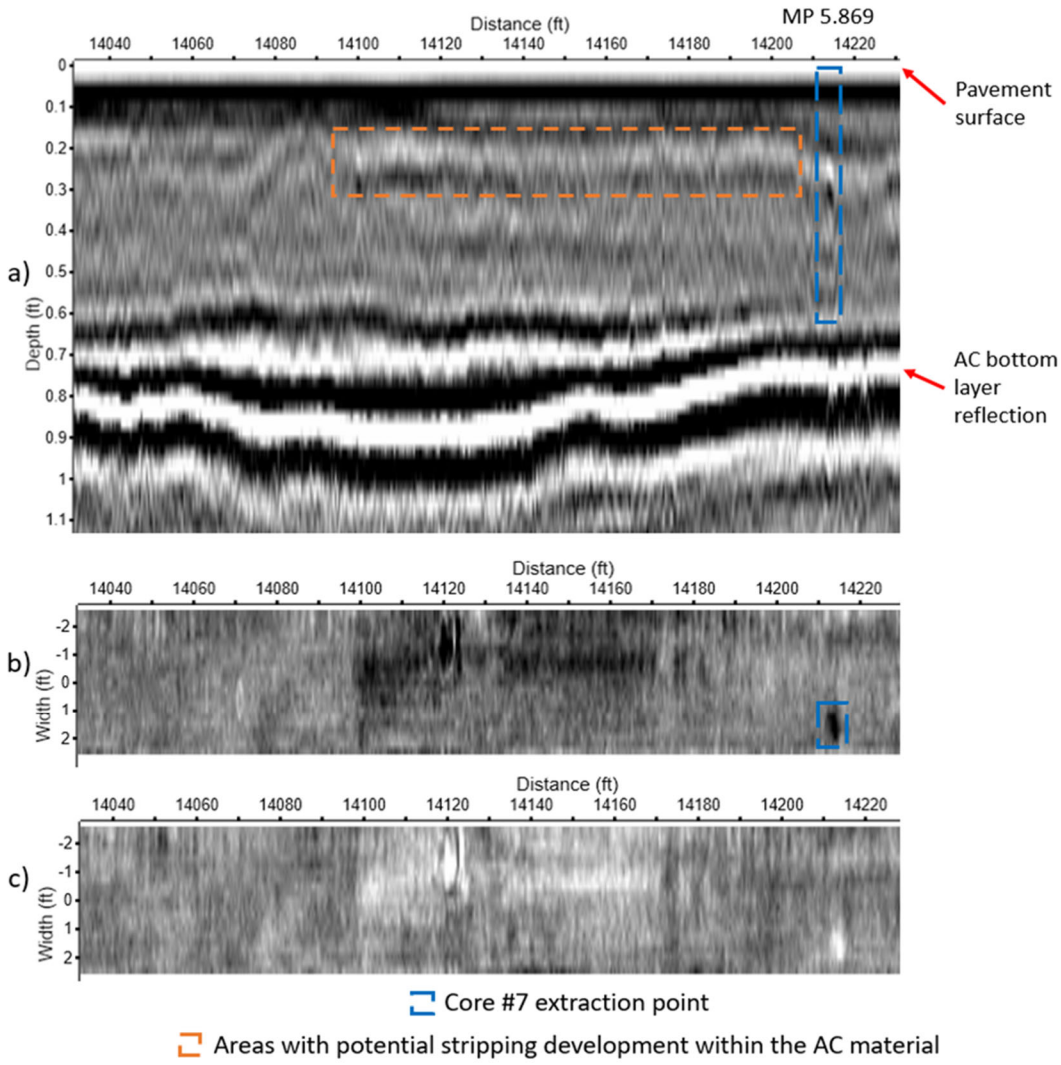

Figure 27: 3D-Radar cross-section through the core #7 extraction point (a); I-10 reflection at the depth of 2.9 inches (b); I-10 reflection at the depth of 3.6 inches (c).

Site 1.3: Interstate 75 – Project # 428803/4-1-52-01 / Roadway ID #: 26260000; (MP 14.5 – MP 27.5), Alachua County – Pavement Subsidence

The purpose of the 3D-Radar survey was to see if the outcomes of the FDOT 2 GHz and 400 MHz GPR system investigation could be replicated with the 3D-Radar system. Four lines of 3D-Radar data were collected on February 14, 2017 – one each in the right and left side of the low speed lane in each direction. The limits of data collection were between state MM's 386 and 401. Samples of data collected in the FDOT study were compared to samples of 3D-Radar data collected at the same location, as discussed below.

MP 14.490-15.520 – Potential Depression. Figure 28 presents a segment of FDOT 2 GHz air-launched GPR data, collected at the south end of the southbound deck over the US-26. The anomaly shown in Figure 28 is considered as a strong indication of subsidence in the area. Figure 29 shows a segment of 400 MHz GPR profile collected over the same area.

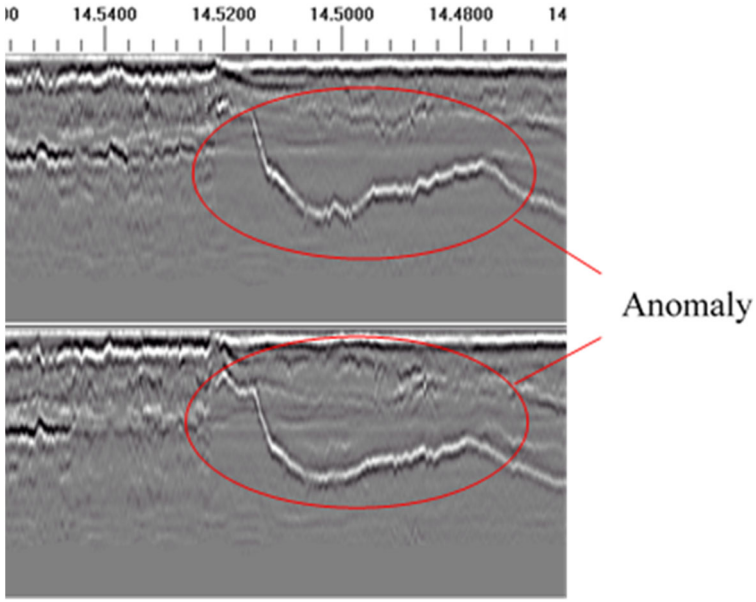

Figure 28: FDOT Air-launched GPR scan showing thickness anomaly at south end of US 26 bridge [2].

Figure 30 shows a segment of 3D-Radar data collected over the same location as it shown in Figure 28 and Figure 29. The red circled area corresponds to the anomaly noted in Figure 28. The green circled area indicates the anomaly associated with potential shifting soil noted in Figure 29. Note that the 2 GHz air launched data was well replicated using 3D-Radar data. The 400 MHz data showing potential shifting soil does not show up as clearly in the 3D-Radar data, and the "moisture" area does not appear up at all.

- **L3 Test Location MP: 14.490 – 14.520**

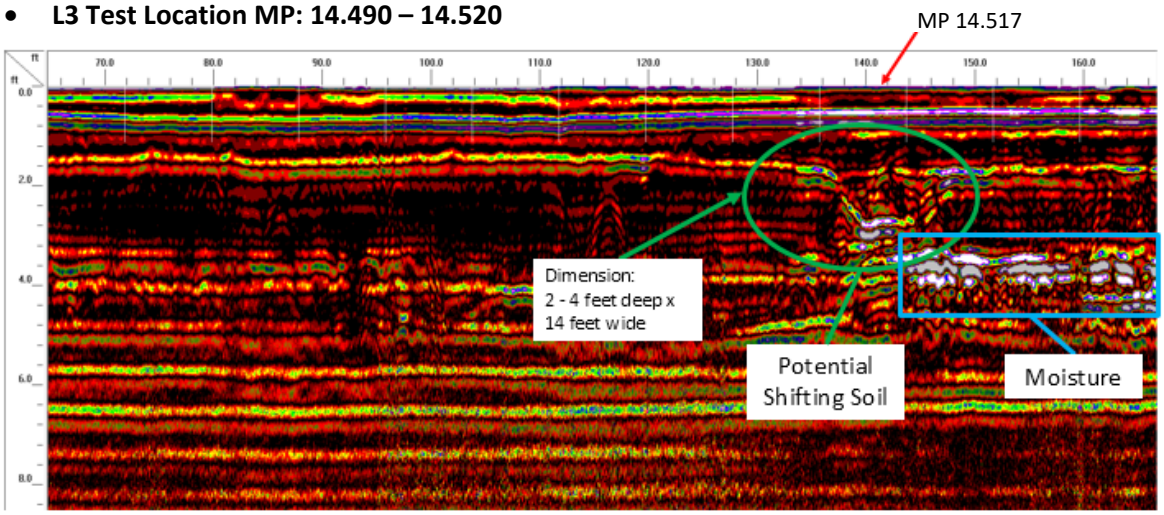

Longitudinal run 4 identified potential shifting soil 140 feet from the starting point (near exit 387). In addition moisture is observed at a depth of 3 to 4 feet beneath the surface. Run 2 was conducted 9 feet east of the white edge line of L3. (left wheel path)

Figure 29: FDOT 400 MHz data collected in southbound lane from bridge joint [2].

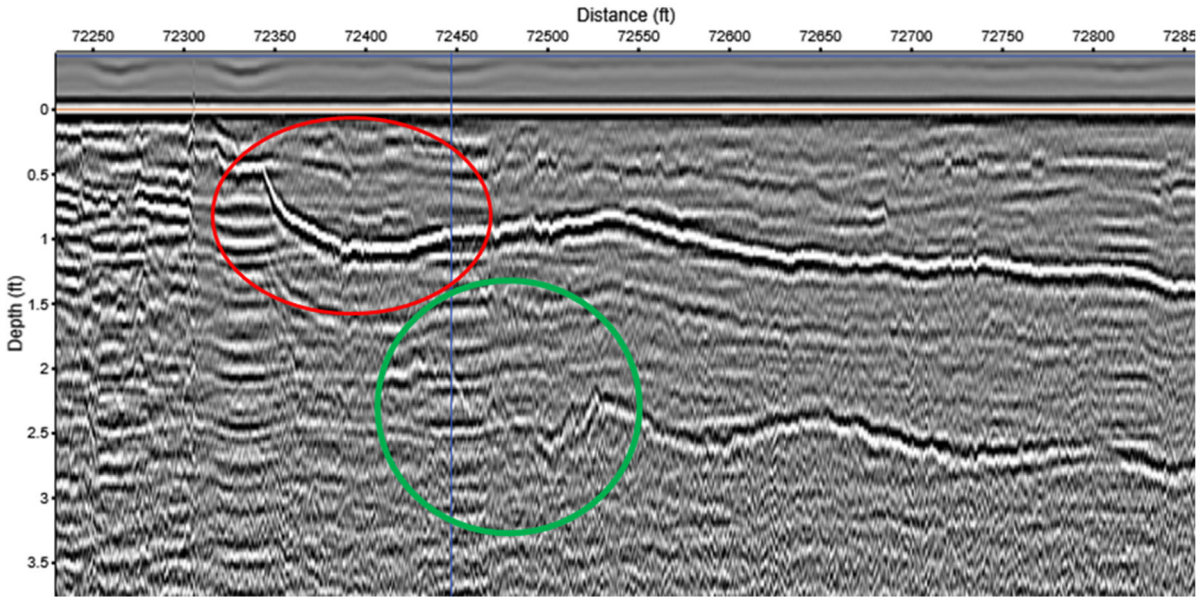

Figure 30: 3D-Radar data collected over the same location as in Figures 28 and 29. Red circled area represents the anomaly associated with potential shifting soil in Figure 28. Green circled area delineates where the evidence of potential soil shifting noted in Figure 29 can be observed on 3D-Radar data.

MP 14.810-14.830 – Potential Depression. Figure 31 below shows a segment of 400 MHz data indicating an area of potential moisture infiltration. Figure 32 shows a segment of 3D-Radar data collected over the same area. The moisture indications that appear in the 400 MHz data does not appear in the 3D-Radar data.

- **L3 Test Location MP: 14.810 – 14.830**

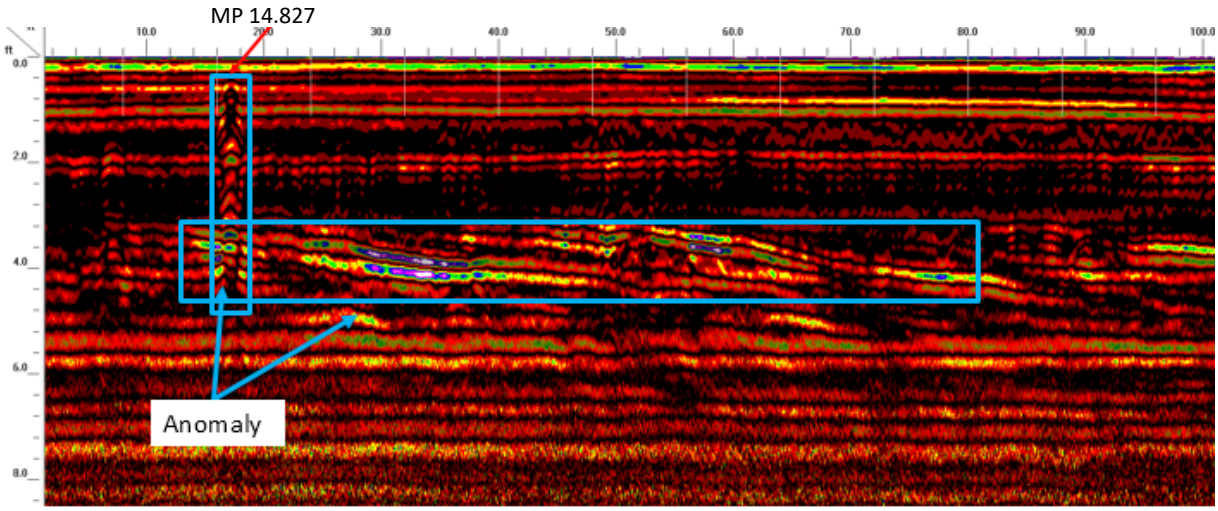

Longitudinal run 1 identified an anomaly (highlighted in green). GPR run 1 was conducted directly over the white edge line of L3.

Figure 31: 400 MHz GPR data showing signs of potential moisture infiltration [2].

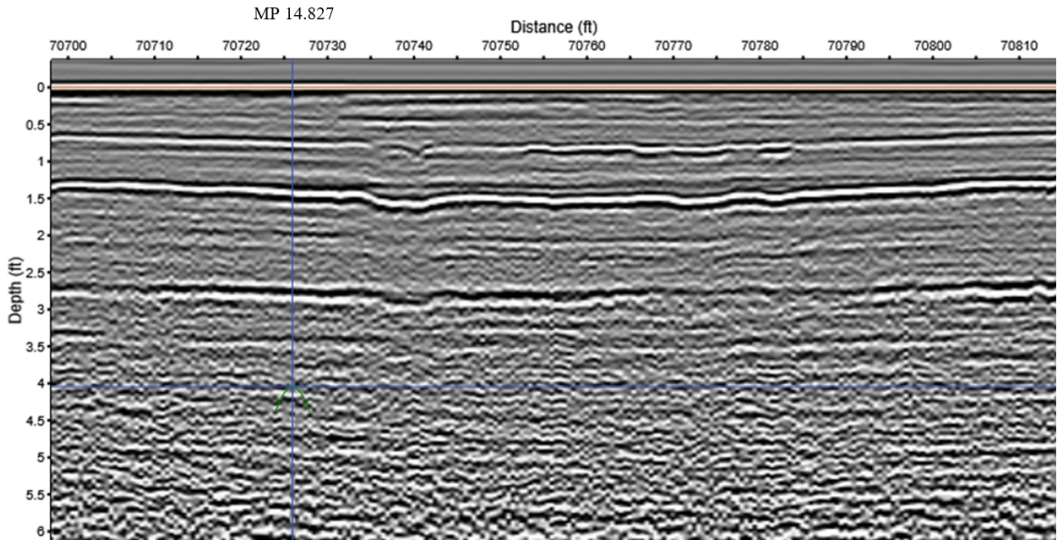

Figure 32: 3D-Radar data collected in the vicinity of MP 14.827.

Figures 33-35 compare 2 GHz air-coupled and 400 MHz GPR data with 3D-Radar data collected over the same location.

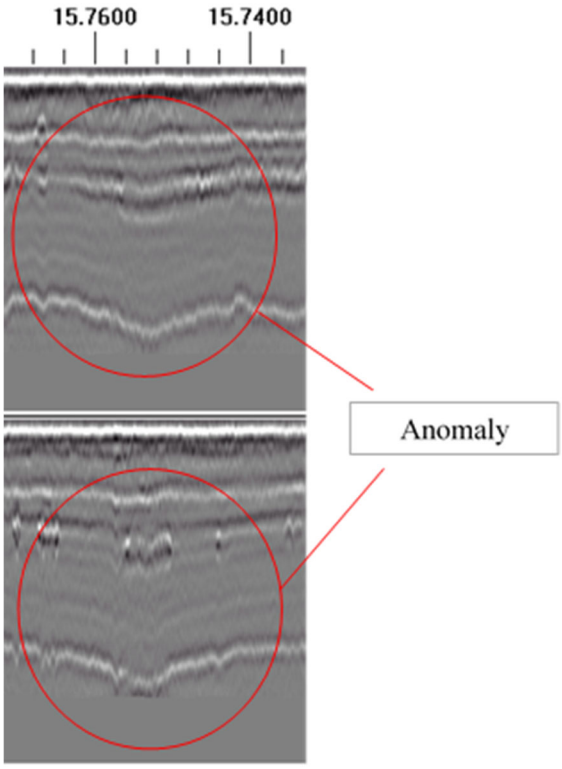

Figure 33: Air-launched GPR scan showing near surface anomalies in vicinity of the MP 15.76 [12].

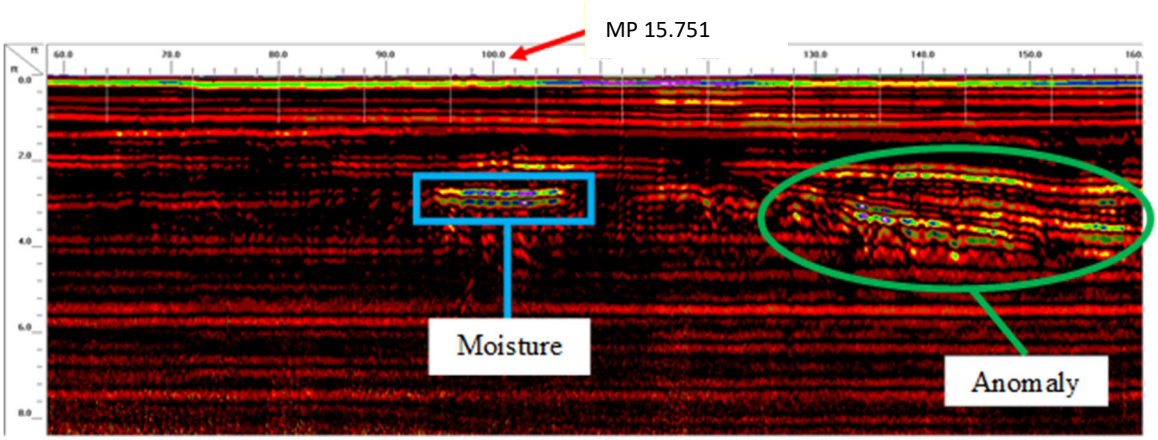

Anomaly was observed from longitudinal run 3 at approximate depths of 2 feet to 4 feet. Area of moisture was identified at approximate depth of 3 feet. Run 3 was ran 6 feet to the east of the white edge line of L3.

Figure 34: 400 MHz GPR data showing signs of potential moisture infiltration [2].

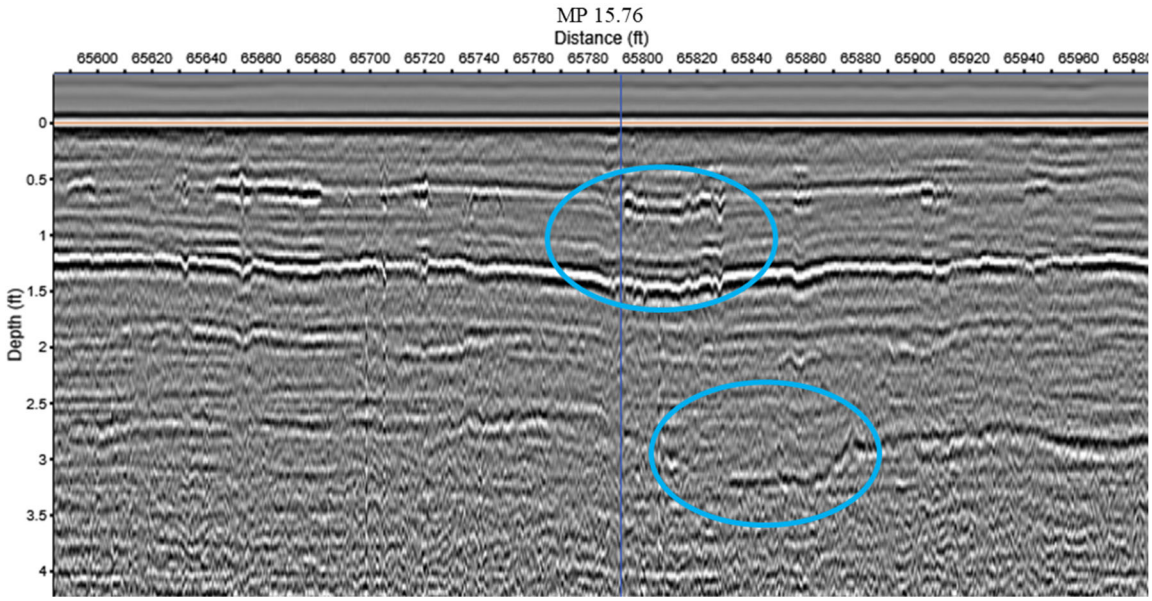

Figure 35: 3D-Radar data showing near surface anomalies which are similar to ones noted in Figure 33 along with anomaly that can be associated with deeper depression at the depth of 3 feet.

In most cases, 3D GPR survey confirmed the presence of previously noted thickness variations and shifting soils. Location and extent of noted anomalies were identified with high precision, without the need for lane closure. However, the depth of penetration of the 3D Radar data was significantly less than that of the 400 MHz ground coupled FDOT system.

Site 1.4: State Material Office (SMO) Asphalt Test Tracks - Flexible Test Lanes 3, 4, and 5 - Interlayer bonding research, density, and segregation study

The purpose of the evaluation described below has been to determine the ability of the 3D-Radar system to detect the conditions embedded into these pavement sections. 3D-Radar data was collected on

February 14, 2017. Two passes were collected in each lane – one in each direction on either side of the lane. Since the coverage of each pass is 5 feet and the lanes are 12 feet wide, there are small gaps in the lateral coverage of the data. Also, since these are test sections, the data was collected at 5 to 10 mph. The data was brought into Examiner software after the survey and evaluated to determine the ability to identify the particular defects.

Lane 3 – Delamination. Figure 3 shows a depth slice of the 3D-Radar data at a depth of approximately 2 inches. The areas circled in blue in Figure 36 are most likely where moisture has infiltrated the sand interface between the two layers – otherwise nothing would show up with GPR in a purely de-bonded condition.

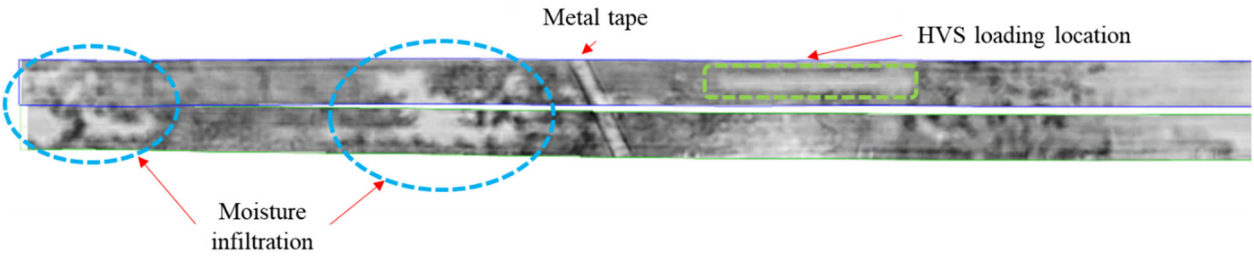

Figure 36: 3D-Radar depth slice at 2 inches in Lane 3.

Lane 4 – Density. This lane was tested with the HVS at 6 various locations within the first 150 feet, and consequently density variations are expected due to the local compaction. Visually examining the depth slices of 3D-Radar at an approximate depth of 0.8 inches over the known areas of HVS loads reveals the testing location pattern and illustrates how the densification can be visually observed in the GPR data. Figure 37 demonstrates the slice of 3-D Radar data revealing the anomalies associated with density variations. Ultimately the pavement surface dielectric would be calculated and plotted, and the relationship between dielectric and density would serve as the basis for the evaluation. At this point in time, the Examiner does not offer this capability.

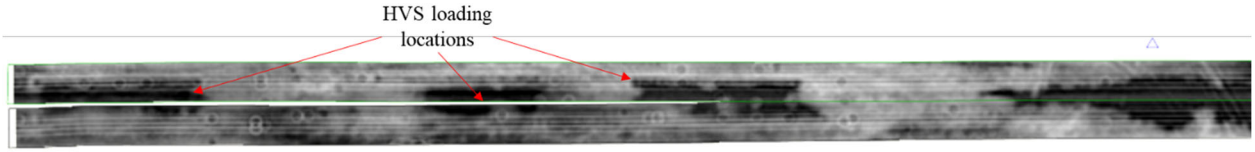

Figure 37: 3D-Radar depth slice at 0.8 inches in Lane 4.

Lane 5 – Segregation. During the construction of Lane 5 the paving process was modified in order to generate localized segregation. The temperature profile measured during paving using an infrared thermal imaging camera confirmed the presence of segregation, as shown in the bottom part of Figure 38. The top part of Figure 38 shows a 3D-Radar depth slice selected to best reveal the effects of segregation. The circled area indicates the anomalous zone, corresponding with the low temperature area denoted on the temperature profile map.

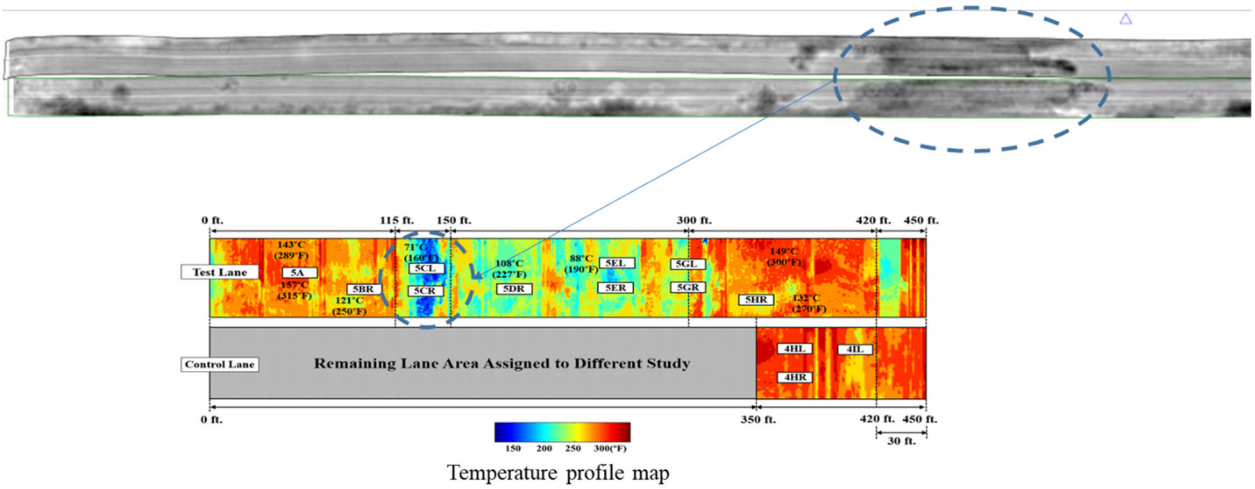

Figure 38: 3D-Radar data depth slice at 1.5 inches in Lane on top; contour map showing spatial distribution of surface temperature values at the bottom.

The data analysis and correlations presented above indicate that, under controlled conditions, 3D-Radar data can reveal delaminations, segregation, and density variations in asphalt pavement.

To test the repeatability of proposed testing procedure, repeat tests were carried out on lanes 3, 4, and 5. Data was collected in both directions for each lane. In each case, the data in the opposite direction was collected on the opposite side of the lane, so close to full lane coverage was obtained for each pair of data files. The primary difference between repeated files is the position of the vehicle, since it is not possible to drive exactly in the same position each time. Since the 3D-Radar data is geopositioned, the display of the data reflects these positional differences. Figure 39 and Figure 40 below show repeat testing depth slice results for Lanes 3 and 4. Note that the primary difference is the spatial geometry of the pass, and not in the underlying data. For Lane 3, there is also some spatial distortion – the middle section is wider in the lower image than in the upper image. This sort of distortion does not occur in the Lane 4 data.

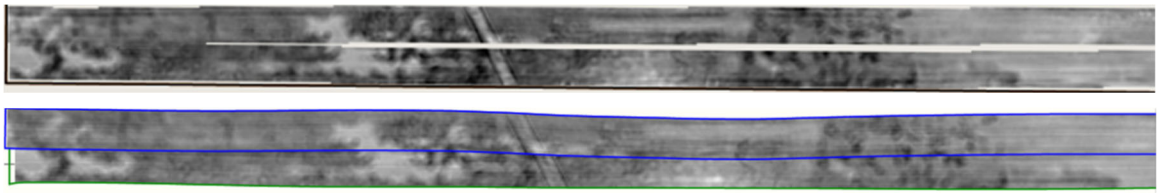

Figure 39: Repeat test results for Lane 3.

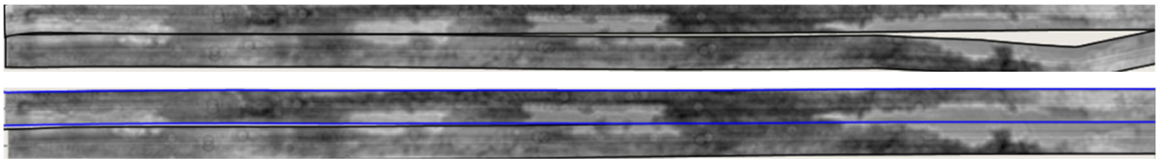

Figure 40: Repeat tests for Lane 4.

In summary, the tests of the 3D GPR system at the SMO facility showed that the system was able to detect the presence and extend of the embedded conditions, and that this detection capability was repeatable.

Site 1.7: SR 20 – Project # 430565-3-52-01 / Roadway ID #: 26080000; (MP 5.000 – MP 6.000), Alachua County – Thickness Evaluation

Florida Department of Transportation survey was conducted on March 1st, 2017 using four 2 GHz air-launched GPR antennas mounted to the FDOT GPR survey vehicle. An evaluation of pavement asphalt thickness presented as a line chart displayed in Figure 41 showing the chart of variation of average thickness (vertical axis) as a function of GPR profile length (horizontal axis).

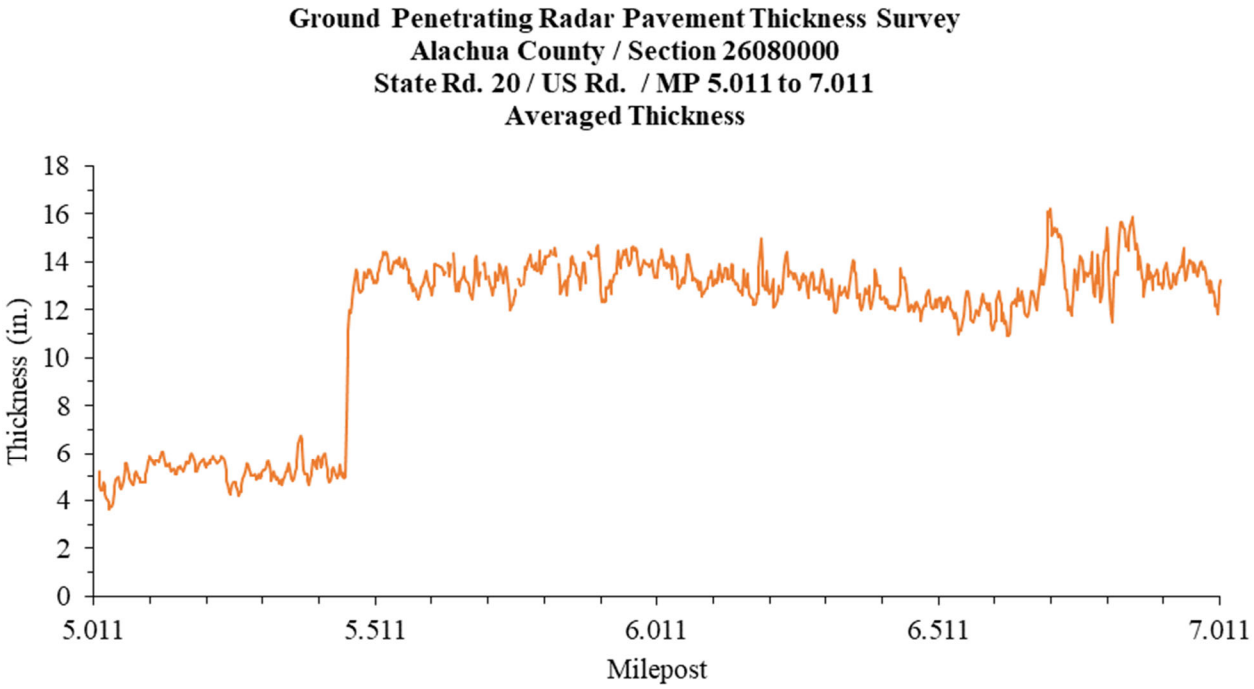

Figure 41: Chart showing the average asphalt thickness (vertical axis) measured using FDOT air-launched GPR system vs distance along the SR 20 (horizontal axis).

The purpose of carrying out the 3D GPR survey has been to see if data collected with 3D-Radar system can be used to perform pavement thickness evaluation. The 3D-Radar survey was carried out on February 14, 2017, between approximately MP 5.0 and 7.0. Two lines of data were collected, in the right and left sides of the outside eastbound lane. Figure 42 displays 3D GPR cross-section through tested area showing significant drop in assumed reflection depth representing the bottom of pavement material at approximate 2400 ft. mark. Figure 43 shows a segment of stitched file containing both left and right sides of eastbound driving lane of SR 20. Red line represents the tracked AC bottom layer interface with significant drop in the depth on approximately 2325 ft. (MP 5.33).

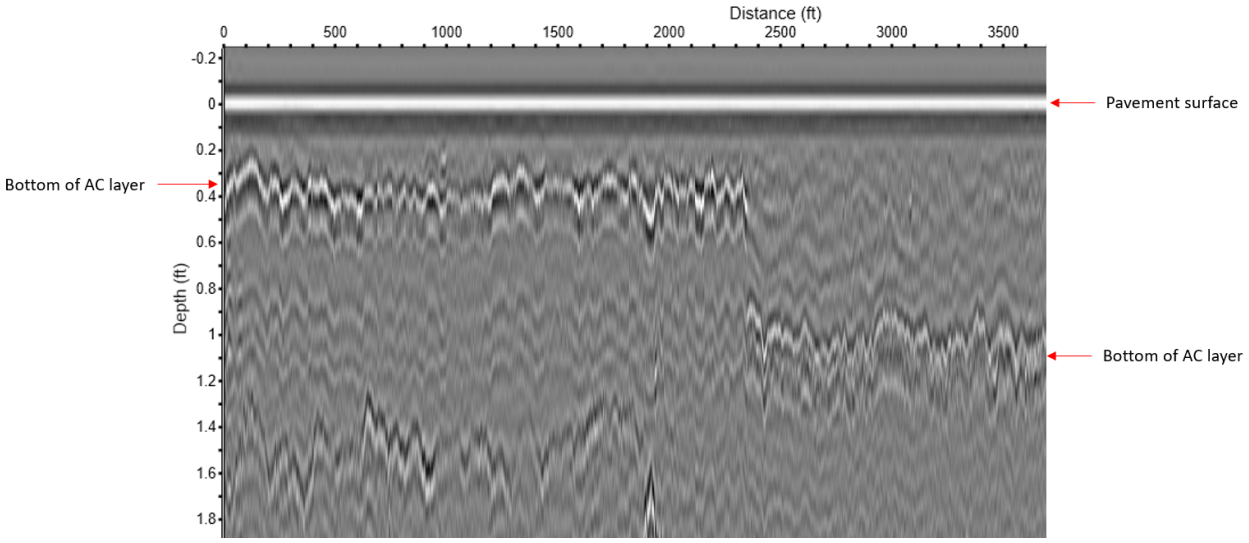

Figure 42: 3D-Radar section through tested area, eastbound Driving lane (right side) of SR 20.

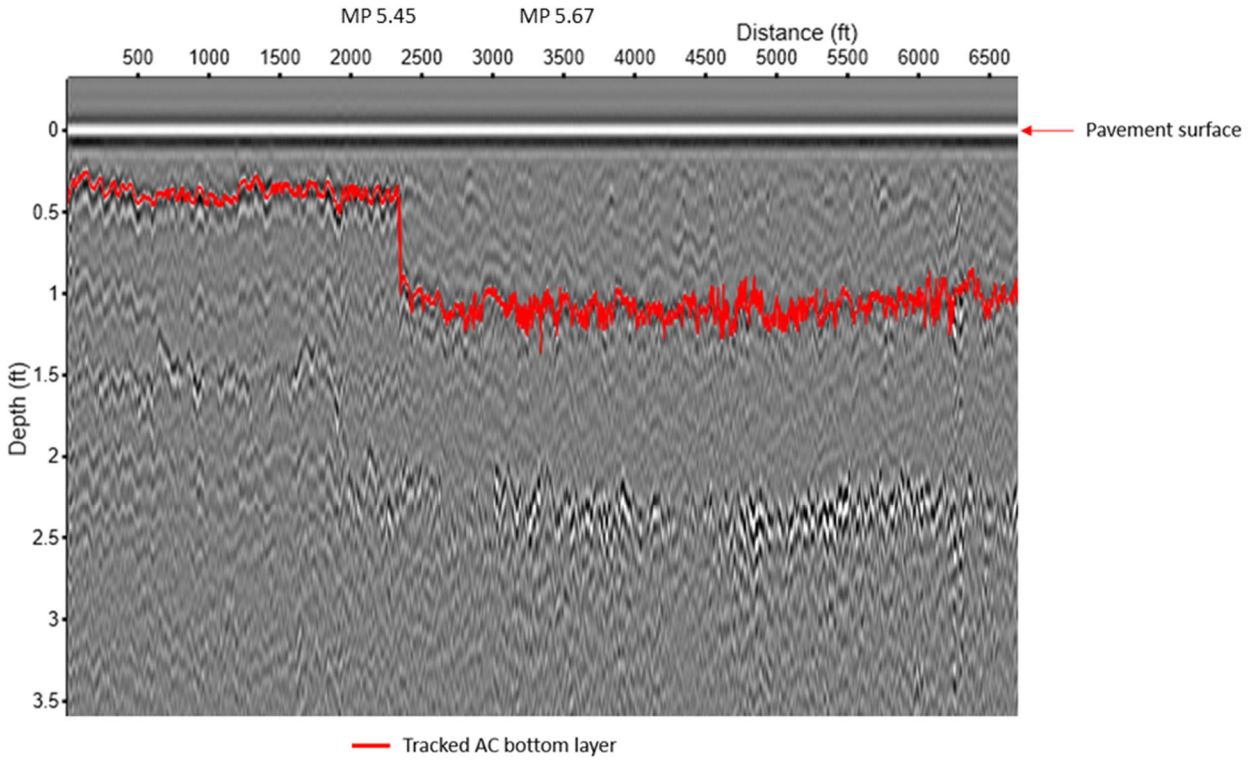

Figure 43: GPR Section through tested area, eastbound driving lane of SR 20.

Using Examiner software, the bottom of AC layer was identified and traced in the same manner as in the related FDOT survey. The AC layer thickness was calculated from the arrival time of the reflection from the top and bottom of the AC layer. The assumed dielectric permittivity of 5 was used to convert reflection times to reflection depths. The value had to be assumed since Examiner does not presently have the ability to calculate dielectric constants. The value of 5 is typical for dry asphalt; the range of calculated reflection depths obtained from the 3D-Radar data with assumed dielectric constant of 5 correlated well with the outcomes of FDOT survey. It should be noted that pavement thickness and its dielectric properties cannot be assumed homogeneous for extended pavement sections and can significantly vary within the relatively short distance. Figure 44 displays the linear plot of AC layer thickness showing the distribution of asphalt thickness values calculated using 3D-Radar system, vs distance along the SR 20. 3D GPR survey provided similar level of thickness evaluation precision as previously performed conventional air-launched investigation.

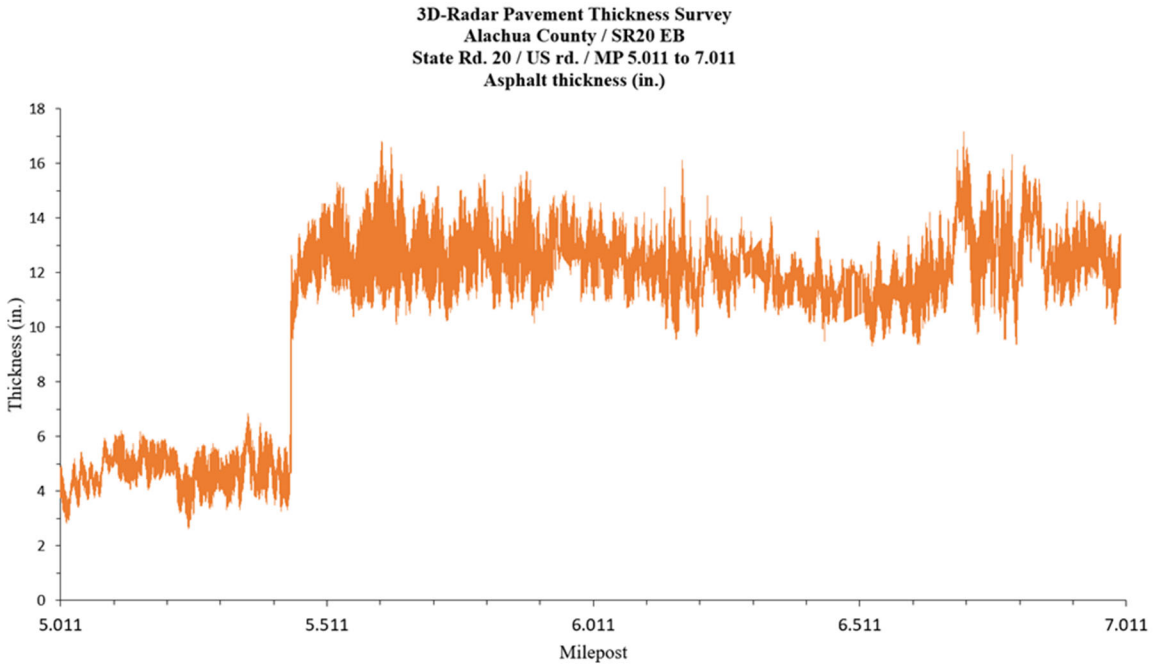

Figure 44: Plot showing the distribution of asphalt thickness values (vertical axis) measured using 3D-Radar system vs distance along the SR 20. (horizontal axis).

Site 1.8: SR 5 (US-1) – Project # 436168-1-32-01 & 436169-1-32-01 Roadway ID #: 78010000; (MP 16.120 – MP 18.692), St. Johns County – Distress and voids detection

The 3D-Radar survey was carried out on February 15, 2017, between 9 and 10 AM. Four lines of data were collected, two each in the northbound and southbound low-speed lanes. The northern limit was W. Castillo Drive (MP 14.425) and the southern limit was the south joint of the bridge over the San Sebastian River (MP 16.815). The goals of carrying out the 3D GPR survey haves been to confirm the findings of a previous extensive low-speed survey and reveal any construction information that was not previously reported. Figure 45 and Figure 46 show the pavement cross section in the northbound and southbound directions as it shown in the 3D-Radar data samples. The predominant pavement construction in the

survey area (other than the bridge deck) appears to be Jointed Plain Concrete pavement (JCPC – see Figure 47), however, the figures show that the pavement composition tend to vary considerably in the northbound and southbound directions in the region where the piles are known to exist. In the northbound section (Figure 45), the segment in the pile area appears to be continuously reinforced (CRCP), with transverse rebar at approximately 6 feet spacing (Figure 48). Note that the southbound profile of Figure 46 shows substantial settlement of the concrete pavement, with asphalt fill having been placed to maintain the horizontal grade of the roadway. Note also that the portion of the southbound roadway that has subsided includes both CRCP and plain concrete pavement with no apparent joints (PCP). It appears likely that the CRCP construction is present to transfer the vehicle loads to the piles. The 3D-Radar survey data has revealed the essential features of the pavement construction, particularly in the pile-supported area. There is no clear evidence of voids or "loose" soil anomalies under the concrete, as mentioned in the EGS report described in Section 3. It is possible that the voids detected in the EGS survey were outside of the range covered by the 3D-Radar survey. The timber piles were not directly observed in the 3D-Radar data. The 3D GPR survey revealed considerable detail regarding the pavement substructure condition. Note that the 3D-Radar survey took one hour to complete and required no lane closures. This is a significant reduction in the time and cost that was associated with the traditional GPR survey approach used by EGS. Also, the nature of the 3D-Radar presentation in Examiner has made pavement features appear clearer during analysis.

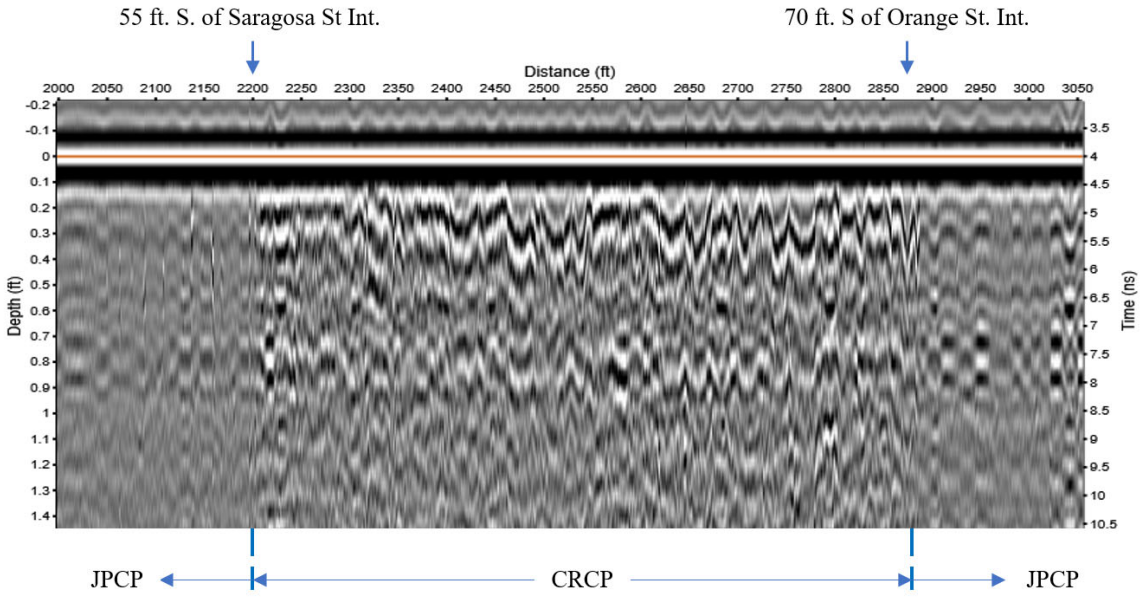

Figure 45: 3D-Radar data cross-section, northbound driving lane, right side.

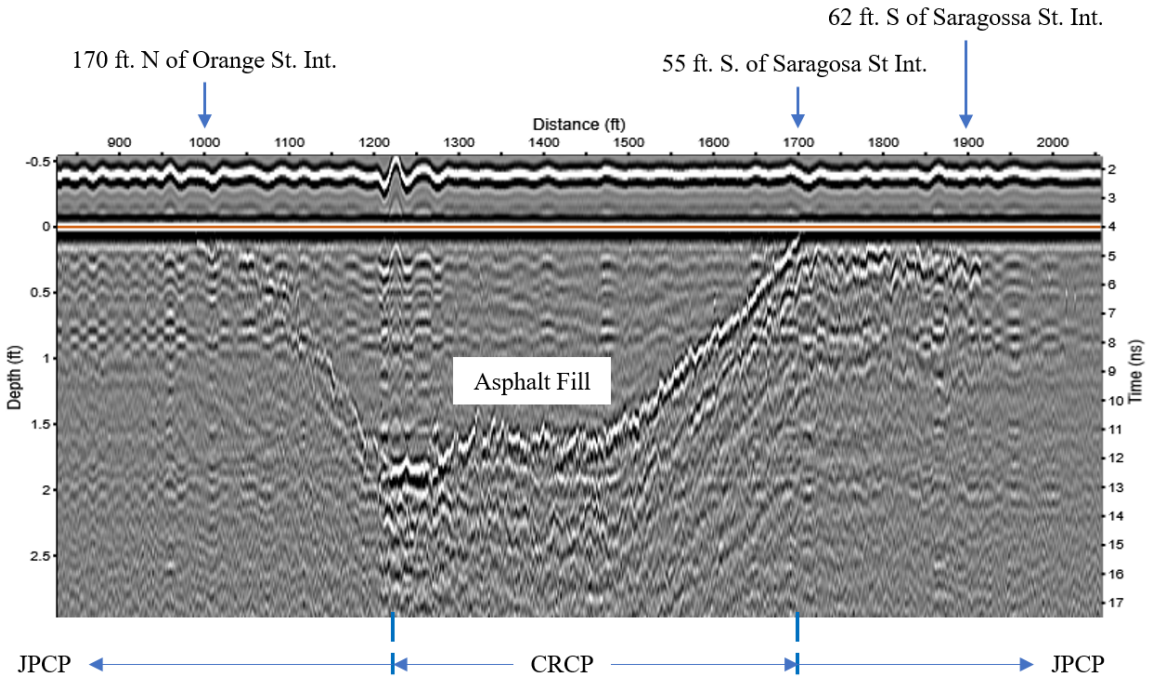

Figure 46: 3D-Radar data cross-section, southbound driving lane, right side.

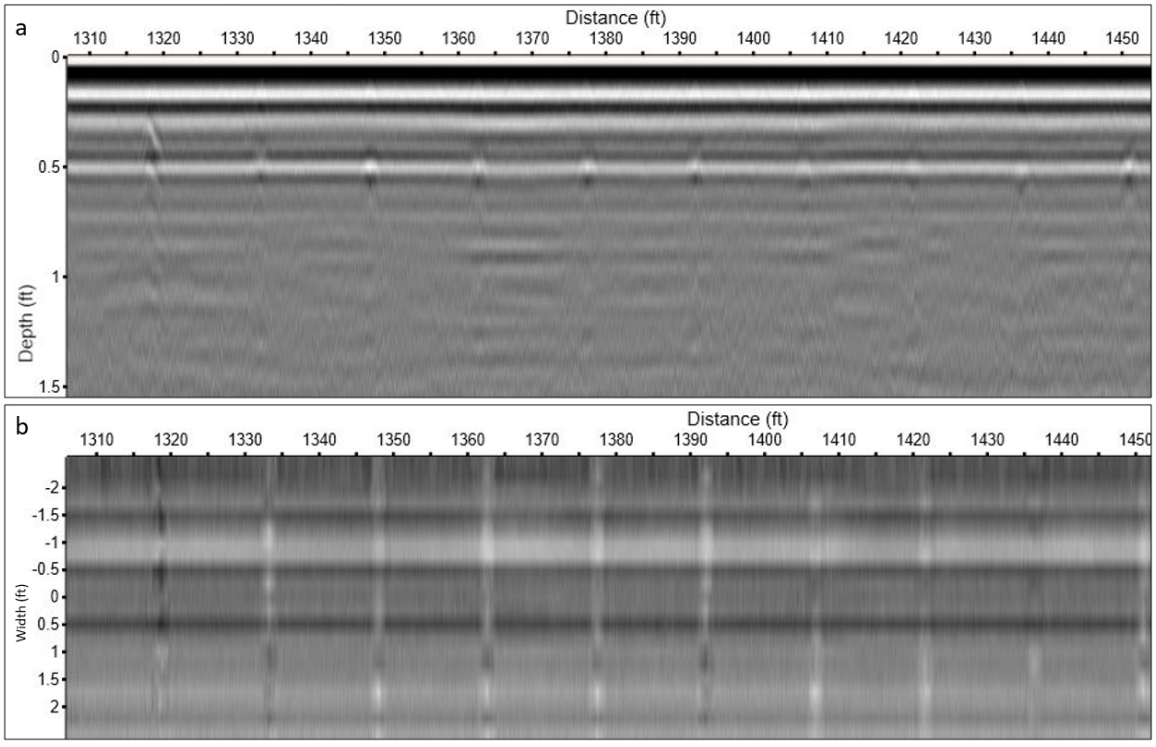

Figure 47: Typical GPR image from SR 5 tested section showing regularly spaced joints reflections on B-scan (a) and C-scan (b) from the depth of 6 inches.

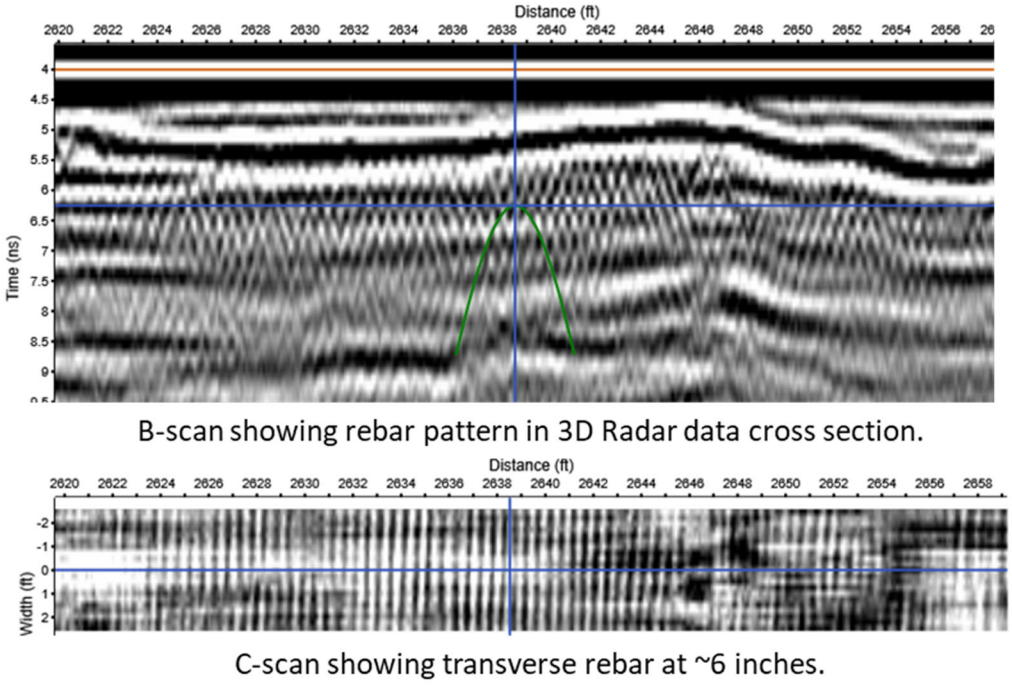

Figure 48: Example of 3D-Radar data collected over the northbound lane, showing details of CRCP construction.

Site 1.9: SR 18 – Project # 207973-2-52-01; Roadway ID #: 28040000; (MP 3.464 – MP 3.596), Bradford County – Evaluation of Pavement Distress

3D-Radar data were collected on February 16, 2017 in the eastbound direction between MP 3.04 and MP 3.80. Two lines of data were collected, one each in the right and left sides of the eastbound lane. Figure 49 and Figure 50 show the cross-sections of 3D-Radar data. The upper asphalt layers and the SBRM layer as described above. Worth of note is the variation of amplitude at the boundary between the asphalt and the SBRM. This variation could be an indication of accumulation of moisture as suggested in the SMO study.

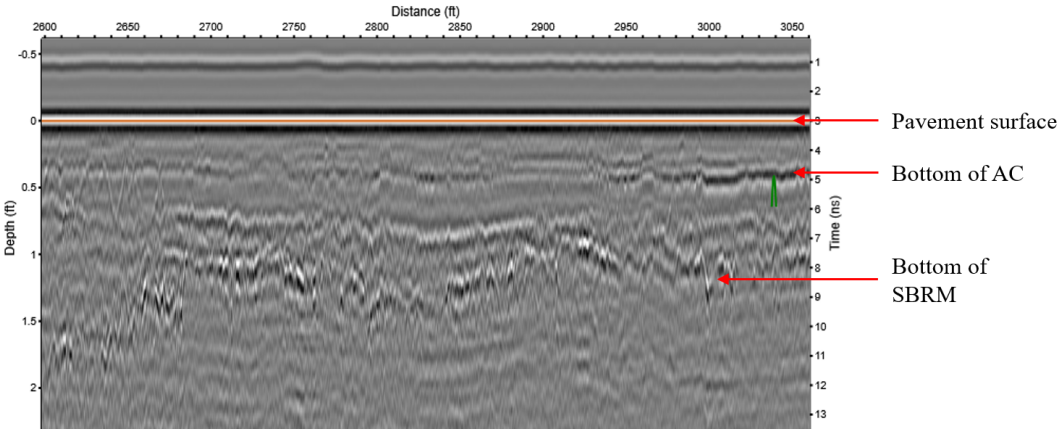

Figure 49: Example of 3D-Radar data section through the distressed area. Left side, eastbound.

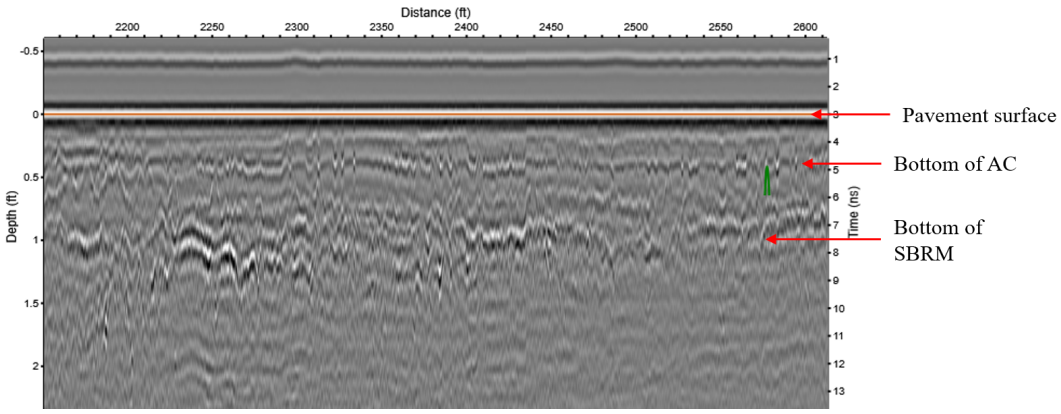

Figure 50: Another example of 3D-Radar data section through the distressed area. Right side, eastbound.

Figure 51 shows a depth slice through the section at a depth of approximately 5 inches, directly below the bottom of the AC. 3D GPR survey showed considerable amplitude variations observed in the "distress" area, much more so than in the "control" area. This observation supports the theory that moisture infiltration into this boundary is contributing to the pavement distress.

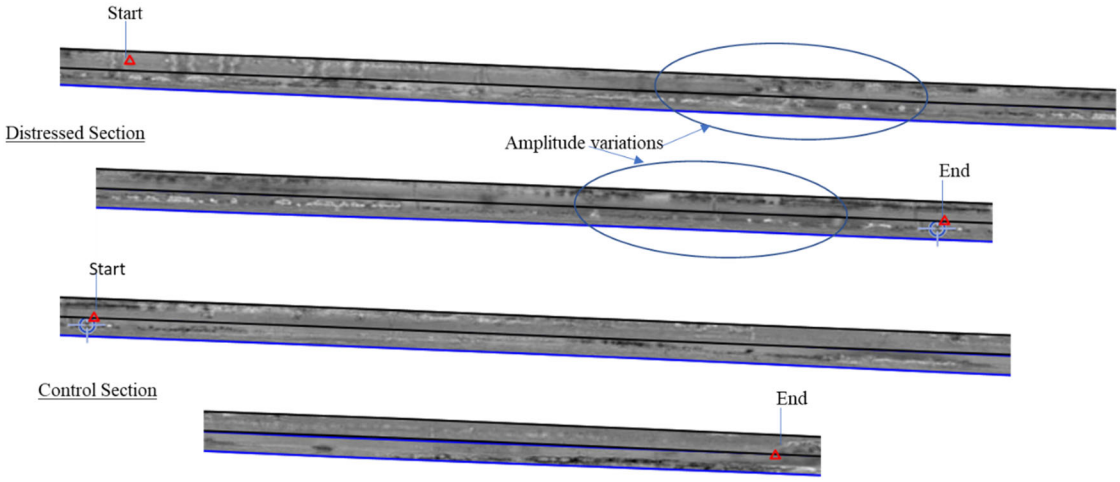

Figure 51: Reflection at the bottom of the AC layer at a depth of 4.8 inches.

Site 1.10: SR 100 – Project 213940-1-52-01; Roadway ID #: 76110000; (~MP 7.800), Putnam County – Monitoring of piles

The objective of carrying out the 3D-Radar survey was to see if any details of the pavement structure can be revealed which explain the observed strength reduction. The survey was carried out on February 15, 2017 between Sipprell Road (MP 6.791) and Indian Lakes Forest Rd., (MP 8.287). Four lines of data were collected – two in the eastbound lane (right and left sides) and similarly two in the westbound lane. As a result, section of the SR 100 with installed piles can be easily delineated on the processed GPR data. The section is approximately 3720-ft. long. Figure 52 and Figure 53 show a depth slice through the section at a depth of approximately 5.7 inches. The beginning and the end of the test area with installed Soil

Stabilization Columns (SSC) can be clearly recognized on the 3D-Radar data. Figure 54 displays the layout of the tested section of SR 100 [4].

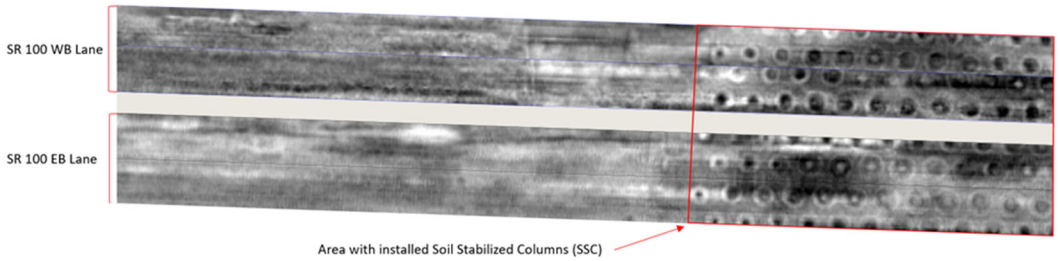

Figure 52: SR 100 eastbound and westbound reflections at the top of the area with installed SSC grid. Beginning of the test area.

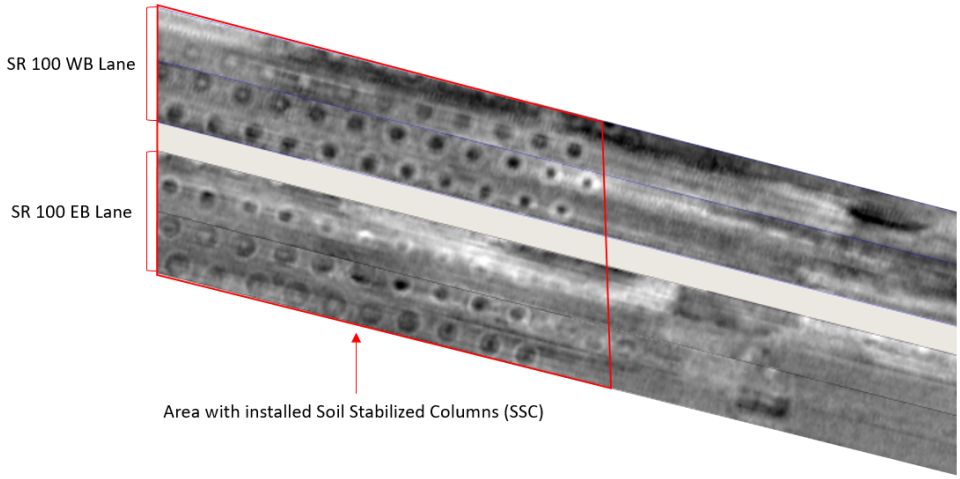

Figure 53: SR 100 eastbound and westbound reflections at the top of the area with installed SSC grid. End of the test area.

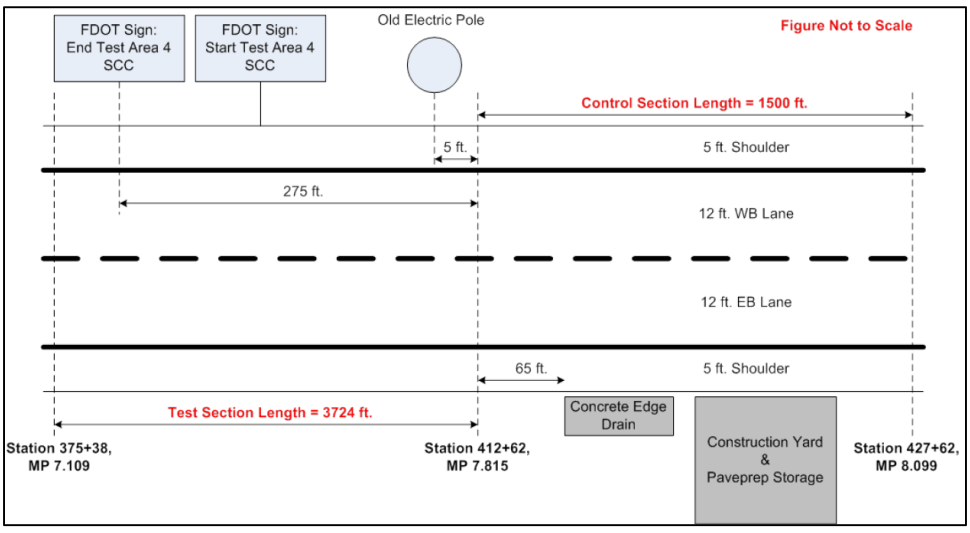

Figure 54: Section layout of tested area of SR 100 in Putnam County [4].

Figure 55 displays the B-scan with corresponding C-scan obtained from depth of 5.9 inches. (55b). Hyperbolic reflections associated with SSC can be clearly seen starting from 6275 ft. mark. An isolated area with approximate length of 30 ft. with no piles installed was noted on the eastbound lane. Figure 56 and Figure 57 display the feature associated with a gap within the SSC grid pattern. Anomaly of similar character was noticed on the left side of eastbound lane.

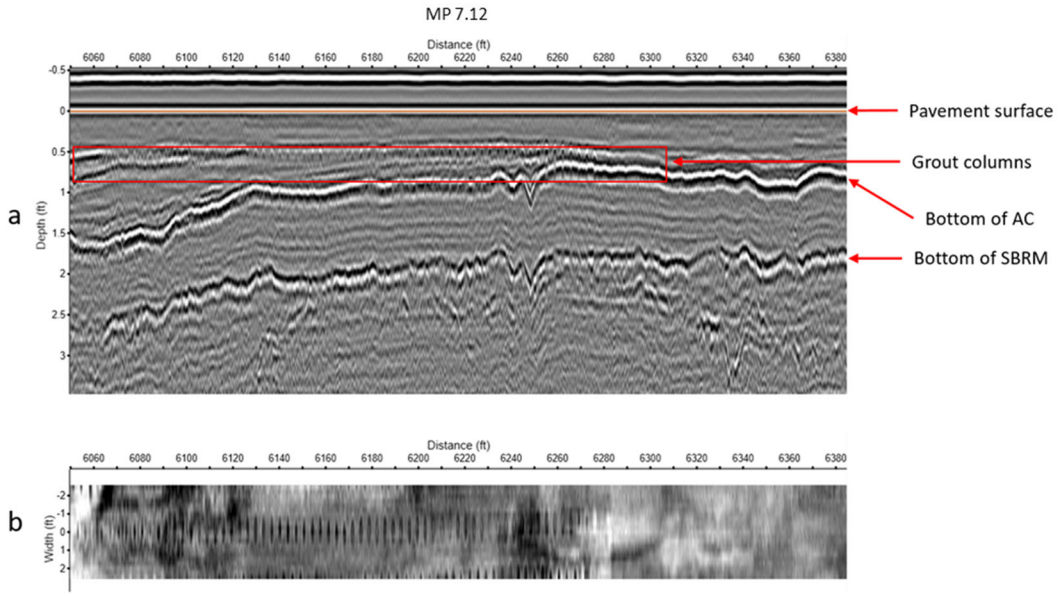

Figure 55: Example of 3D-Radar data cross-section collected over the through the area with installed grout columns.

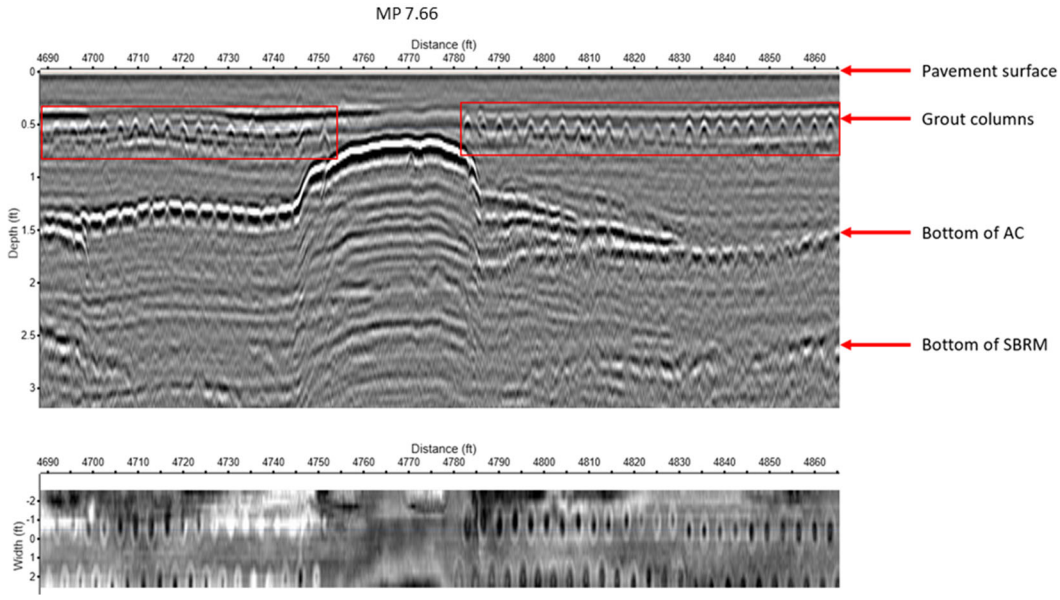

Figure 56: Another example of 3D-Radar data cross-section collected over the through the area with installed grout columns.

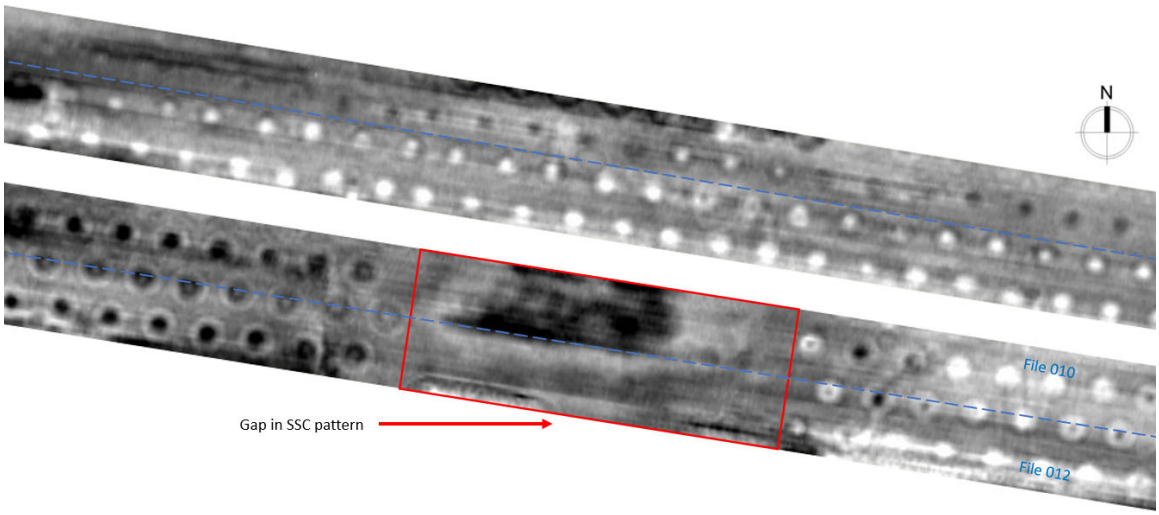

Figure 57: SR 100, westbound lane (top) and eastbound lane (bottom) reflections, showing the gap in SSC grid pattern.

The precise location and layout of individual piles can be obtained as it shown in Figure 58 showing the GPR section at the depth of 5.15 inches. Location and disposition of piles (~3 ft. lateral and ~3.5 ft. transverse spacing according to the 3D-Radar data) can be clearly seen along with their approximate dimensions (11 – 12.5 inches in diameter according to the 3D-Radar data).

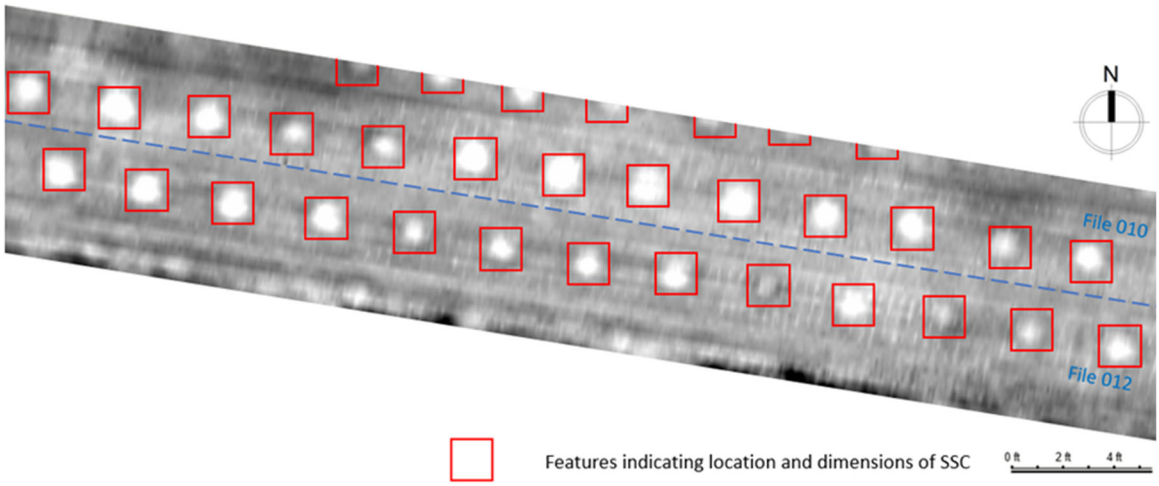

Figure 58: SR 100, eastbound lane. Reflection, showing the pattern of installed SSC arrangement.

Figure 59 shows the grid pattern of installed SSC [4]. It should be noted that final design of SSC grid employed the 3 X 3.5 ft. pattern [5].

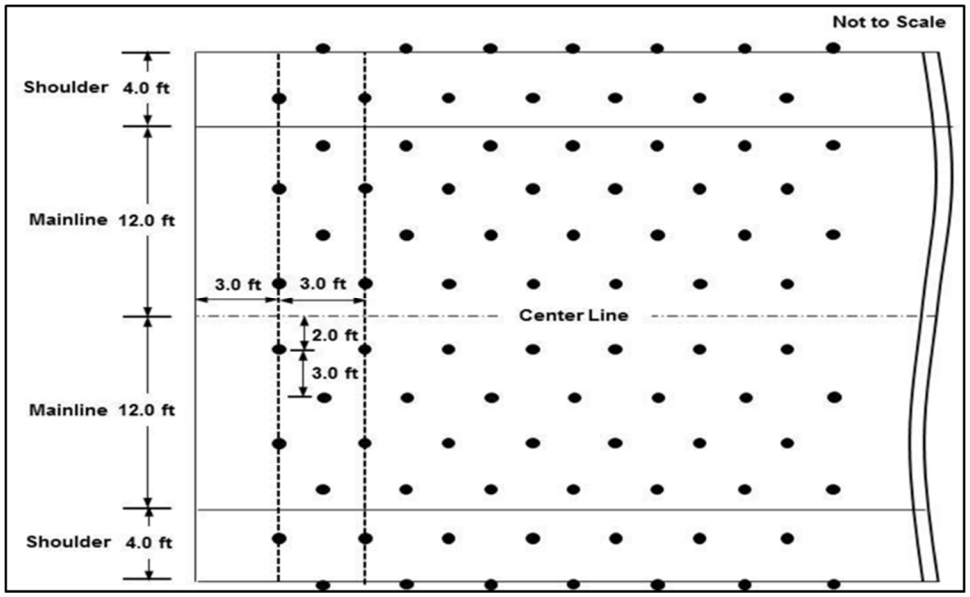

Figure 59: Schematic of piles arrangement pattern [4].

According to the report [4], the AC thickness varies from 8 to 14.5 inches in the test area and from 7 to 13.9 inches in the control area, while on GPR data, the AC thickness fluctuates from 9.6 to 19.2 inches in the test area and from 4.8 to 11 inches in the control area (The dielectric permittivity of 5 was used for time to depth conversion). Figure 60 displays the extended GPR cross-section through the right side of the westbound lane showing the area where the settlement possibly occurs. The AC layers' thickness as well as the depth to the bottom of SBRM vary significantly in along the GPR image. Multiple asphalt layers can be seen on the 3D-Radar data. 3D GPR survey results have shown the extent, spacing, and size of SSC piles. The extent of subsidence and its exact location can be observed and evaluated with high precision.

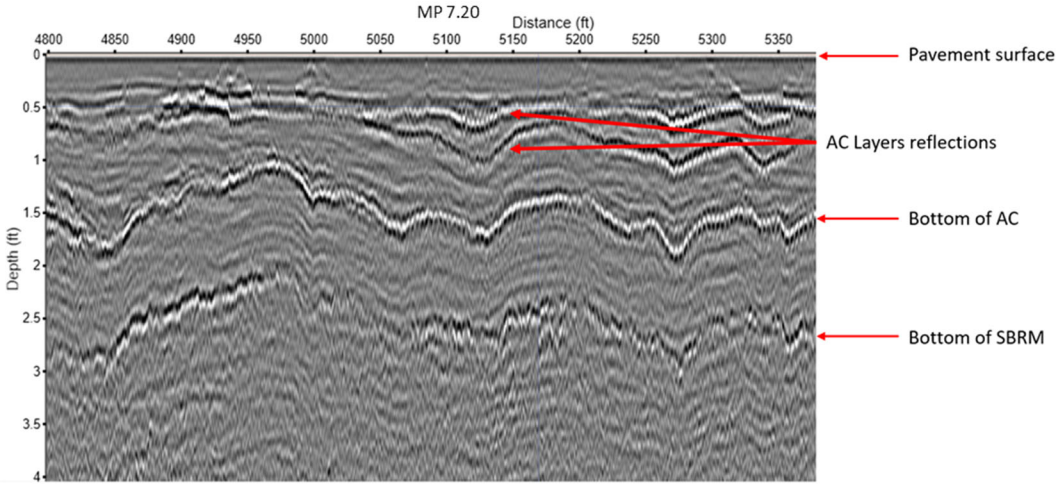

Figure 60: Example of 3D-Radar data cross-section through the area with observed signs of possible settlement development. Right side, eastbound lane.

Site 1.11: Pablo Creek Bridge – (Bridge# 720509) – SR 202 Roadway ID #: 72292000; (~MP 10.358 – MP 11.228), Duval County – Condition, cover

The 3D-Radar survey was carried out on February 16, 2017 between 11:00 and 12:30 AM. Ten lines of data were collected, five each in the westbound and eastbound lanes. The 3D-Radar system was used to comparatively evaluate the concrete cover. Rebar reflections appear as a layer in the 3D-Radar data as it is illustrated in Figure 61:

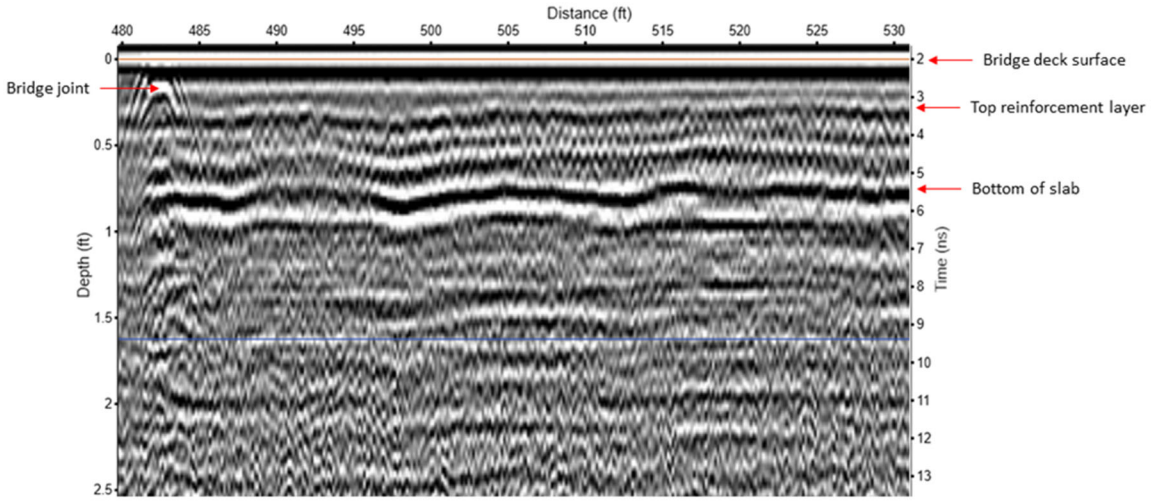

Figure 61: GPR cross-section showing the identified rebar layer. Left side, eastbound lane.

Using dedicated software (Examiner), x- and y-coordinates from each hyperbolic maximum were matched with a measure of two-way travel time of electromagnetic waves propagation to calculate a depth of rebar cover. A dielectric permittivity of 6 was used to convert reflection times to reflector depths. This value had to be assumed since Examiner does not currently have the capability to directly measure dielectric constant for each channel. Figure 62 displays the enlarged area of GPR cross-section through the stitched file (covers the eastbound lane) showing the area with traced reinforcement reflector. The 3D-Radar system demonstrated the ability to identify areas of variable concrete cover thickness. Figure 63 shows the contour map of the concrete cover depths to the rebar, generated from the 3D-Radar data (top) compared to the results obtained with FDOT system (bottom). The distribution of cover depth values over the bridge deck surface demonstrated reasonably good correlation for air-launched and 3D-Radar data sets. The discrepancies in spatial distribution and degree of concrete cover observed between the air-launched and 3D-Radar GPR interpretations can be explained by several factors including different GPR systems employed, and differences in tracking of the rebar layer. 3D GPR data were used to generate a contour plot of rebar depth, which is generally agrees with the FDOT results, generated using 2 GHz horns, with some minor discrepancies.

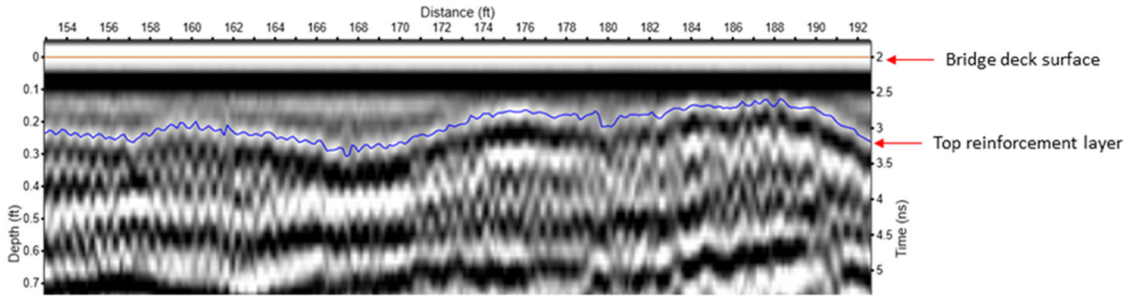

Figure 62: Example of 3D-Radar data cross-section showing the identified rebar layer (blue line).

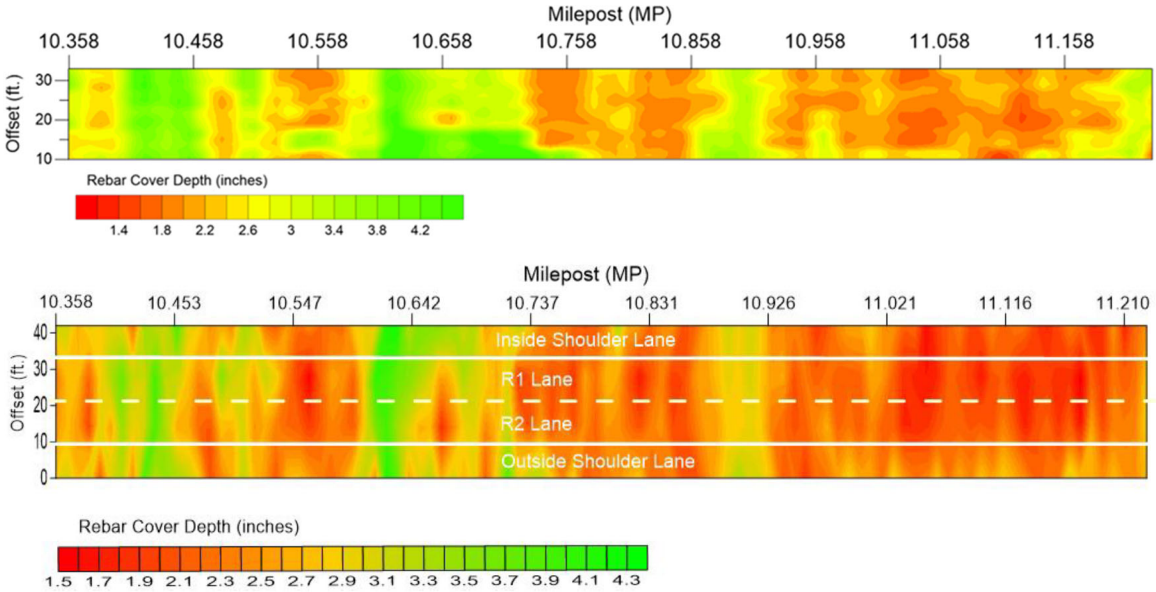

Figure 63: Contour map showing concrete cover depth to rebar, generated from 3D-Radar survey data (top); contour map showing concrete cover depth to rebar, generated from 2 GHz air-launched GPR data (bottom). Not to scale - axis were adjusted for better data representation.

Site 1.12: Waldo Road (SR 24) – Roadway ID #: 26050000; (~MP 4.150 – MP 5.733), Alachua County – detection objective – voids over culverts

The objective of the 3D Radar survey was to see if the system could replicate the findings of the FDOT 400 MHz survey in a quicker and more efficient way. The 3D-Radar survey was carried out on February 14 and February 15, 2017. Three lines of data were collected, covering the whole width of the right side of the southbound lane. A dielectric permittivity of 5 was used to convert reflection times to reflector depths. GPR cross sections that are shown in Figure 64, show two segments of GPR data collected on the first test location [8] using ground-coupled GPR unit equipped with 400 MHz antenna (top) and 3D-Radar system (b). Blue frames represent features identified as potential shifting soils. Figure 65 displays two segments of GPR data collected on the second test location [8] using ground-coupled GPR unit equipped with 400 MHz antenna (top) and 3D-Radar system (bottom). Blue frames represent features identified as potential shifting soils; red frames represent features which were not noticed on 3D-Radar data in proximity of the second test location. Figure 66 displays two segments of GPR data collected on the third test location [8] using ground-coupled GPR unit equipped with 400 MHz antenna (top) and 3D-Radar system (bottom).

Blue frames represent features identified as potential shifting soils; green frames indicate features that were detected on both 3D-Radar and ground-coupled GPR unit data; orange frames represent features that were noticed on 3D-Radar data only; red frames represent features which were not noticed on 3D-Radar data in proximity of the third test location.

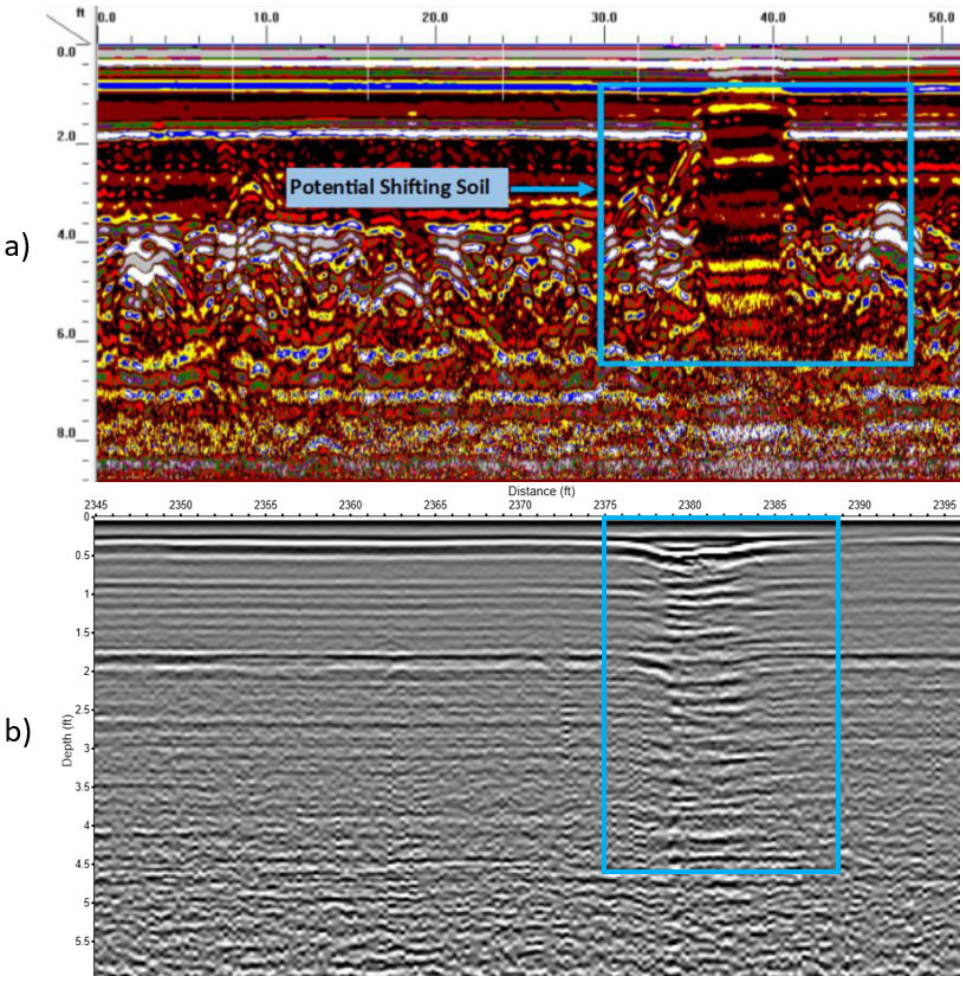

Figure 64: Segment of the 400 MHz GPR data showing reflections associated with shifting soil (a); segment of 3D-Radar data collected in proximity to the first test location displaying similar features (b).

Figure 67 displays two segments of GPR data collected on fourth test location [8] using ground-coupled GPR unit equipped with 400 MHz antenna (4a) and 3D-Radar system (4b). Blue frames represent features identified as potential shifting soils; orange frames represent features that were noticed on 3D-Radar data only. 3D-Radar data reveals more distinct features as it can be seen in Figure 67 (bottom). The reflection pattern that can be associated with metal plate (green frame) is approximately 5 ft.-long on the 3D-Radar data; even though it doesn't exhibit typical ringing effect on 3D-Radar data, the corresponding area of subjacent interface reflection is absent (marked with purple frame). The 3D-Radar survey revealed some subsidence related conditions, but not as thorough as 400 MHz ground coupled GPR.

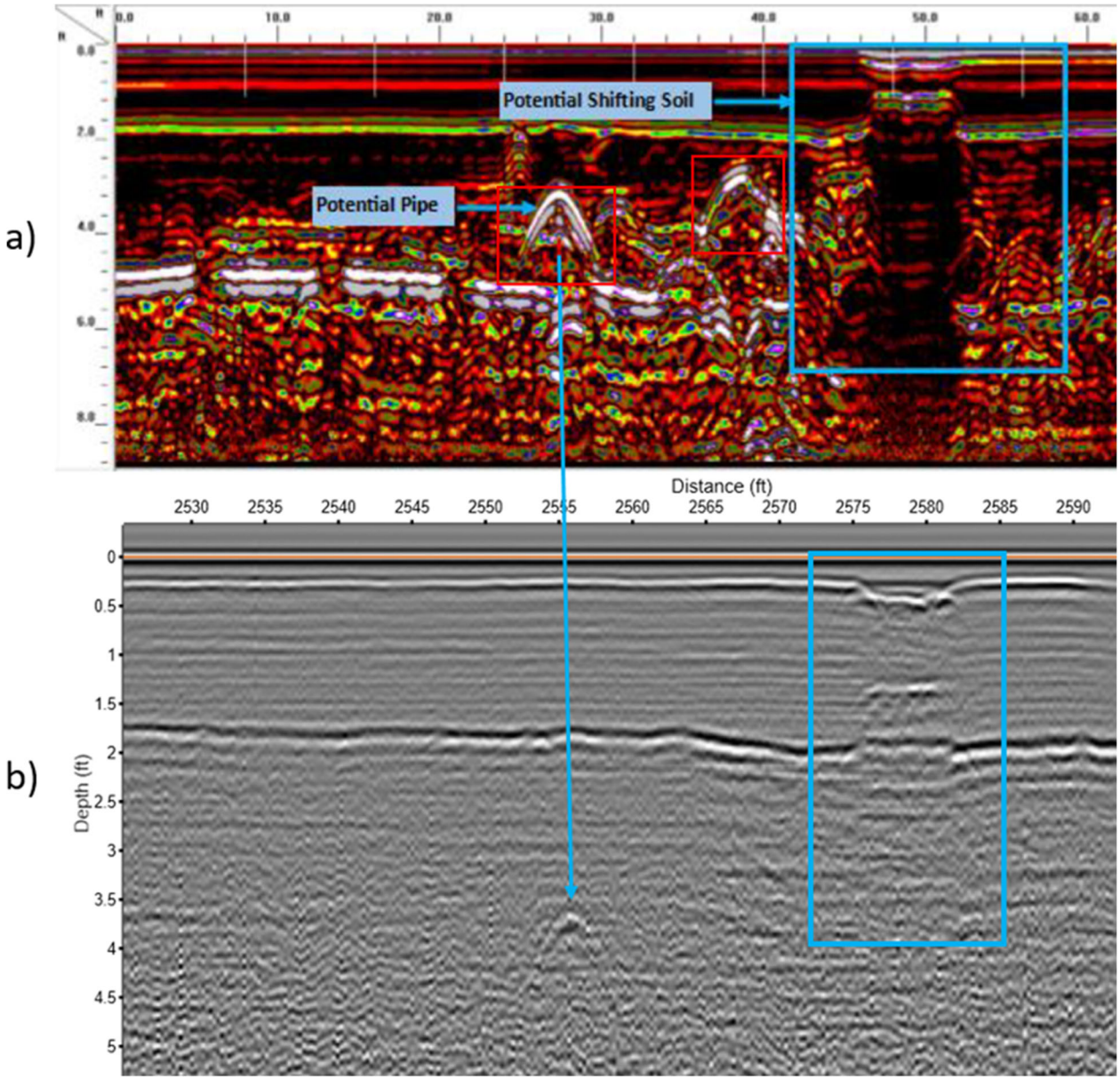

Figure 65: Segment of the 400 MHz GPR data showing reflections that can be associated with pipe and shifting soil (a); segment of 3D-Radar data collected in proximity to the second test location displaying similar features (b).

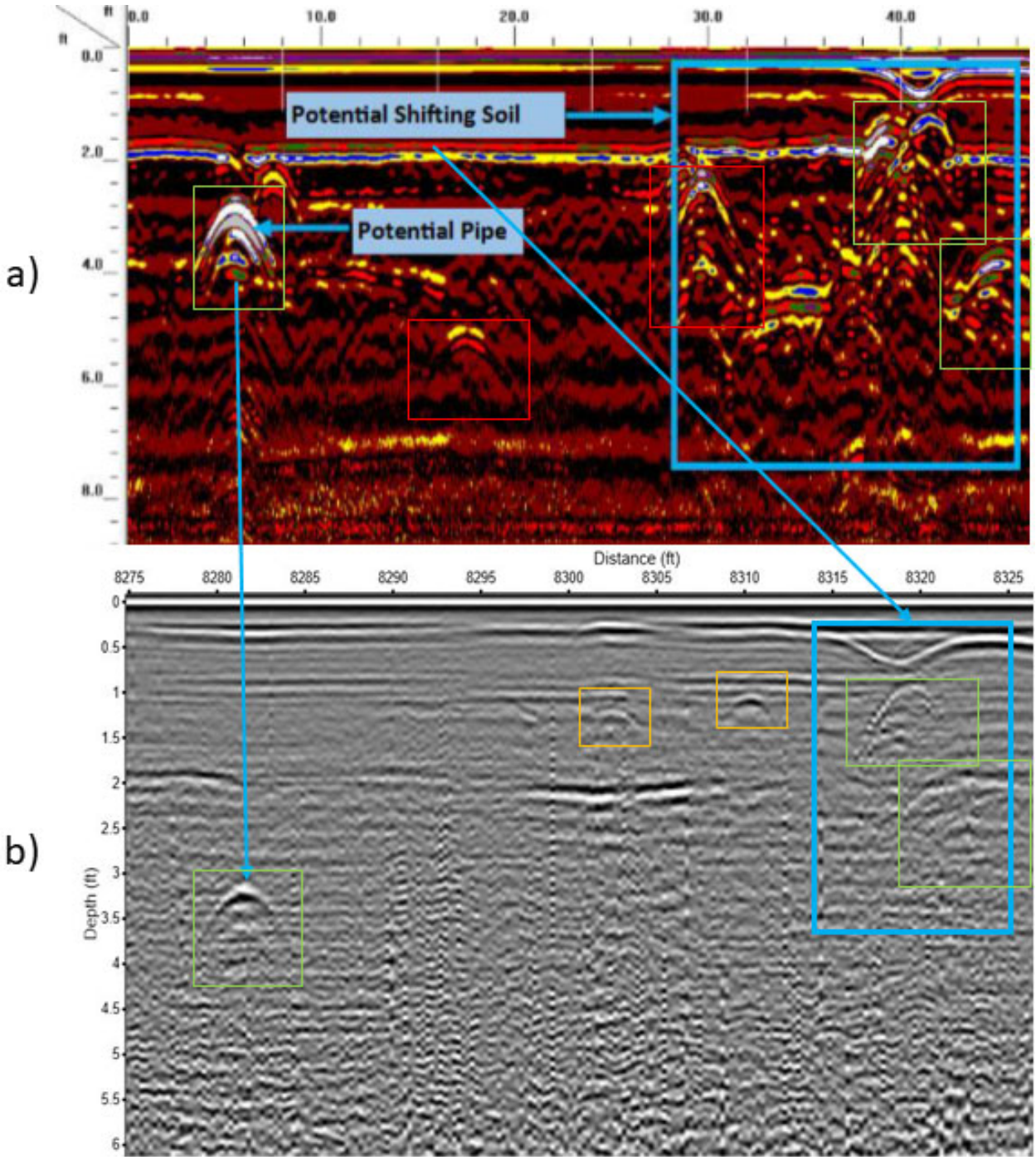

Figure 66: Segment of the 400 MHz GPR data showing reflections associated with potential pipe and shifting soil (a); segment of 3D-Radar data in proximity of the third test location displaying similar features (b).

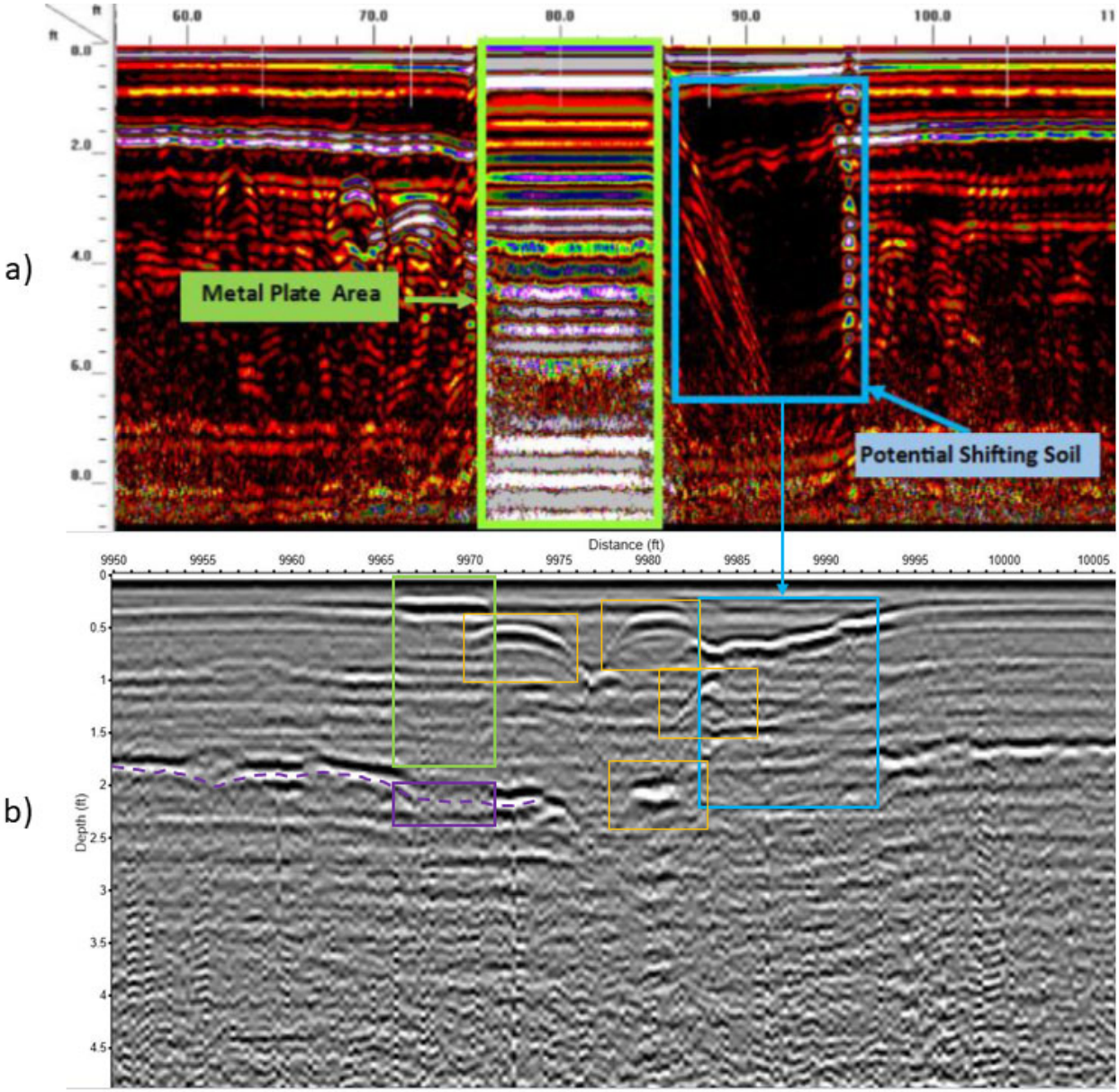

Figure 67: Segment of the 400 MHz GPR data showing reflections associated with potential pipe and shifting soil (a); segment of 3D-Radar data in proximity of the fourth test location displaying similar features (b).

Sites 2.1 and 2.2: SR 22 – Project # 41641-1-52-01 / Roadway ID #: 51030000; (MP 5.418 – MP 12.136) and Gulf County and SR 77 – Project # 424625-1-52-01 / Roadway ID #: 61080000; (MP 26.217 – MP 29.826), Washington County

Site 1, SR 22, Gulf County, Asphalt Roadway Section. Four lines of data were collected, two each in the westbound and eastbound lanes. The goal of carrying out the 3D-Radar survey has been to see if data collected with 3D-Radar system can be used to non-destructively identify the locations and extent of stripping, delamination, and "road worms" phenomena. Reported limits of observed roadway worms damage includes the SR 22 pavement section from MP 7.609 to MP 8.886. Core samples were acquired at

five locations (MP 7.6091, MP 7.7485, MP 8.7899, MP 8.8551, MP 8.8858). Figure 68 shows the condition of pavement section in proximity of MP 7.6091. Figure 69 shows photographs of core samples. The photographs reveal intensive cracking on specimen labeled 1A and 2A; porous nature of the cores can be observed as well. Figure 70 shows a full-depth vertical slice of 3D-Radar data, collected in westbound lane, near MP 7.6. Figure 70b shows a corresponding horizontal slice of 3D-Radar data at approximate depth of 4.2 inches (converted from two-way travel time with dielectric of 5).

Figure 68: Photographs of pavement distress in proximity of core extraction point (MP 7.6091): a view of the lane (top) and signs of the distress on the pavement surface (bottom).

Figure 69: Core samples extracted over the Site 1 (Gulf County, SR 22) Pavement section.

Figure 71 displays the example of Reflection Activity mode of ExploreGPR software showing the segment of 3D-Radar data collected in proximity of MP7.6. Figure 71a shows the b-scan and Figure 71b shows, with color-coded amplitude, the spatial distribution of reflection activity patterns over the specified depth interval shown by the opaque orange shape overlaid on the B-Scan axes.

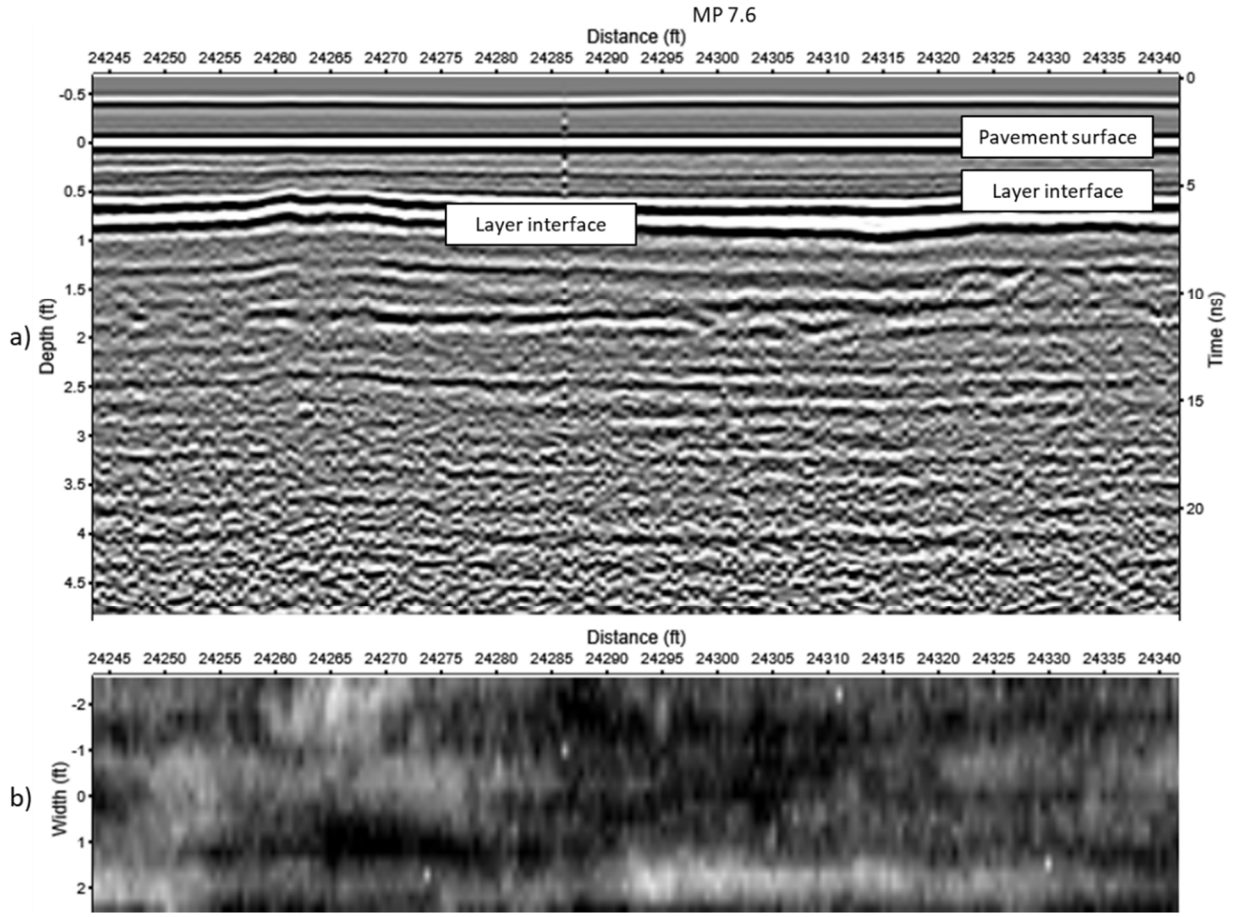

Figure 70: Vertical (a) and horizontal (b) slices of 3D-Radar data in proximity of MP 7.6, SR 22 westbound, right lane. Depth is converted from two-way travel time with dielectric of 5. Horizontal slice (b) was taken from the depth of 4.2 inches.

Activity is defined as the average of the sum of the GPR amplitudes at every point of the GPR scan within the analysis window. The upper boundary of the window is indicated by a blue line at the top of the orange patch, while the lower boundary of the window is indicated by a green line at the bottom of the orange patch. The analysis was carried out on the depth interval defined by the upper limit of 3.5 ns (to exclude the strong surface reflection obtained at 3 ns from analysis) and by a 0.48 ns offset from the traced asphalt layer on the bottom. Interface dip in the right part of the Figure 71 associated with located trench with approximate length of 15 feet.

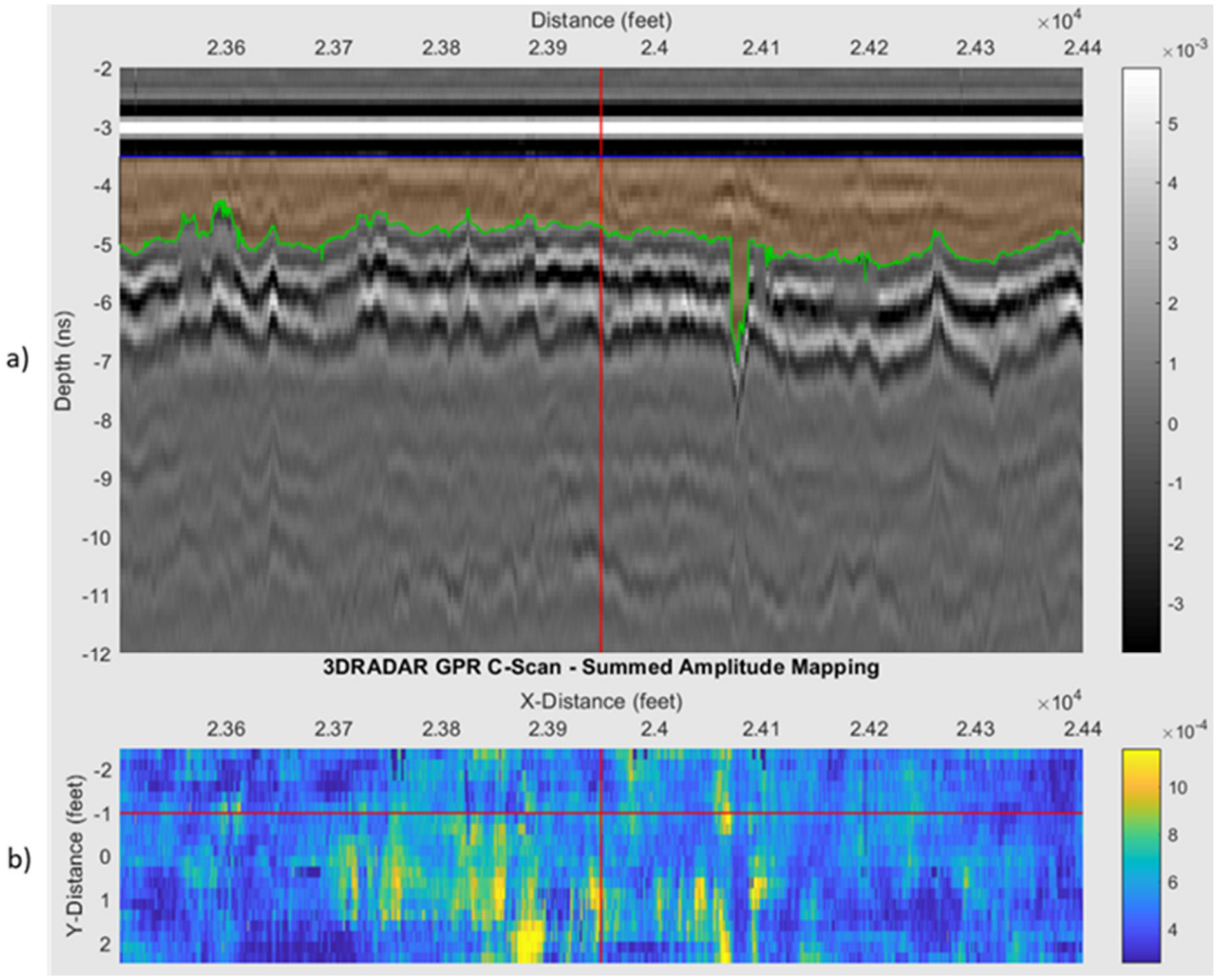

Figure 71: ExploreGPR interface showing the activity analysis performed on interval limited by 3.5 ns on top and offset of 0.48 ns on top of the traced layer interface on the bottom: a) is the b-scan; b) is a color-coded reflection activity plot for the window specified in a).

Figure 72 shows the spatial distribution of increased reflection activity within the AC layer covering the SR 22 from MP 7.59 to MP 7.76 in the westbound direction, right driving lane. The map was generated from the ExploreGPR output table using a thresholded Surfer contour plot. Shades of salmon color represent the anomalous reflection activity presented within the selected depth interval. The output data was normalized to a mean of 1.0, and a threshold of 1.5 was used to highlight significant reflection activity. Two parallel 3D-Radar profiles in proximity to the core extraction points have been stitched together with Examiner to enable analysis of the full width of the road lane. Figure 73 displays the Reflection Activity mode of ExploreGPR software showing the stitched section of 3D-Radar data, covering the SR 22 from MP 7.535 to MP 7.913. The analysis was carried out on the depth interval defined by the upper limit of 3.5 ns (0.5 ns. down from the surface) and by a 0.48 ns offset from the traced asphalt layer on the bottom. Figure 73a demonstrates the reflection analysis performed on the specified depth interval, Figure 73b is a spatial distribution of reflection activity patterns over the specified depth interval selected by the opaque orange shape overlaid on the B-Scan axes. It should be mentioned that plotting software interpolates data, filling the gaps between the stitched profiles. Considering the rationale of the proposed analysis method, it does not affect the deliverables.

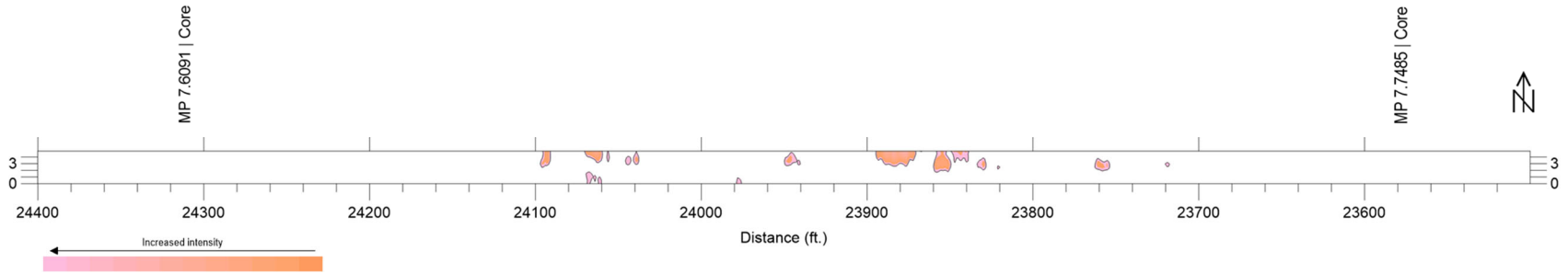

Figure 72: Reflection activity map covering core locations at MP 7.7485 and MP 7.6091. Westbound direction, right driving lane

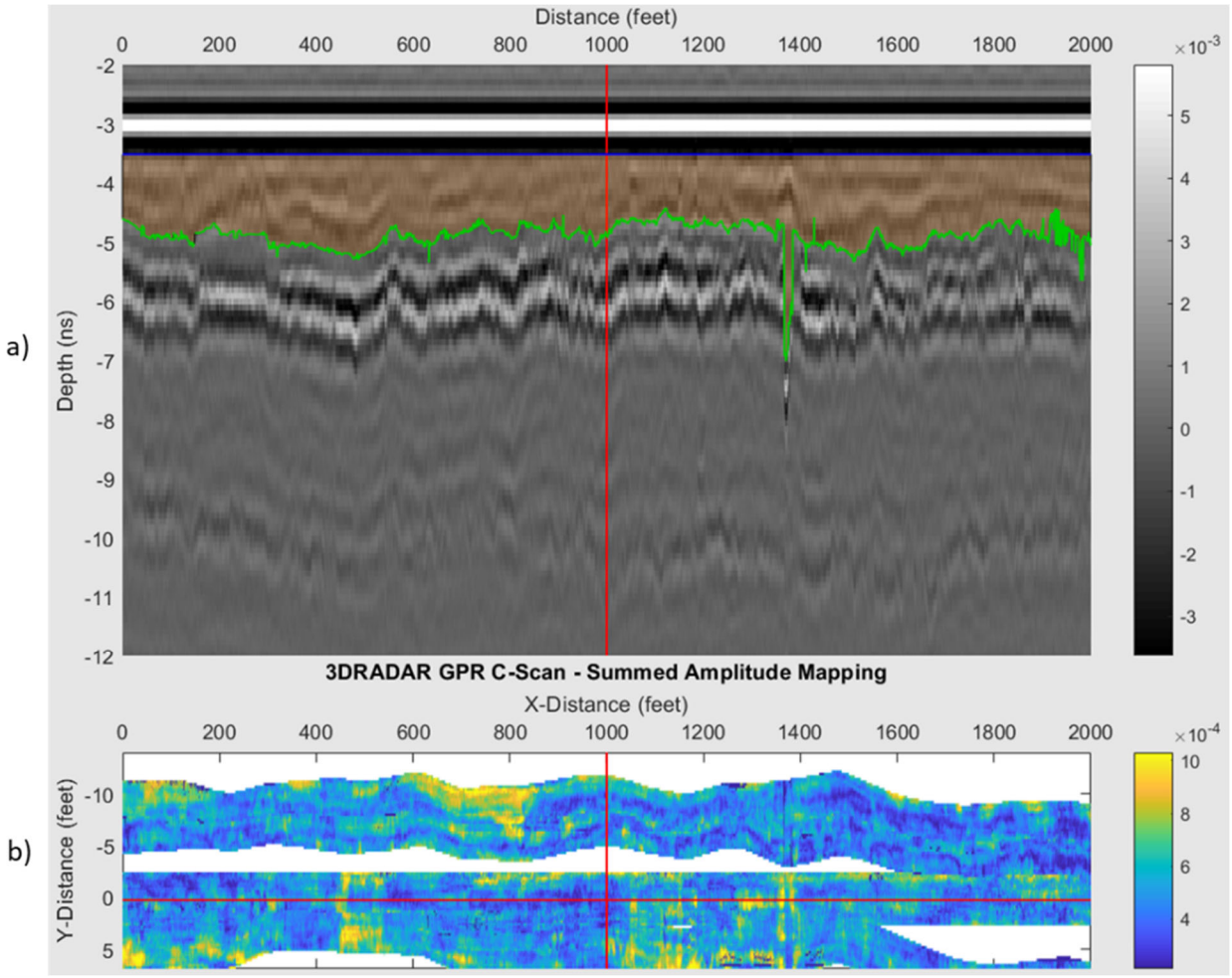

Figure 73: ExploreGPR interface showing the activity analysis performed on interval limited by 3.5 ns on top and offset of 0.48 ns on top of the traced layer interface on the bottom for stitched File: a) is the b-scan; b) is a color-coded reflection activity plot for the window specified in a).

Figure 74 shows the spatial distribution of increased reflection activity within the AC layer of the stitched section of 3D-Radar data covering the whole width of SR 22 from MP 7.535 to MP 7.913. Figure 75 shows the spatial distribution of increased reflection activity within the AC layer of the second stitched section of 3D-Radar data covering the whole width of SR 22 from MP 8.625 to MP 9. It should be noted that due to partial overlap of collected 3D-Radar profiles in proximity to the core extraction points, resulting plots have different roadway widths.

To test the ability of 3D-Radar to provide data that will allow to distinguish the area of pavement which is affected by road worms from the control section, comparative analysis of a control section outside the damage zone was performed. Figure 76 displays the Reflection Activity mode of ExploreGPR software showing the stitched section of 3D-Radar data covering the SR 22 from MP 5.96 to MP 6.34, and Figure 77 shows the corresponding plot of spatial distribution of increased reflection activity within the AC layer.

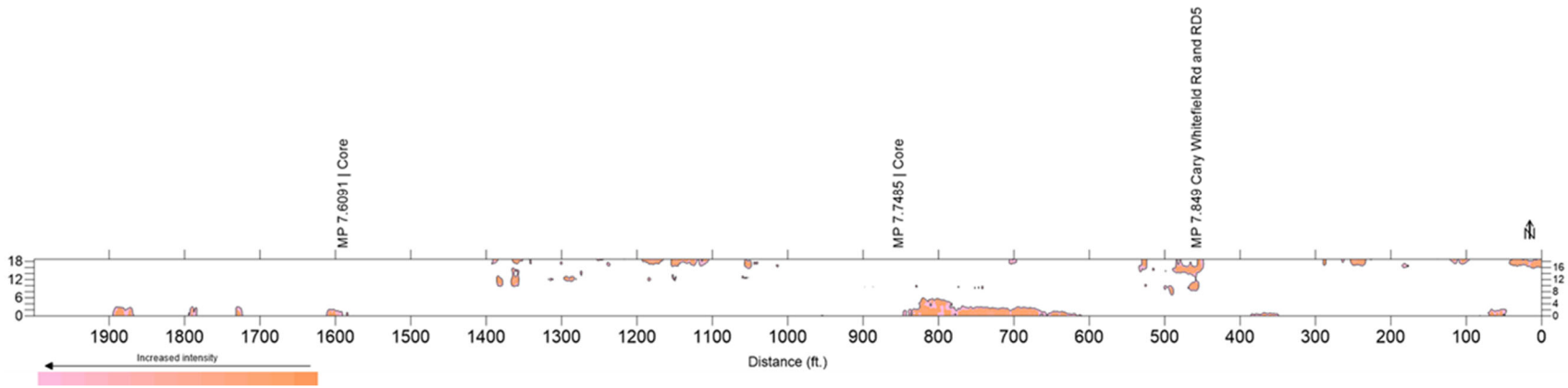

Figure 74: Reflection activity map of pavement section covering Core locations at MP 7.6091 and MP 7.7485.

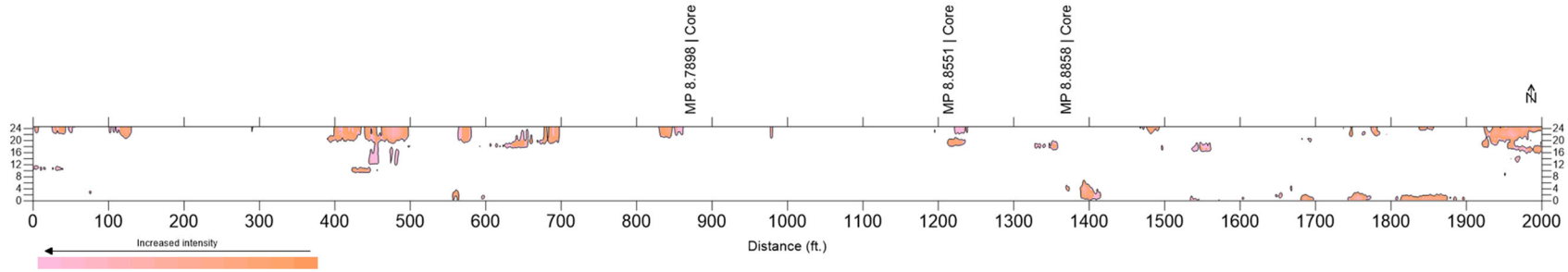

Figure 75: Reflection activity map of pavement section covering Core locations at MP 8.7898, MP 8.8551, and MP 8.8858.

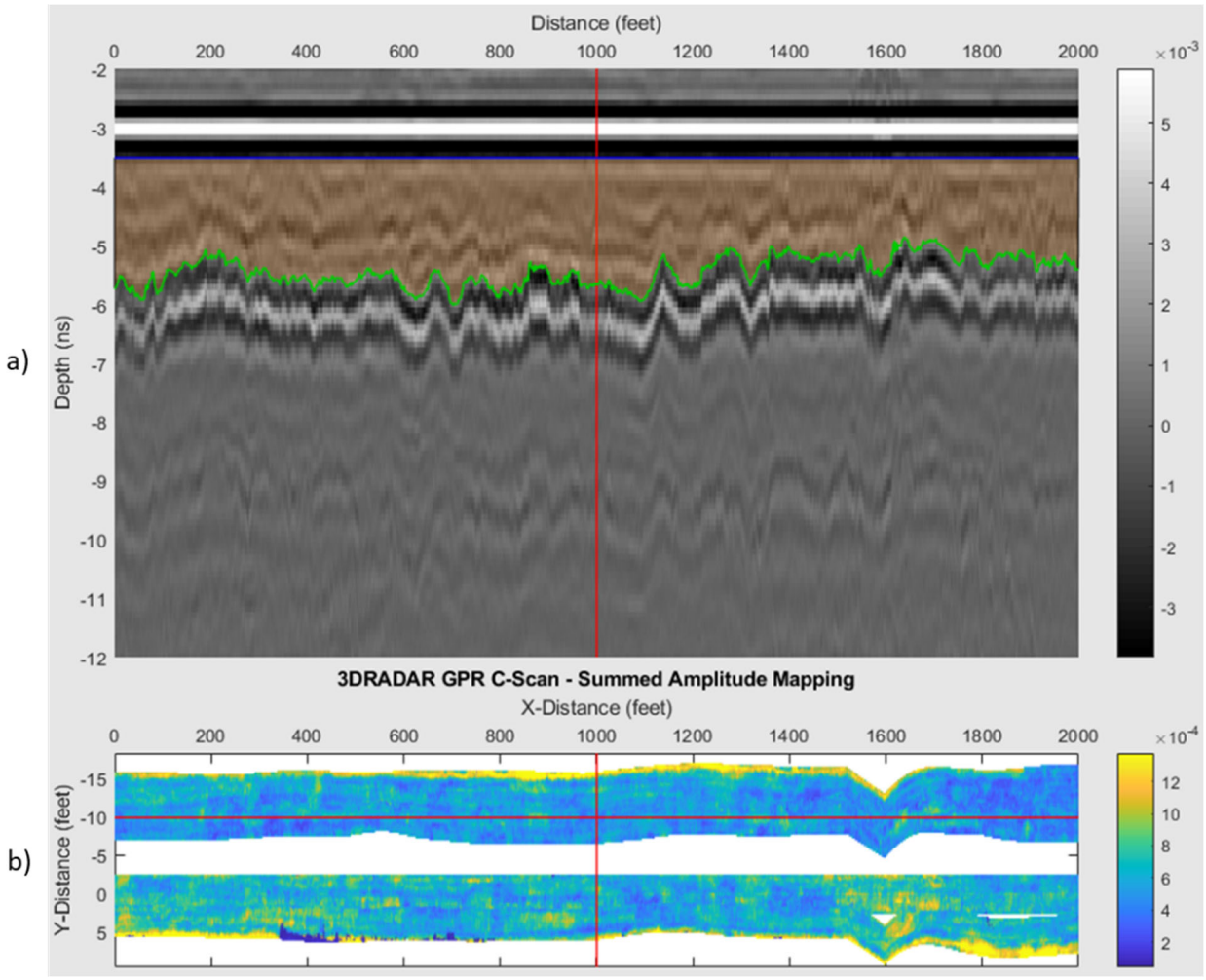

Figure 76: ExploreGPR interface showing the activity analysis performed on interval limited by 3.5 ns on top and offset of 0.48 ns on top of the traced layer interface on the bottom for SR 22 control section stitched File: a) is the b-scan; b) is a color-coded reflection activity plot for the window specified in a).

Patterns of increased reflection activity can be observed along the curbs and the turning lane. Resulting map represents the spatial distribution of reflection activity patterns within the isolated depth interval. This type of analysis examine data for deviations of dielectric properties of material and presence of internal reflectors at variable depths which are not normally seen within intact materials and can be indicative, but not limited to the indication of presence of "road worms" distress. Increased reflection activity can be considered as a precursor of developing deterioration and/or delamination, as well as appearance of thin asphalt layers in the upper part of the roadway. The 1.5 threshold (50% above the mean) used in this work is arbitrary, and modification can be made to reflect or eliminate precursor conditions.

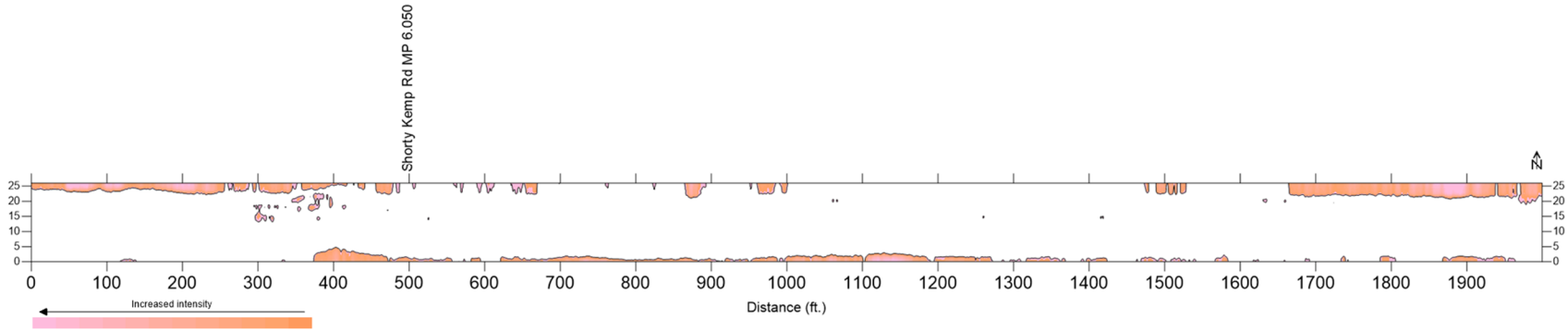

Figure 77: Reflection activity map of the control section covering the SR 22 from MP 5.96 to MP 6.34.

This is a 2 – lane rural highway with 5 feet shoulders running in the north and south direction near Chipley in Washington County. This roadway comprised of asphalt pavement. The roadway was reported to experience severe ride issues related to ripples. The roadway continues to deteriorate. The objective of this project is to investigate the cause of the premature failure with respect to the rippling.

2SR 77 – Project # 424625-1-52-01 / Roadway ID #: 61080000; (MP 26.217 – MP 29.826), Washington County. Four lines of data were collected, two each in the northbound and southbound lanes. The southern limit was MP 26.217 and the northern limit was MP 29.826 on SR 77 in Washington County. The goal of carrying out the 3D GPR survey has been to see if data collected with 3D-Radar system can be used to non-destructively identify the locations and extent of the observed "road worms" phenomena. No core samples were acquired at the test location. A series of photographs, showing the road worms damage, were taken at MP 28.438, MP 29.179, and MP 29.401. Reported limits of observed roadway worms damage includes the SR 77 pavement section from MP 28.438 to MP 29.179. Figure 78 shows the condition of pavement section in proximity of MP 28.438 (top) and MP 29.401 (bottom).

Figure 78: Photographs of pavement distress in proximity of MP 28.438 (top) and MP 29.401 (bottom).

Figure 79 left, demonstrates segment of 3D-Radar data collected in northbound lane in proximity of MP 28.08 (outside of the road worms section). Figure 79, right, displays another segment of the same file, collected in proximity of MP 28.72 (within the road worms section). It should be noted that displayed scans represent the internal condition of pavement in proximity of particular mileposts only, and it can greatly vary from point to point. Approximate points where the photographs were taken were located using reference MP 28.068 (Knotch Pond Ln) and MP 28.326 (Bahoma Rd).

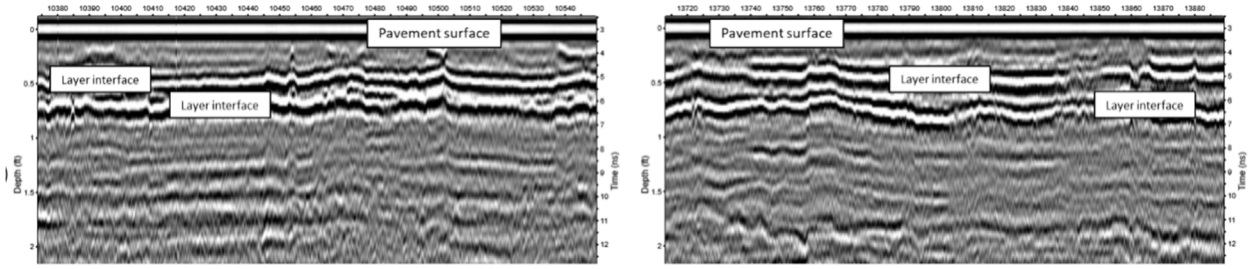

Figure 79: Vertical slices of 3D GPR data collected outside of the "road worms" section (left), and inside the "road worms" section (right). Northbound direction, left lane.

Six pavement sections in proximity to the core extraction points were selected to demonstrate the Reflection Activity analysis, three each in northbound and southbound lanes, respectively. Files collected on left and right sides of southbound and northbound lanes have been stitched together with Examiner to enable the analysis of the full lane width for southbound and northbound lanes, respectively.

Figure 80 displays the Reflection Activity mode of ExploreGPR software showing the stitched section of 3D-Radar data covering the southbound lane of SR 77 from MP 28.2 to MP 28.49. Figure 80a demonstrates the reflection analysis performed on the specified depth interval. Figure 80b is a spatial distribution of reflection activity patterns over the specified depth interval selected by the opaque orange shape overlaid on the B-Scan axes.

Figure 81 displays the spatial distribution of increased reflection activity within the AC layer of the first stitched section, covering the SR 77 from MP 28.2 to MP 28.49 in southbound direction. Figure 82 shows the spatial distribution of anomalous reflection activity within the AC layer of the second stitched section, covering the SR 77 from MP 28.21 to MP 28.47 in northbound direction. Figure 83 and Figure 84 show the spatial distribution of increased reflection activity within the AC layer of the third stitched section, covering the SR 77 from MP 29.08 to MP 29.27 in southbound and northbound directions, respectively. Figure 85 and Figure 86 show the spatial distribution of increased reflection activity within the AC layer of the third stitched section, covering the SR 77 from MP 29.31 to MP 29.5 in southbound and northbound directions, respectively.

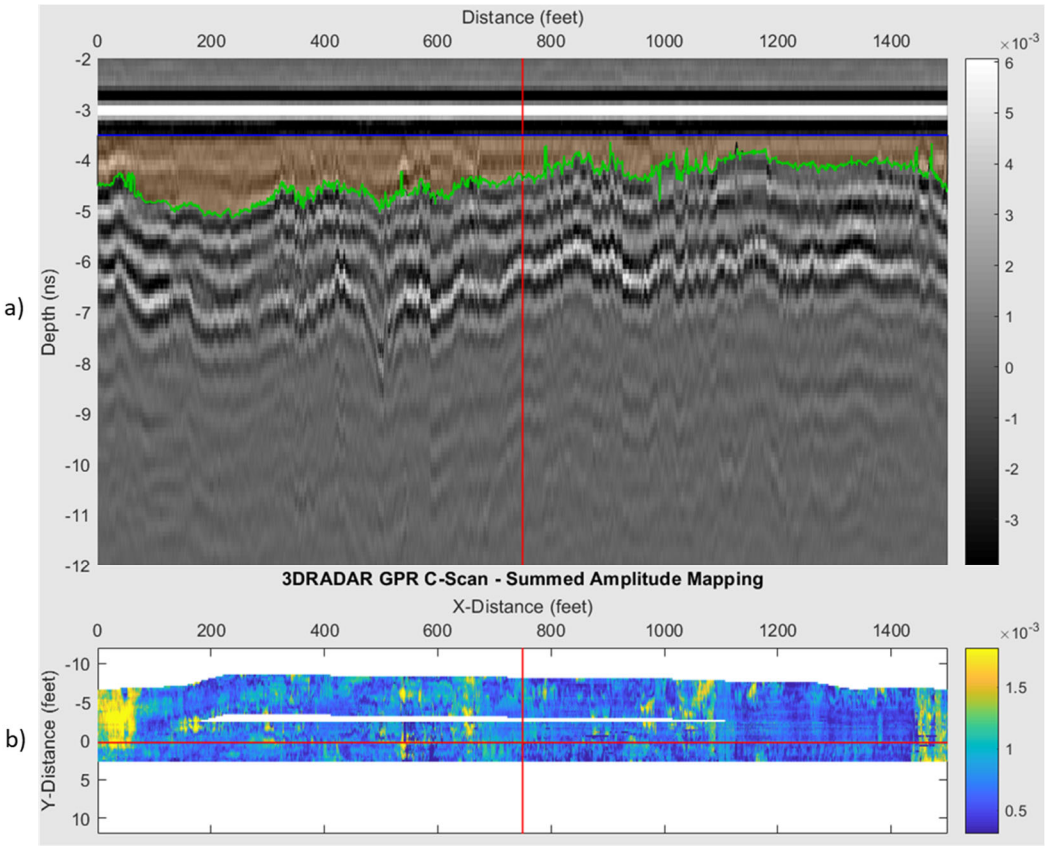

Figure 80: ExploreGPR interface showing the activity analysis performed on interval limited by 3.5 ns on top and offset of 0.48 ns on top of the traced layer interface on the bottom for the first stitched File, covering the southbound lane of SR 77 from MP 28.2 to MP 28.49: a) is the b-scan; b) is a color-coded reflection activity plot for the window specified in a).

To test the ability of 3D-Radar to provide data that will allow to distinguish the area of pavement which is affected by road worms from the control section, comparative analysis of a control section outside the damage zone was performed. Figure 87 displays the Reflection Activity mode of ExploreGPR software showing the stitched section of 3D-Radar data covering the southbound lane of SR 22 from MP 28.047 to MP 28.33.Figure 88 shows the corresponding plot of spatial distribution of increased reflection activity within the AC layer.

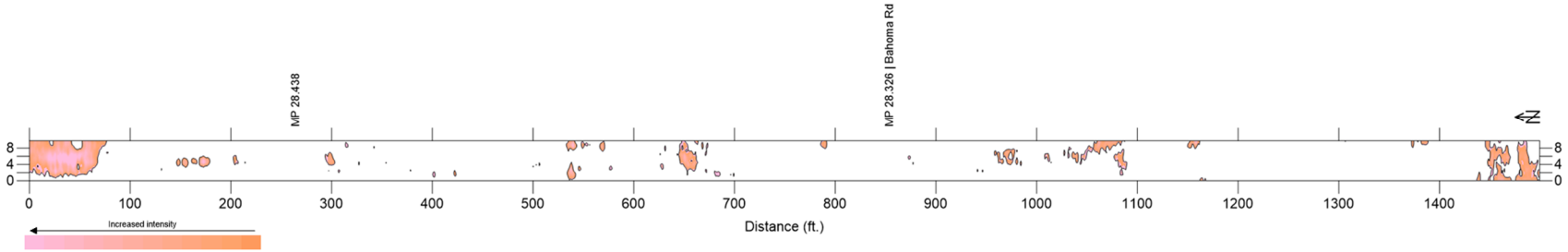

Figure 81: Reflection activity map of pavement section covering the SR 77 from MP 28.2 to MP 28.49. Southbound lane.

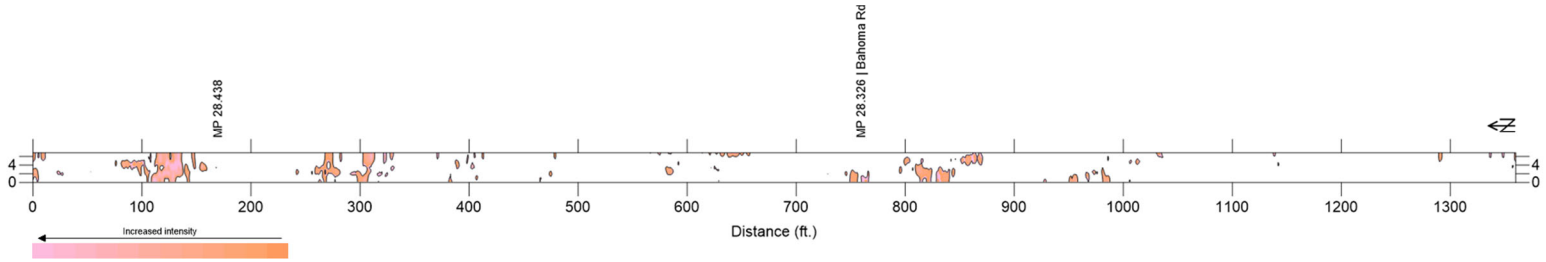

Figure 82: Reflection activity map of pavement section covering the SR 77 from MP 28.21 to MP 28.47. Northbound lane.

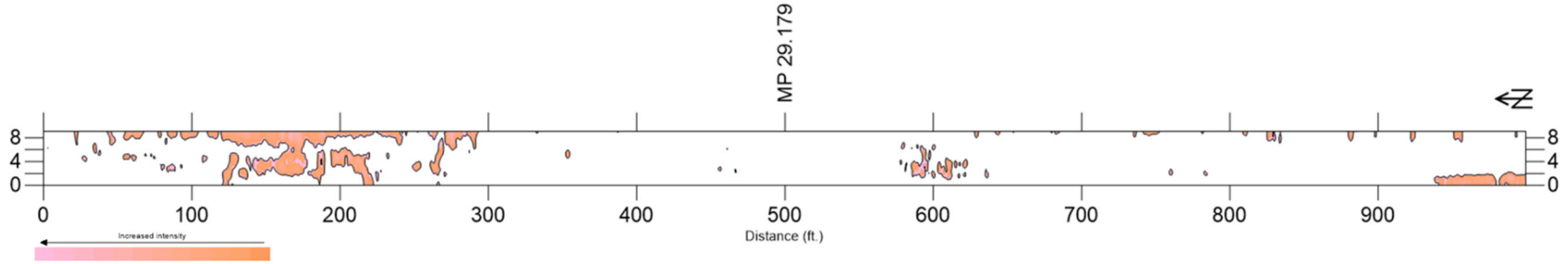

Figure 83: Reflection activity map of pavement section covering the SR 77 from MP 29.08 to MP 29.27. Southbound lane.

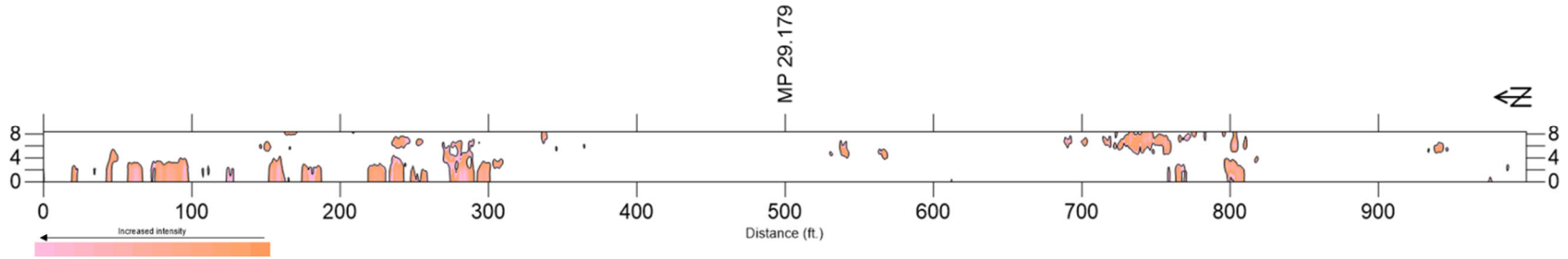

Figure 84: Reflection activity map of pavement section covering the SR 77 from MP 29.08 to MP 29.27. Northbound lane.

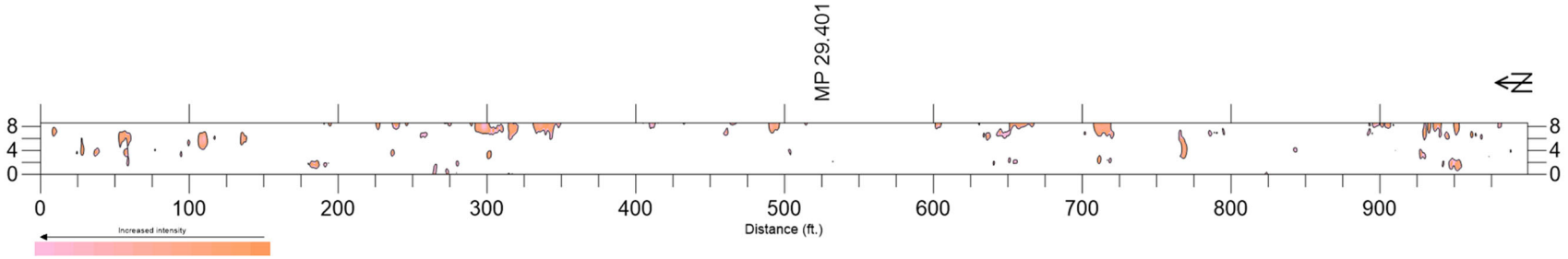

Figure 85: Reflection activity map of pavement section covering the SR 77 from 29.31 to MP 29.5. Southbound lane.

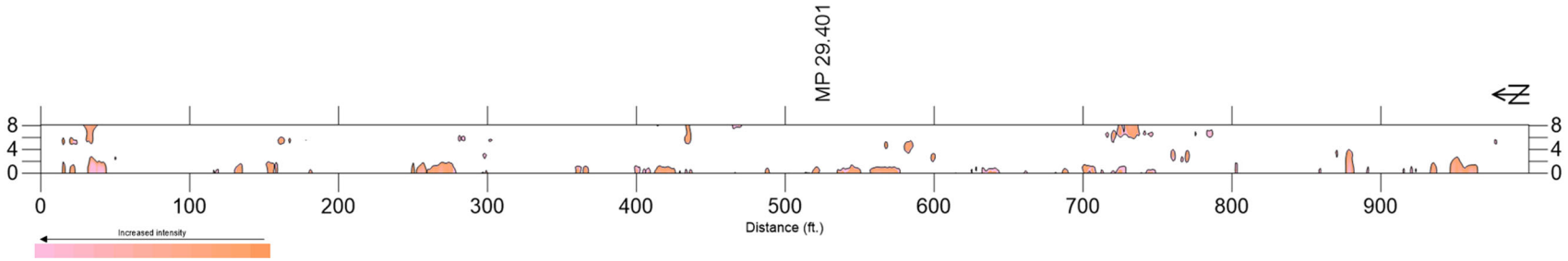

Figure 86: Reflection activity map of pavement section covering the SR 77 from 29.31 to MP 29.5. Northbound lane.

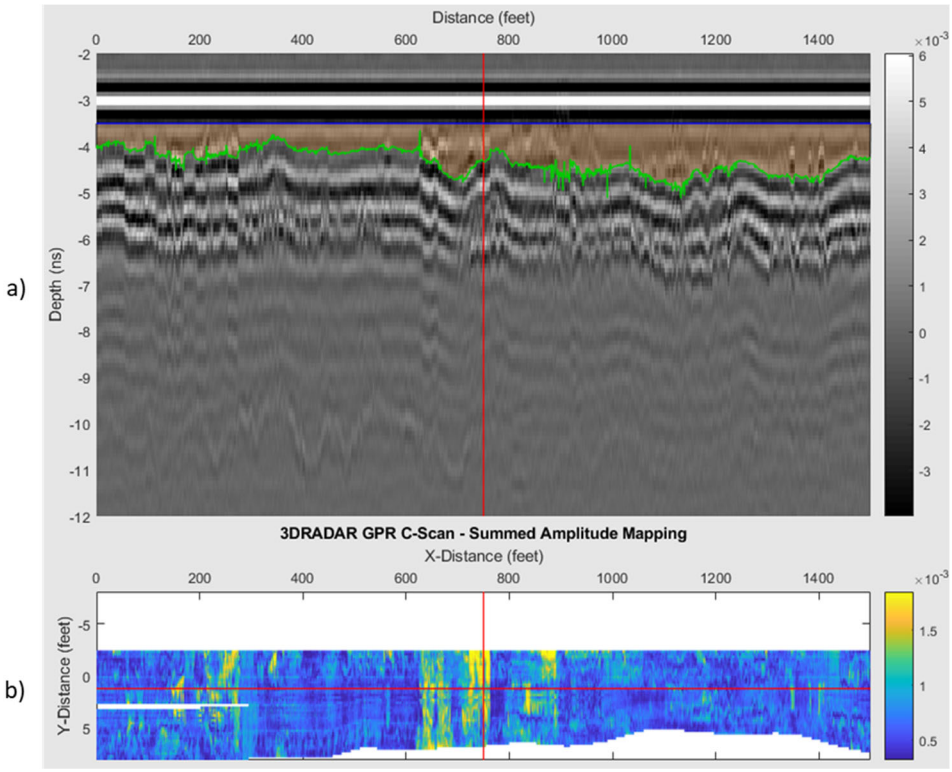

Figure 87: ExploreGPR interface showing the activity analysis performed on interval limited by 3.5 ns on top and offset of 0.48 ns on top of the traced layer interface on the bottom for SR 77 control section stitched File: a) is the b-scan; b) is a color-coded reflection activity plot for the window specified in a).

Patterns of increased reflection activity can be observed in the middle part of the control section. Resulting map represents the spatial distribution of reflection activity patterns within the isolated depth interval. This type of analysis examine data for deviations of dielectric properties of material and presence of internal reflectors at variable depths which are not normally seen within intact materials and can be indicative, but not limited to the indication of presence of "road worms" distress. Increased reflection activity in the middle of test section can be considered as a precursor of developing deterioration and/or delamination, as well as appearance of thin asphalt layers in the upper part of the roadway, that does not manifest itself on the pavement surface.

In summary, the use of ExploreGPR software allowed to quickly process large amount of data and identify locations and extent of potential stripping development.

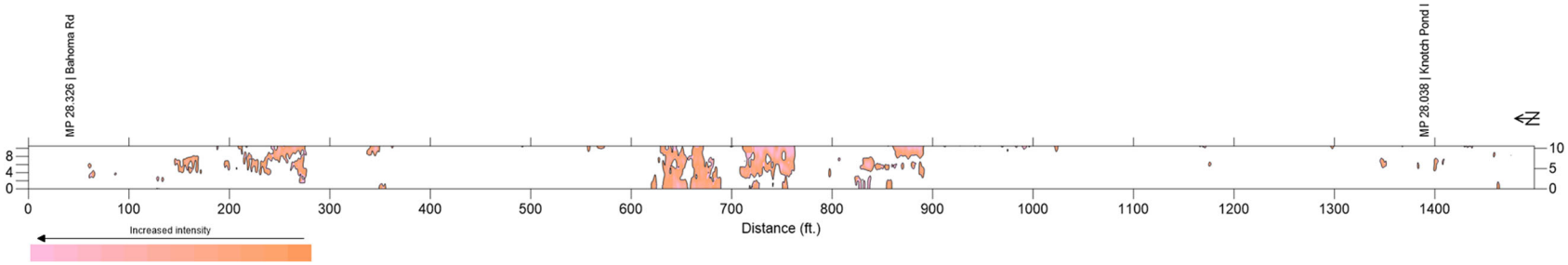

Figure 88: Reflection activity map of the control section covering the SR 77 from MP 28.047 to MP 28.33 in southbound direction.

Site 2.3: Interstate 10 – Project # 432736-1-52-01 / Roadway ID #: 58002000; (MP 24.520 – MP 26.300), Santa Rosa County - Subsurface Investigation

One line of 3D-Radar data was collected in the right side of eastbound lane. Issues with 3D-Radar equipment prevented the collection of additional lines of data at this site. Amount of the collected data was considered sufficient for the proposed goal of the survey. The eastern limit of data collection was MP 23.543 and the western limit was MP 26.0 on I-10 in Santa Rosa County. The objective of this Task is to investigate the pavement depression and upheaval between this section and to understand the nature, source, and extent of the problem. The repair zone can be recognized on 3D-Radar data as it shown in Figure 89.

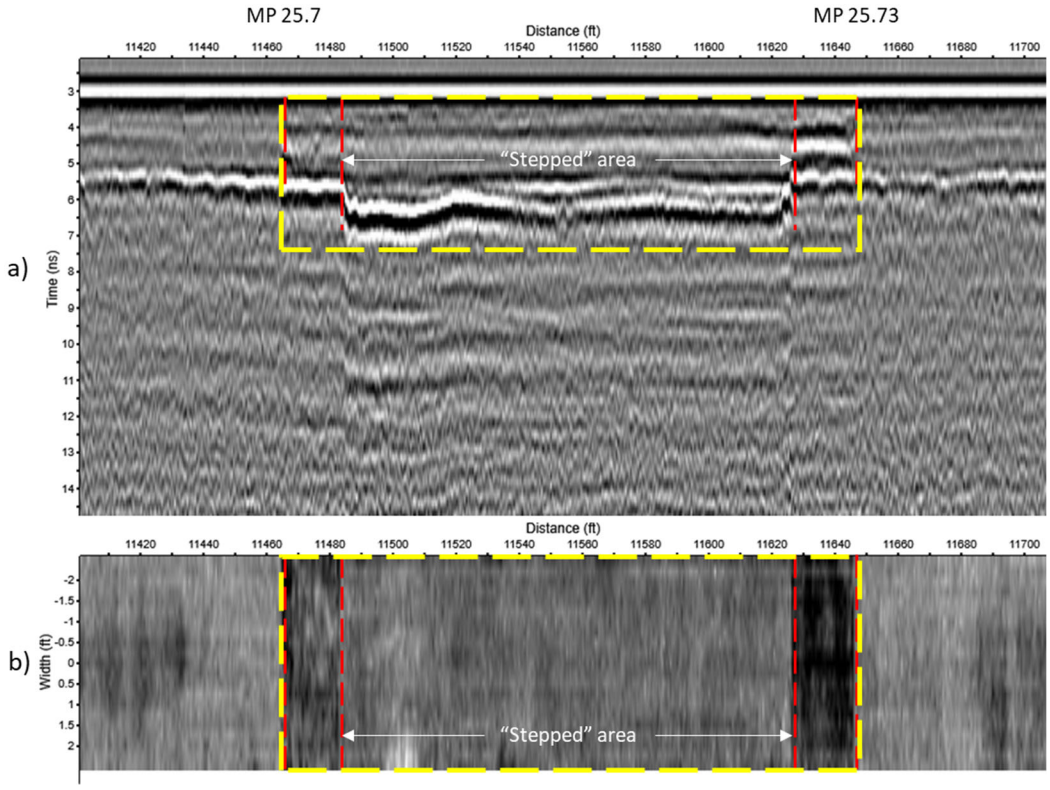

Figure 89: Vertical (a) and horizontal (b) slices of 3D-Radar data in proximity of MP 25.7. Eastbound direction, right lane.

Exact location and difference of the material removal depth on the both 140 feet long repair area itself and two additional milled segments can be observed in the part of 3D-Radar data collected in eastbound lane, where the vertical axis represents the depth expressed in ns. Yellow frames indicate the limits of a repaired zone. Red dashed lines delineate areas, where an additional 3 inches milling was performed starting 20 ft. from the begin of repair station to 20 ft. in advance of the end repair station to provide a "stepped" area [11]. Figure 90 represents a series of horizontal depth slices of 3D-Radar data, where the design and depth of the proposed repair area elements can be observed. Converting two-way travel time to depth, with average dielectric of 6, the depth in the B-scans correlate well with the proposed milling depth of 2 inches on the sides and 7 inches depth of the "stepped" area, which correlates with the proposed description of the repair [11]. While the 3D-Radar clearly reveals the repaired area, there are

no obvious indications in the data as to the nature and source of the underlying problem. No significant soil shifts and/or moisture pockets were observed below the repair area at depths up to 4.5 ft. Figure 91 shows full-depth vertical slice of 3D-Radar data in proximity to the repair section (depth was converted from two-wat travel time with dielectric of 5).

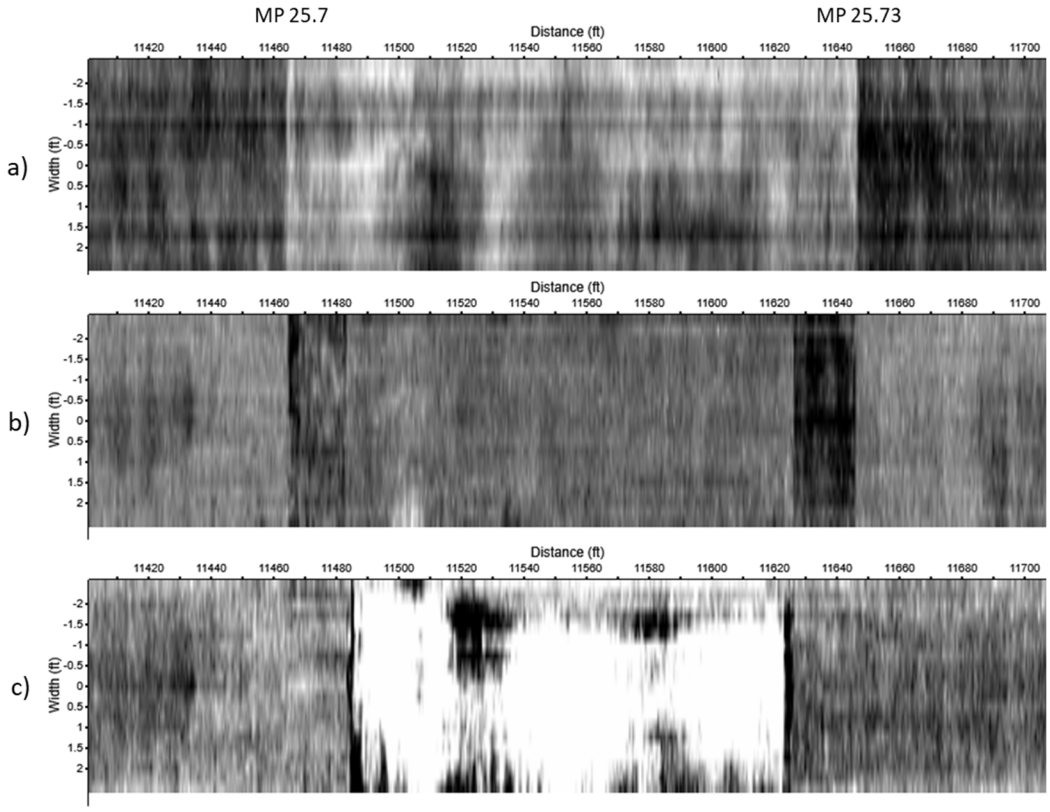

Figure 90: Horizontal slices of 3D GPR data in proximity of MP 25.7. Eastbound direction, right lane, at depths of 1 in. (a), 2.2 in. (b), and 7.2 in. (c).

Exact location and extent of repaired section were noted using 3D GPR system. Variations of the material removal depths on the repair area itself and two additional milled segments were also identified.

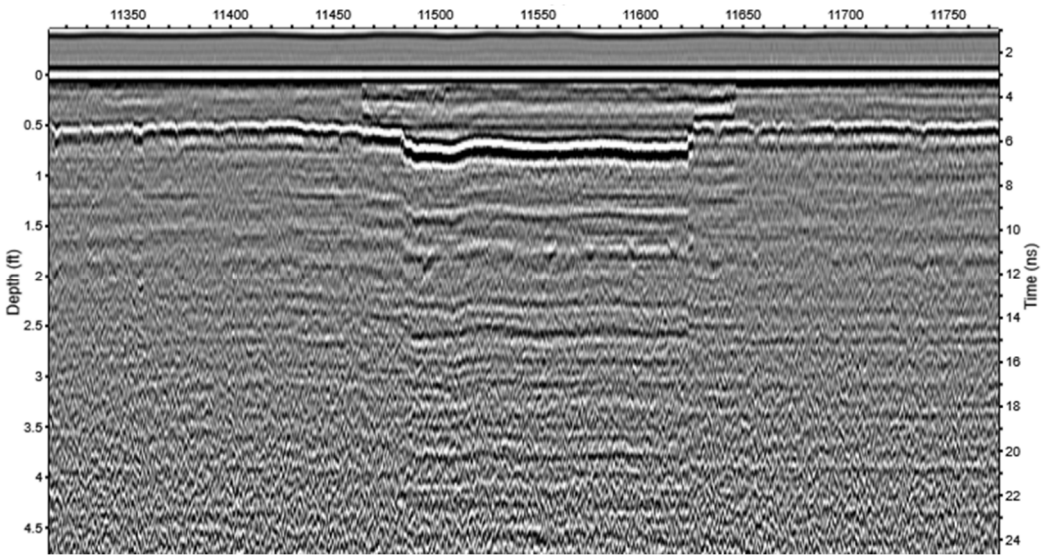

Figure 91: Full-depth vertical slice of 3D GPR data in proximity of the repaired area. Depth is converted from two-wat travel time with dielectric of 5.

Site 2.4: SR 75/US 231, Panama City, Bay County, Composite (asphalt + concrete*) Roadway Section – Confirm the nature and extent of the underlying pavement layers

Four lines of data were collected, two each in the northbound and southbound lanes. The southern limit was MP 0.873 Intersection of Harrison Ave and E 13th St) and the northern limit was MP 11.970 (intersection of SR 75/US 231 and Penny Rd/Commerce Blvd) on SR 75/US 231 in Bay County. Figure 92 demonstrates aerial view of SR 75/US 231 Test Section in proximity of Transmitter Rd and US 231 intersection.

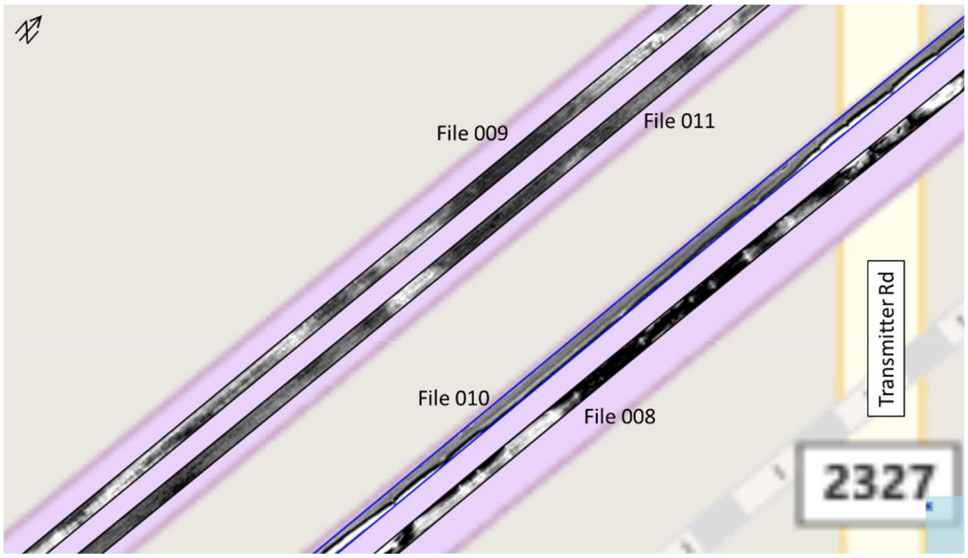

Figure 92: 3D-Radar files collected over the test section. Area in proximity of Transmitter Rd and US 231 intersection (~MP 5.2).

The 3D-Radar data, collected over the northbound pavement section, revealed the presence of sand-asphalt hot mix (SAHM) layer below the asphalt layer. As it can be seen in Figure 93-99 composition of northbound lane pavement is different from the southbound lane design. The presence of SAHM layer was registered on the northbound section, starting from the MP 1.18 (intersection of Harrison Ave and SR 75/US 231.

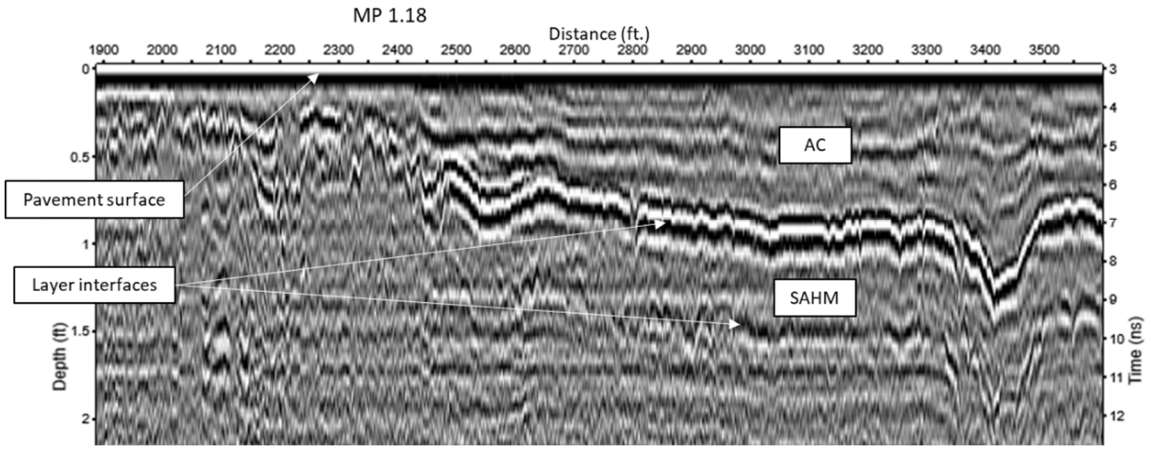

Figure 93: Vertical slice of 3D GPR data collected in southbound direction on the right lane. In proximity of MP 1.18 (the beginning of two-layered AC over SAHM design).

No SAHM layer signatures were observed in area limited by MP 5.17 on the south and MP 5.53 on the north (Figure 94), and over the area limited by MP 10.59 on the south and MP 510.73 on the north (Figure 95).

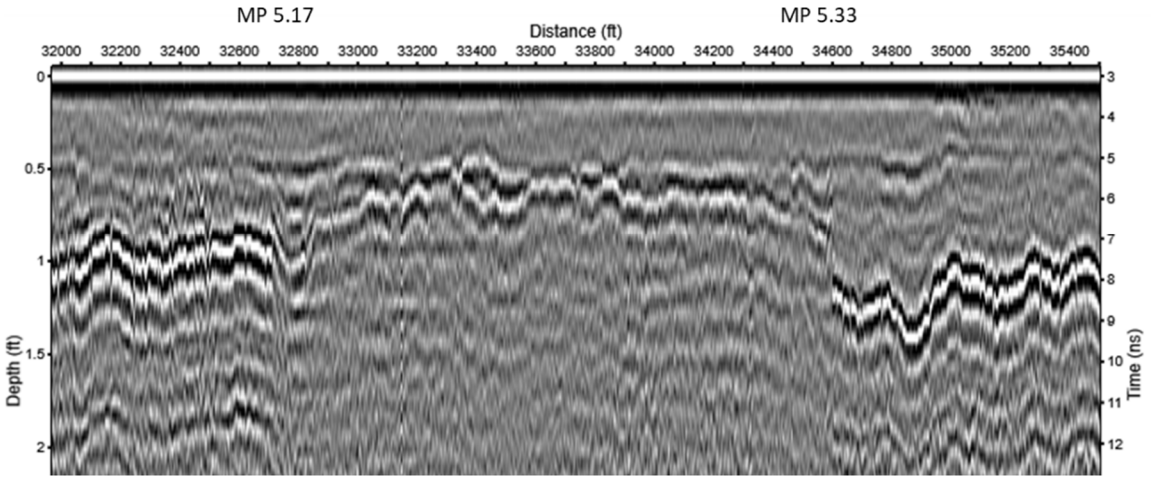

Figure 94: Vertical slice of 3D GPR data collected in southbound direction on the right lane. Different pavement composition noted between MP 5.17 and MP 5.33.

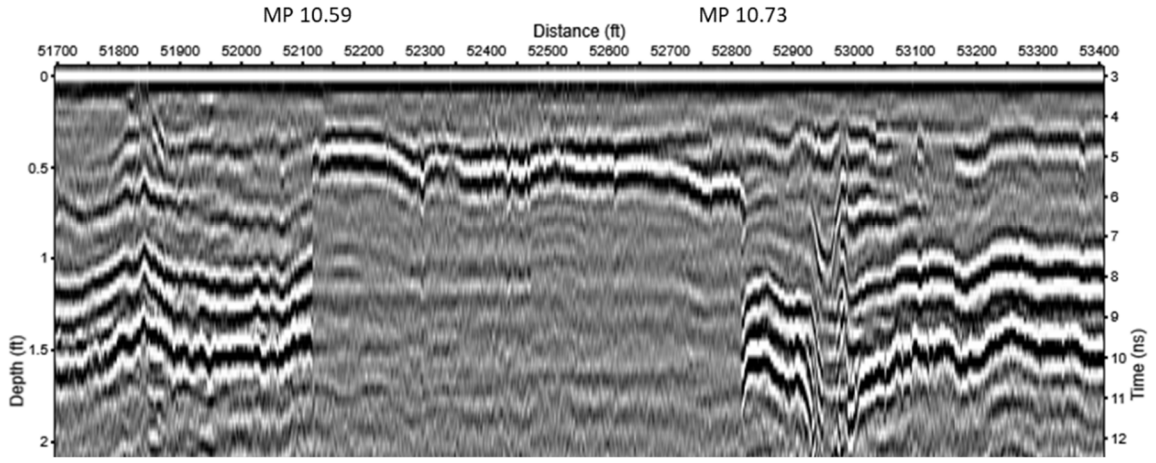

Figure 95: Vertical slice of 3D GPR data collected in southbound direction on the right lane. Different pavement composition noted between MP 10.59 and MP 10.73.

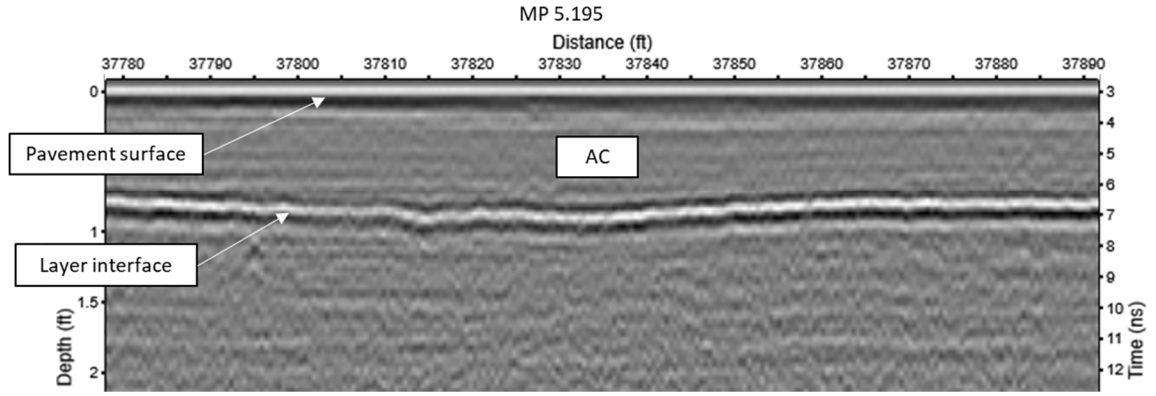

Figure 96: Vertical slice of 3D GPR data collected in southbound direction on the right lane. Displayed part represents the data from 320 ft. south from the intersection with Transmitter Rd, MP 5.195. Pavement design is represented by single AC layer, overlaying the base material.

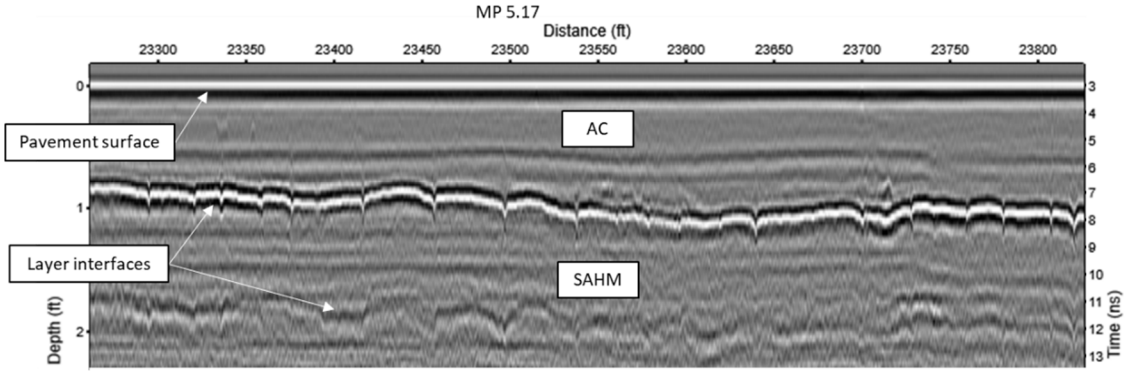

Figure 97: Vertical slice of 3D GPR data. Northbound direction, left lane, 320 ft. south from the intersection with Transmitter Rd. Very clear illustration of pavement design, which is represented by AC material overlaying the SAHM layer.

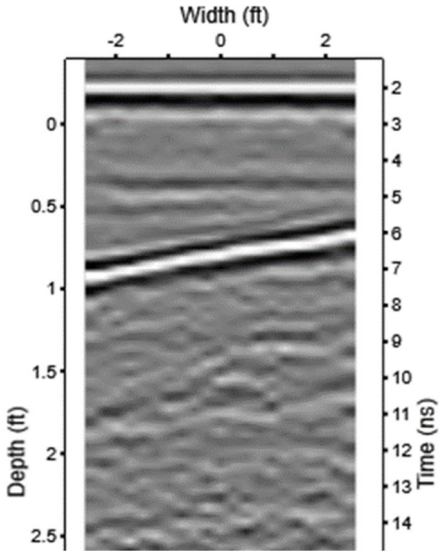

Figure 98: Typical section across the width of the pavement. The AC layer thickness varies by over 2".

It can be seen from 3D-Radar data (Figure 99), that both material layers greatly vary in depth over the distance. Figure 100 and Figure 101 display the contour maps of AC and cemented material layer (SAHM) thicknesses, observed over the selected control section (northbound lane, SR 75/US 231 from MP 4.79 to MP 5.84). Y-axes were expanded for better data representation.

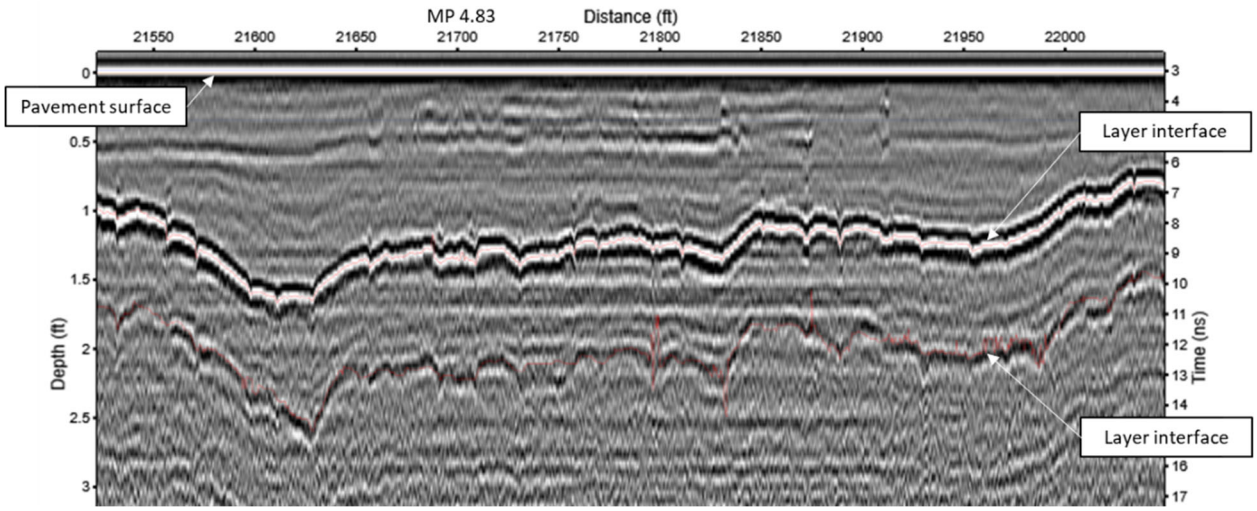

Figure 99: Vertical slice of 3D GPR data. Settlement occurs at 21, 600-foot mark.

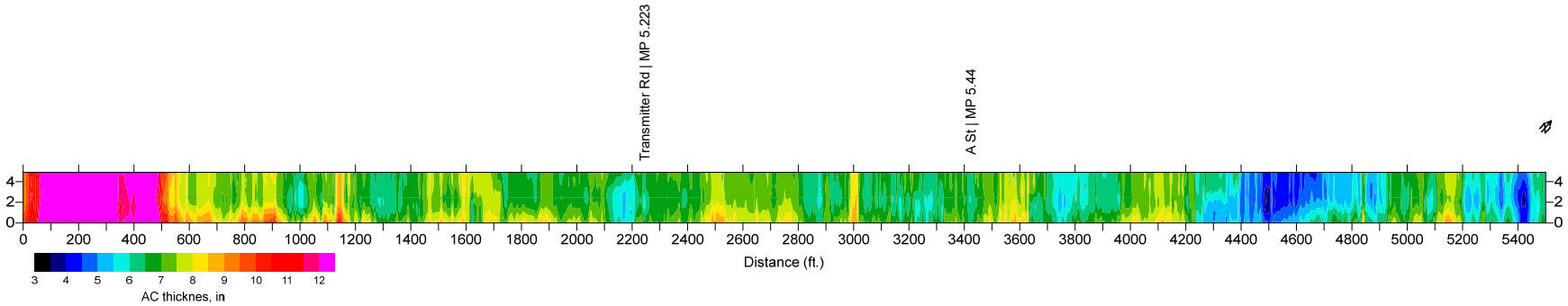

Figure 100: Contour map, showing spatial distribution of asphalt thickness values, calculated from 3D-Radar data, collected in northbound direction over the selected segment of SR 75/US 231.

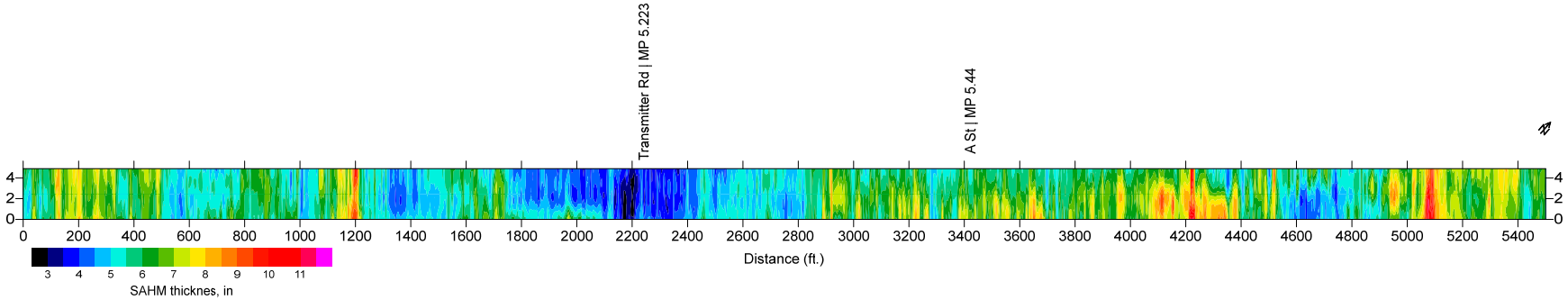

Figure 101: Contour map, showing spatial distribution of underlaying cemented layer thickness values, calculated from 3D-Radar data, collected in northbound direction over the selected segment of SR 75/US 231.

Site 2.5: SR 5 (Whitetopping Project) – Roadway ID #: 79010000; (~MP 9.600 – MP 11.458), Volusia County - Dowel bar detection and alignment

The 3D-Radar survey was carried out on November 13, 2017, between MP 9.6 and 11.458. Six lines of data were collected in SB direction in in the right and left sides of testing section (6 data sets, 3 passes per lane). Acquisition of 3D-Radar data started 250 feet to the north from the beginning of the Test Section. The purpose of the 3D-Radar survey was to confirm the ability of 3D-Radar system to detect the presence and alignment of the dowel bars. 3 Figure 102-106 display examples of 3D-Radar data showing standard dowel configuration, alternative dowel configuration, and undoweled section between the SP and SD designs. Figure 105 displays overlay thickness variations.

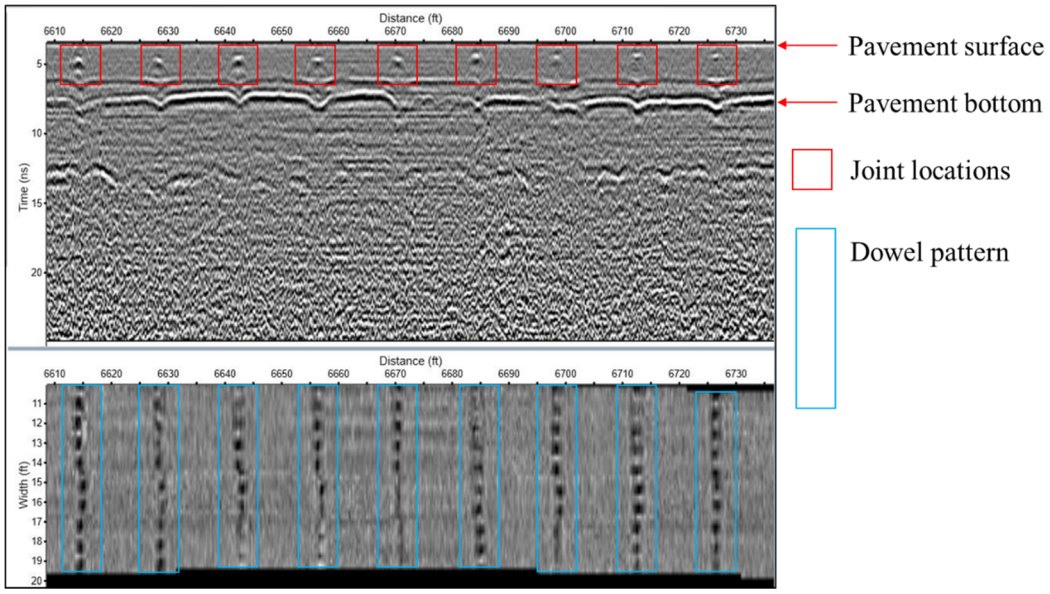

Figure 102: Standard (ST) dowel configuration.

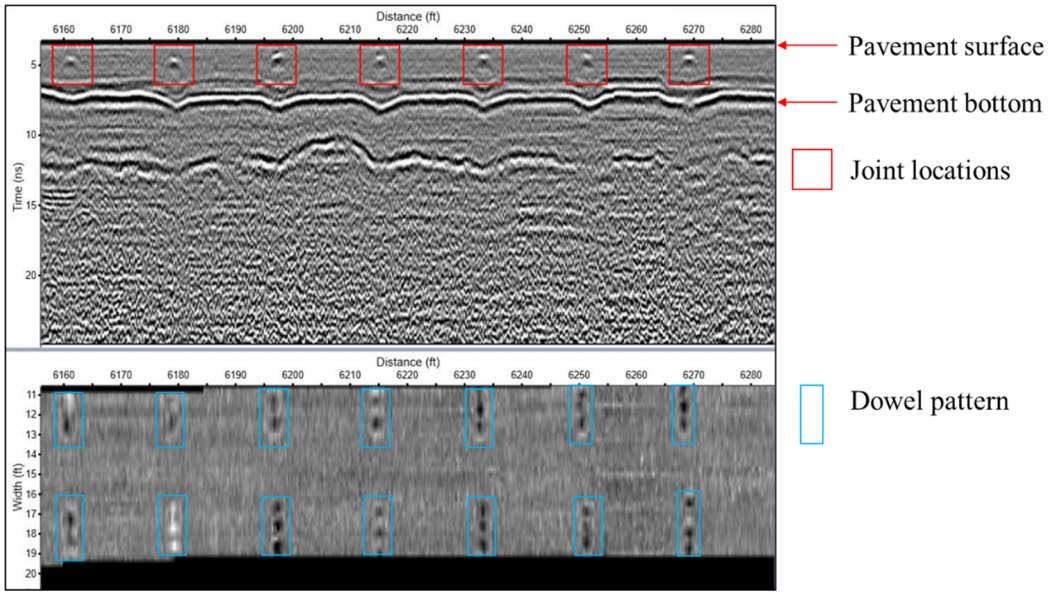

Figure 103: Alternative (SP) dowel configuration.

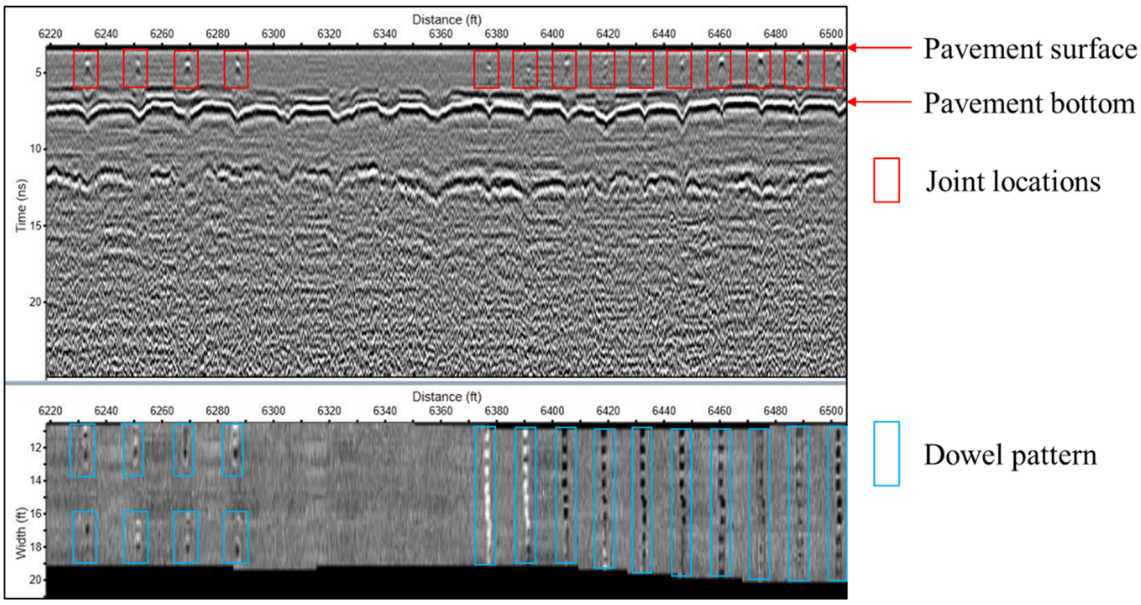

Figure 104: Undoweled section (left) between the SP and SD designs.

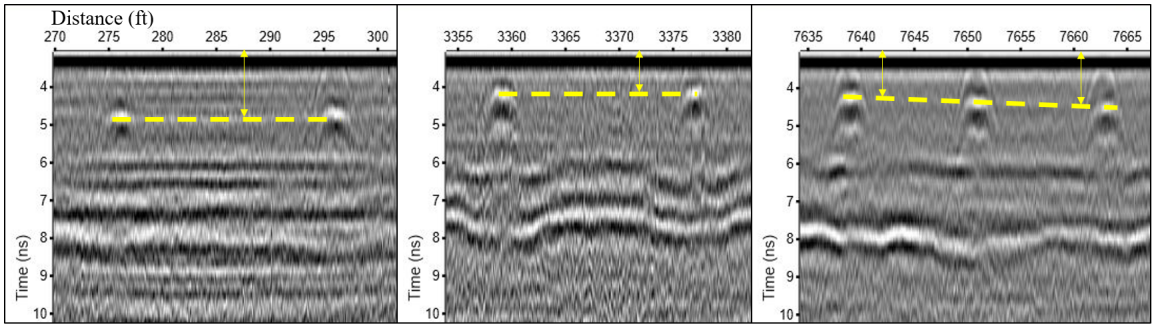

Figure 105: Various dowel depths observed on 3D-Radar data collected over the Test Section.

Measurements of dowel bars signatures on 3D-Radar data confirmed 18" dowel length and 12" dowel spacing. Proposed slab dimensions were confirmed with 3D-Radar survey results with minor discrepancies. Example is shown in Figure 106.

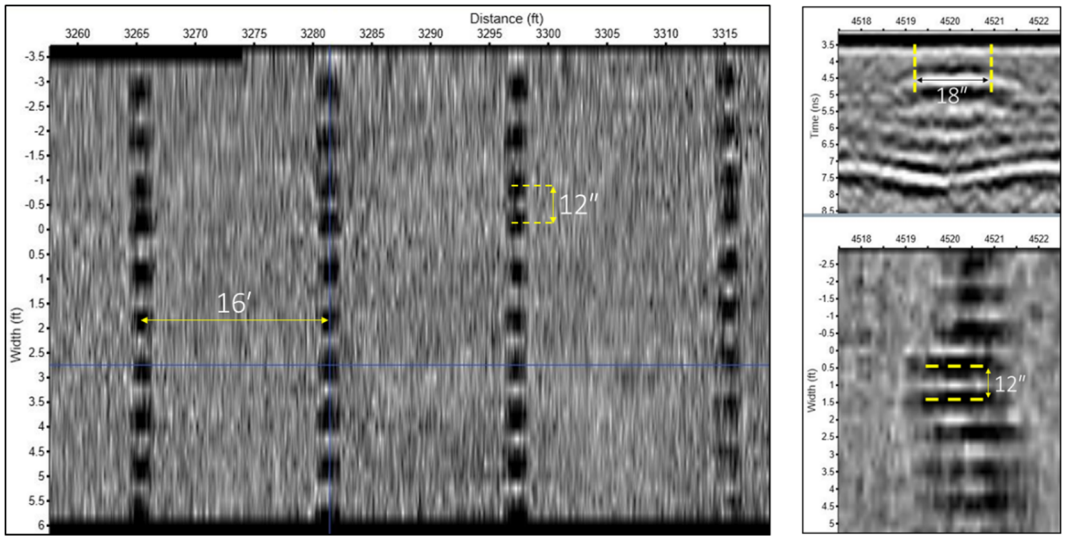

Figure 106: Measured dowels dimensions and spacing.

3D-Radar did not reveal the presence of proposed transition zones between the sections 13 and 12, 7 and 6, and 1 and 0; however, 3D-Radar clearly indicated existence of undoweled joints located in the last four slabs between the special (SP) and standard (SD) dowel subsections. Figure 107 exhibits the proposed Test Section design (left) and the Test Section design obtained from 3D-Radar survey results.

The design of the proposed transition zones with no dowels do not agree with the plan. As it can be seen on the 3D-Radar data (Figure 108, first of the proposed transition zones), transition zone contains additional ST doweled joints. Figure 109 contains the comparison of proposed (left) and measured by 3D-Radar slab length for sections 18 - 0. The misalignment (horizontal skew and vertical tilt) of dowel bars can be accessed and examined to the limited extent, as it shown in Figure 106 . However, it is difficult to evaluate the lateral positioning of a single dowel bar.

In summary, the 3D-Radar survey successfully confirmed the ability of utilized system to locate slabs (installment pattern, dimensions, and reinforcement design) joints, and dowel configuration.

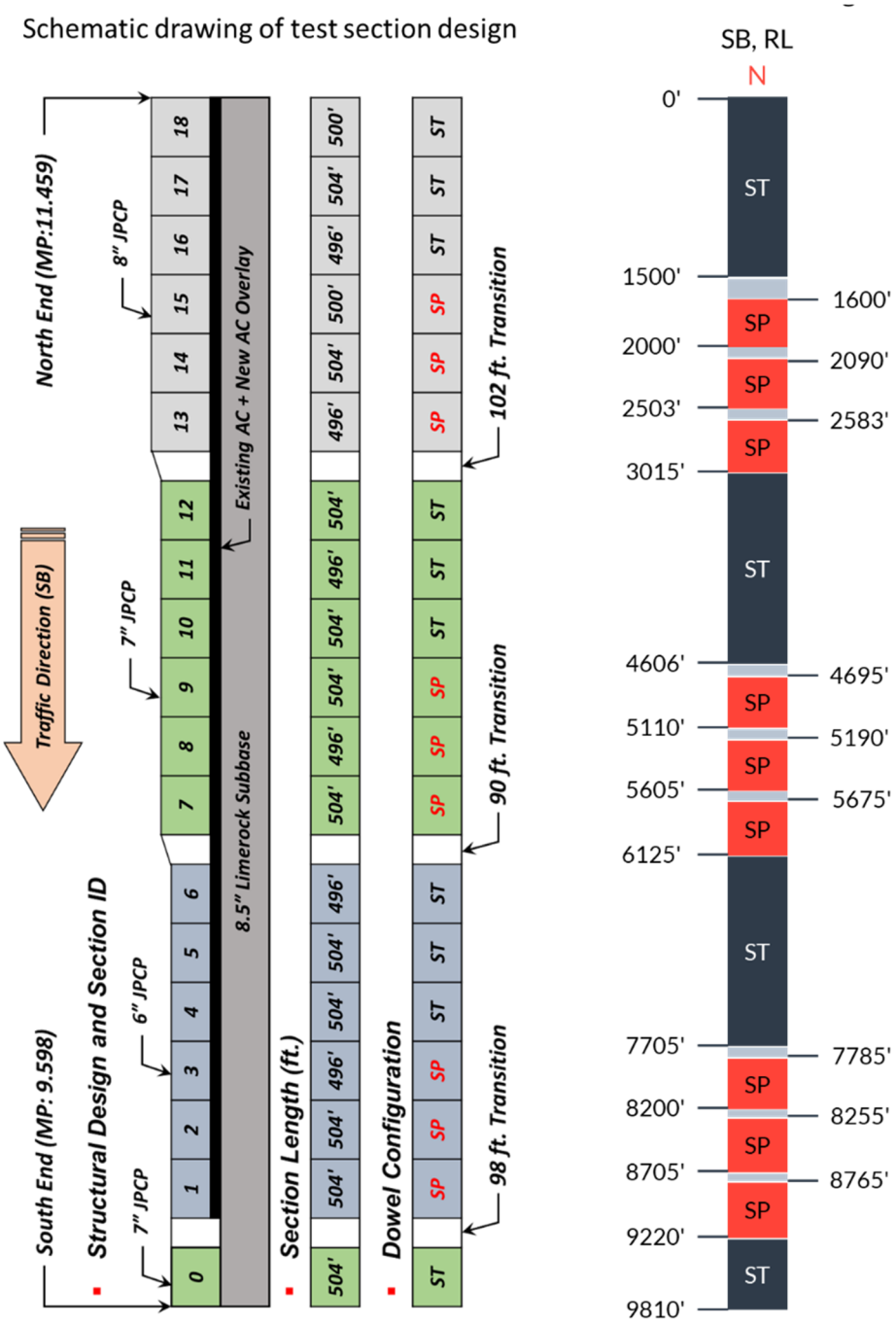

Figure 107: Schematic drawing of test section design dimensions provided by FDOT (left). Figures on the right represent the difference between the proposed and observed Test Section designs.

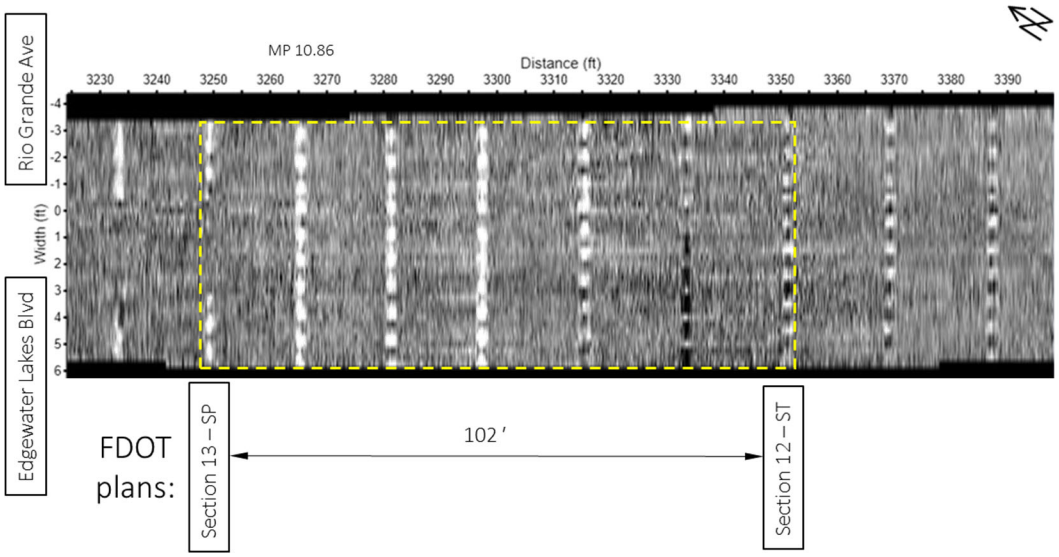

Figure 108: Segment of 3D-Radar data in proximity of the proposed transition section location (framed with dashed yellow line).

		FDOT plans Slab length		3D Radar Slab length
1500 ′	ST	20 ′	✓	20.122 ′
	ST	18 ′	✓	17.925 ′
	ST	16 ′	✓	16.058 ′
1500 ′	SP	20 ′	✓	19.946 ′
	SP	18 ′	✓	17.926 ′
	SP	16 ′	✓	15.992 ′
	T			
1504 ′	ST	18 ′	✓	18.188 ′
	ST	16 ′	✓	15.992 ′
	ST	14 ′	✓	13.972 ′
1504 ′	SP	18 ′	✓	18.189 ′
	SP	16 ′	✓	15.992 ′
	SP	14 ′	✓	14.113 ′
	T			
1504 ′	ST	16 ′	✓	16.08 ′
	ST	14 ′	✓	14.059 ′
	ST	12 ′	✓	12.038 ′
1504 ′	SP	16 ′	✓	15.905 ′
	SP	14 ′	✓	14.147 ′
	SP	12 ′	✓	12.126 ′
	T			
504 ′	ST	14 ′	✓	14.147 ′

Figure 109: Proposed and measured slab length by section.

Sites 2.6-2.8 – Bridge Decks

2.6: SR 816 (W. Oakland Park Blvd) Roadway ID #: 86090000; (~MP 2.263 – MP 2.323), Broward County - Bridge Deck Delamination Mapping

2.7: SR A1A (Blue Heron Blvd.) Blue Heron Bridge – Roadway ID #: 93080000; (~MP 0.414 – MP 0.788), Palm Beach County - Bridge Deck delamination/deterioration mapping

2.8: SR A1A/ North Causeway (Shorewinds Dr.) North Bridge over ICWW – Roadway ID #: 94060000; (~MP 0.330 – MP 0.719), St. Lucie County - Bridge Deck Delamination/deterioration mapping

For the following Sites, data was initially processed using 3D-Radar's "Examiner" software. Once the data was stitched using Examiner, then it was processed using Infrasense's "ExploreGPR" software to calculate the amplitude of each of the picked layers. These amplitudes are then displayed in a contour plot format. The displayed areas of deck deterioration are based on setting an amplitude threshold below which the deck is considered "deteriorated". The entire analysis process can be summarized as follows:

1. Import the 3D-Radar files into Examiner;
2. Stitch together of the individual survey passes to form a complete 3D image of the entire deck;
3. Identify the beginning and the end of the deck, and check of the radar distance measurement against the known length and other features within the deck;
4. Identify features (top rebar, bottom of deck) that appear as dielectric discontinuities in the GPR data;
5. Track selected detected layers using the Examiner "picking" tool;
6. Import the stitched data and the tracking data into ExploreGPR, and compute rebar depth, amplitude at the rebar-level and the bottom deck and/or reflection activity within the deck;
7. Contour plot the results;
8. Using the top rebar data display areas where the amplitude is below a specified threshold.

Bridge # 860245. The 3D-Radar survey was carried out on November 14, 2017. Twelve lines of data were collected, six each in the westbound and eastbound lanes. The purpose of survey was to confirm the ability of 3D-Radar system to map the distribution of deterioration. The overall purpose of this task has been to evaluate the condition of the westbound and eastbound lanes of bridge deck.

Rebars reflections appear as a layer reflector in the 3D-Radar data as it is shown in Figure 110. Figure 111 displays the horizontal slice of the 3D-Radar data at 3.5 inches. Longitudinal and transverse reinforcing bars and bridge joint can be identified. GPR signatures that can be associated with bridge girders are visible on 3D-Radar data as well as it shown in Figure 112.

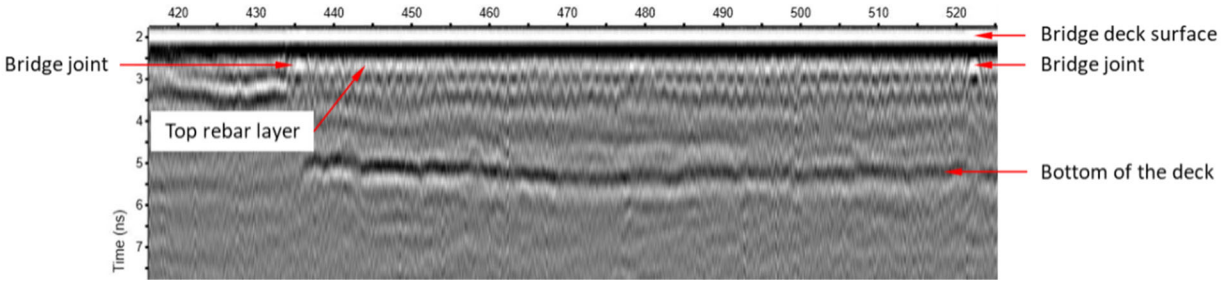

Figure 110: GPR cross-section showing the identified rebar layer and deck bottom, left side of the right driving lane, westbound direction.

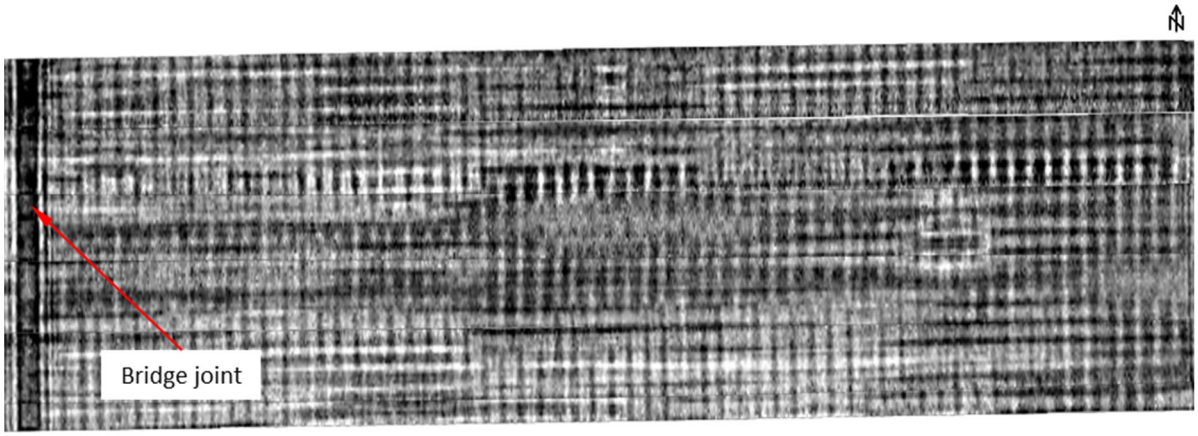

Figure 111: Depth slice at 3.5" showing longitudinal and transverse rebar and bridge joint – segment of a stitched area covering the westbound lane.

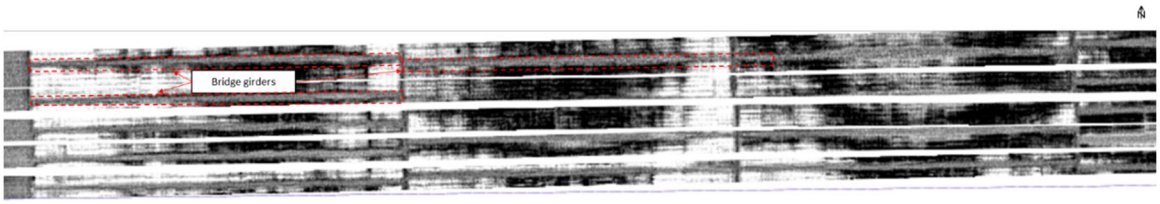

Figure 112: Horizontal slice of stitched 3D GPR section, representing the northwestern part of the bridge with visible signatures of girders.

Data was initially processed using 3D-Radar's "Examiner" software, where files were converted from the frequency to time domain data, filtered, and stitched. Top rebar layer was picked across the deck to obtain the reflection amplitude and two-way travel times of electromagnetic energy (Figure 113). Once the data is stitched with Examiner and processed using Infrasense's ExploreGPR software to calculate the amplitude of each of the picked layers. The attenuation (loss of signal strength) of the radar signal, as measured from the top rebar reflection was used as a measure of concrete delamination, since contaminated and delaminated concrete cause the GPR signal to dissipate and lose strength as it travels through the deck and reflects back from the rebar. Due to the bridge deck design and the influence of girders on deck bottom reflection amplitude values, only top rebar reflection was used for deterioration analysis.

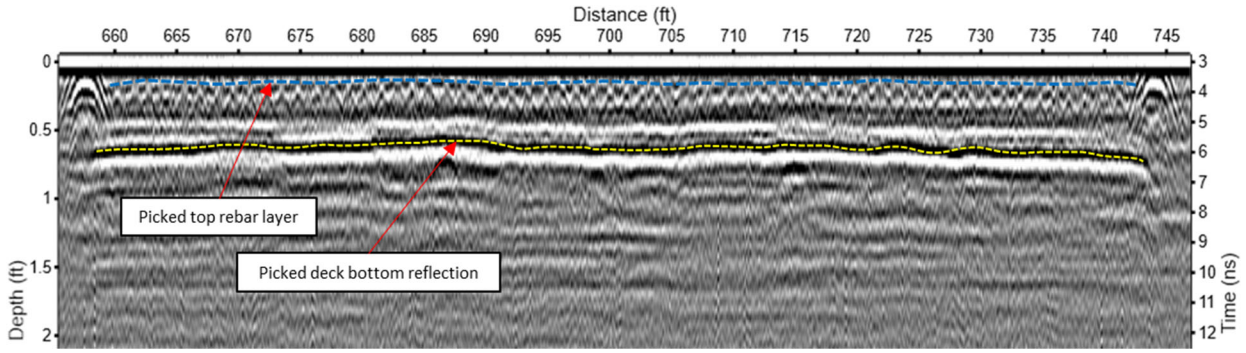

Figure 113: Vertical cross-section of 3D-Radar data showing the picked top rebar layer (blue line) and deck bottom reflection (yellow line). X- and Y-axes are arbitrary.

Representative results for Broward County bridge are shown in Figures below. Figure 114 and Figure 115 show the spatial distribution of deterioration detected with GPR using a thresholded contour plots for westbound and eastbound lanes, respectively. Areas shown are those where the attenuation levels exceed a threshold value, indicating chloride contamination and corrosion. The color scale indicates the degree to which the threshold is exceeded, which represents the severity. Shades of blue delineate areas, where detected deterioration level exceeds the set threshold, shades of magenta color indicate more severe deterioration. Figure 116 and Figure 117 show contour maps of the rebar depth for westbound and eastbound lanes, respectively. Shades of blue and green colors represent rebar cover from 1.4 to 2.25 inches, and shades of yellow and brown represent rebar cover from 2.5 to 3.2 inches.

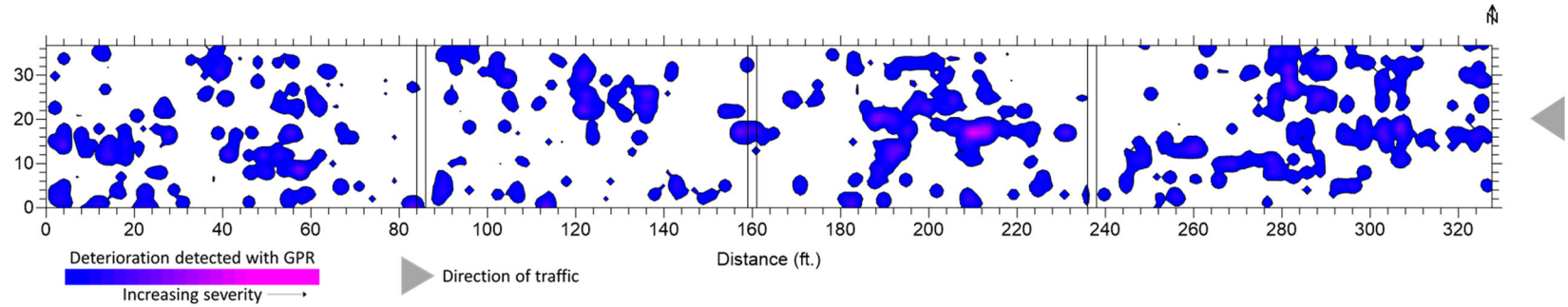

Figure 114: Concrete deterioration distribution map, generated from the results of 3D-Radar survey on westbound lane.

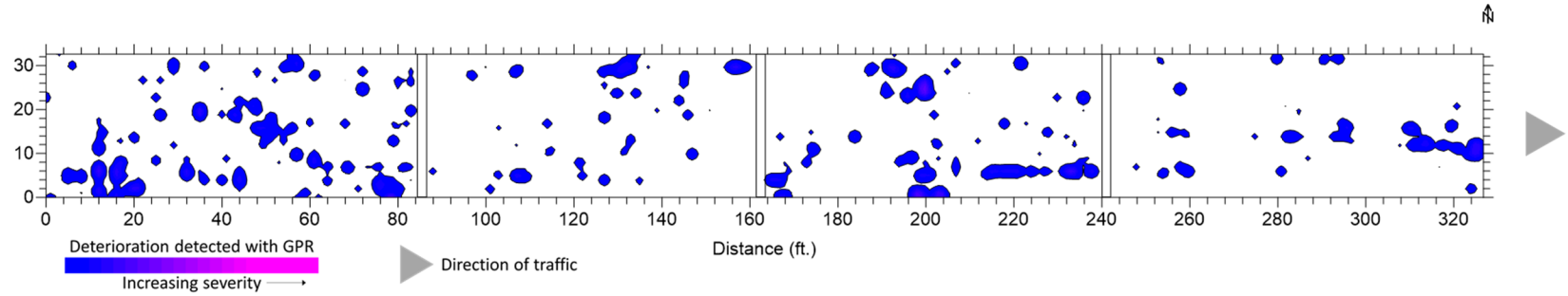

Figure 115: Concrete deterioration distribution map, generated from the results of 3D GPR survey on EB lane.

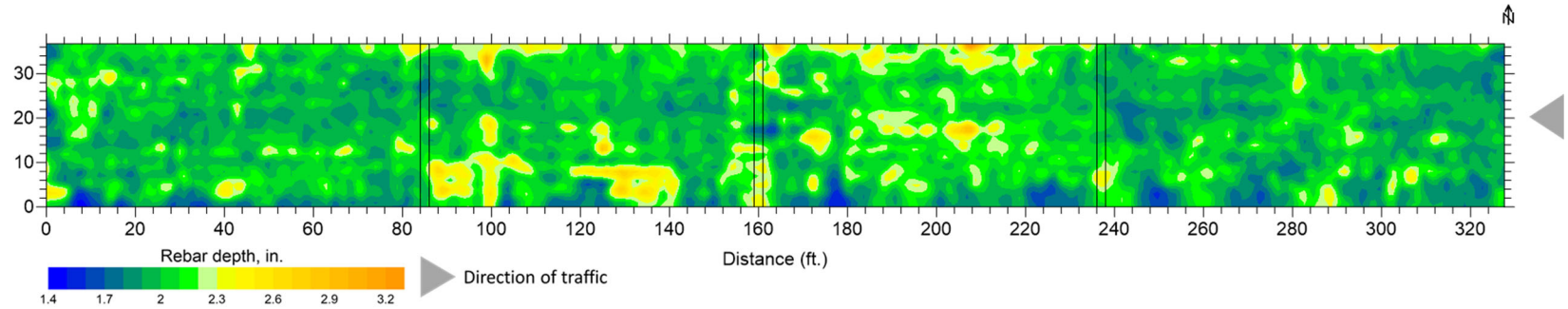

Figure 116: Rebar depth contour plot, generated from the results of 3D-Radar survey on westbound lane.

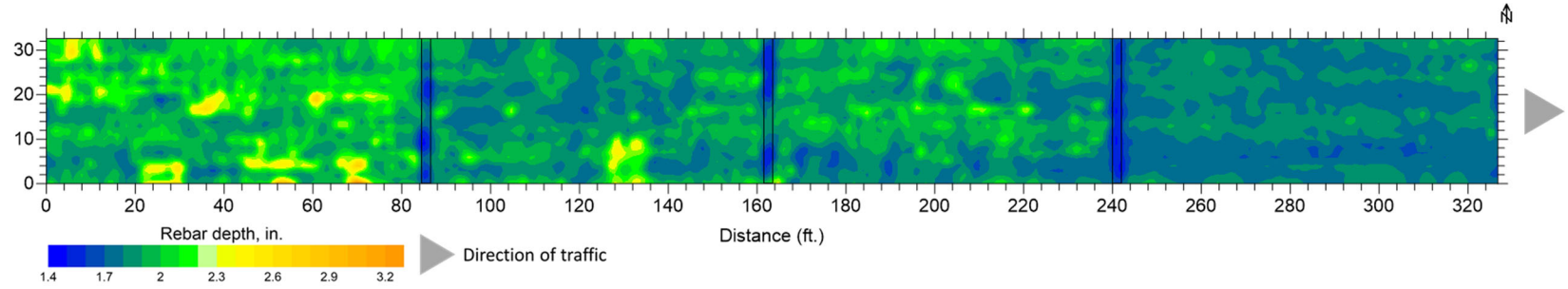

Figure 117: Rebar depth contour plot, generated from the results of 3D GPR survey on EB lane.

Bridge # 930269 (Blue Heron). The 3D-Radar survey was carried out on November 14, 2017. Twelve lines of data were collected, six each in the westbound and eastbound lanes. The purpose of the survey was to confirm the ability of 3D-Radar system to map the distribution of deterioration. Rebars reflections appear as a layer reflector in the 3D-Radar data as it is illustrated in Figure below. As it can be seen in Figure 118, top rebar layer appears as a weak, inconsistent reflection. Due to the specifics of bridge deck design and resulted from it limited capacity of layer identification, alternative approach to data analysis was employed.

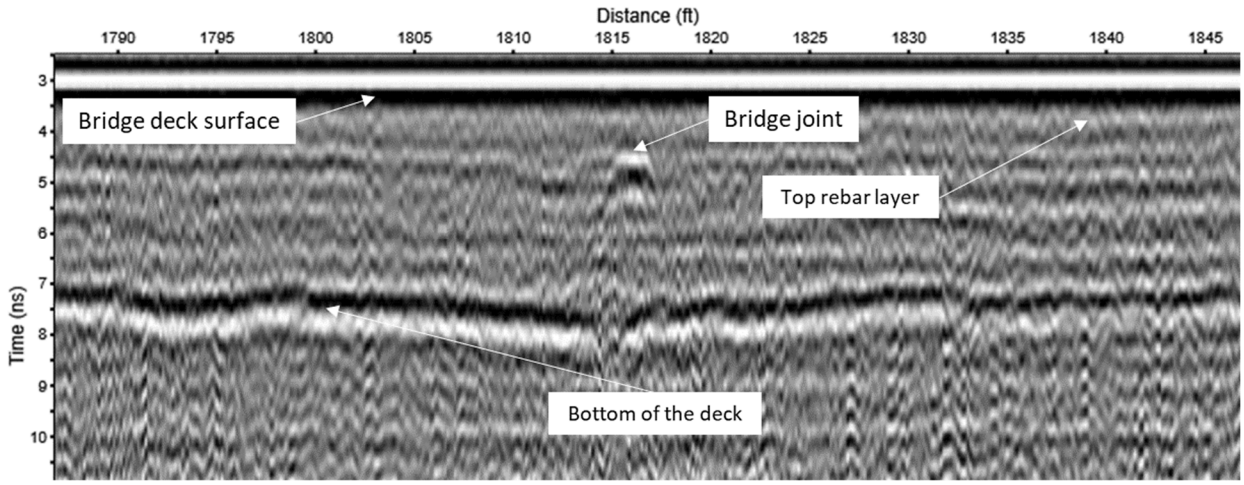

Figure 118: Vertical 3D-Radar cross-section showing the identified rebar layer and deck bottom, left side of the right driving lane, eastbound. Top layer rebar reflection is barely detectable.

Reflection Activity analysis approach was employed for this project. As it can be seen from Figure 118, the quality of 3D-Radar data does not allow to precisely pick the rebar layer reflector. As an alternative, ExploreGPR was used to examine and analyze 3D GPR data collected both in the westbound and eastbound lanes. Each span's activity was analyzed individually to neglect the possible smoothing of anomalous reflection activity and to avoid the impact of strong joint reflections on amplitude values distribution. Interval of 1 ns (from 3.5 to 4.5 ns) was selected to represent the activity within the upper part of bridge deck, where the top layer of rebar is present. Figure 119 displays the reflection activity mode of ExploreGPR software showing the segment of stitched file, covering the eastbound lane of the bridge. Figure 119b displays horizontal slice of 3D-Radar data with color-coded reflection activity distribution patterns. Shades of orange/yellow represent lower resulting amplitudes, shades of blue represent higher reflection activity.

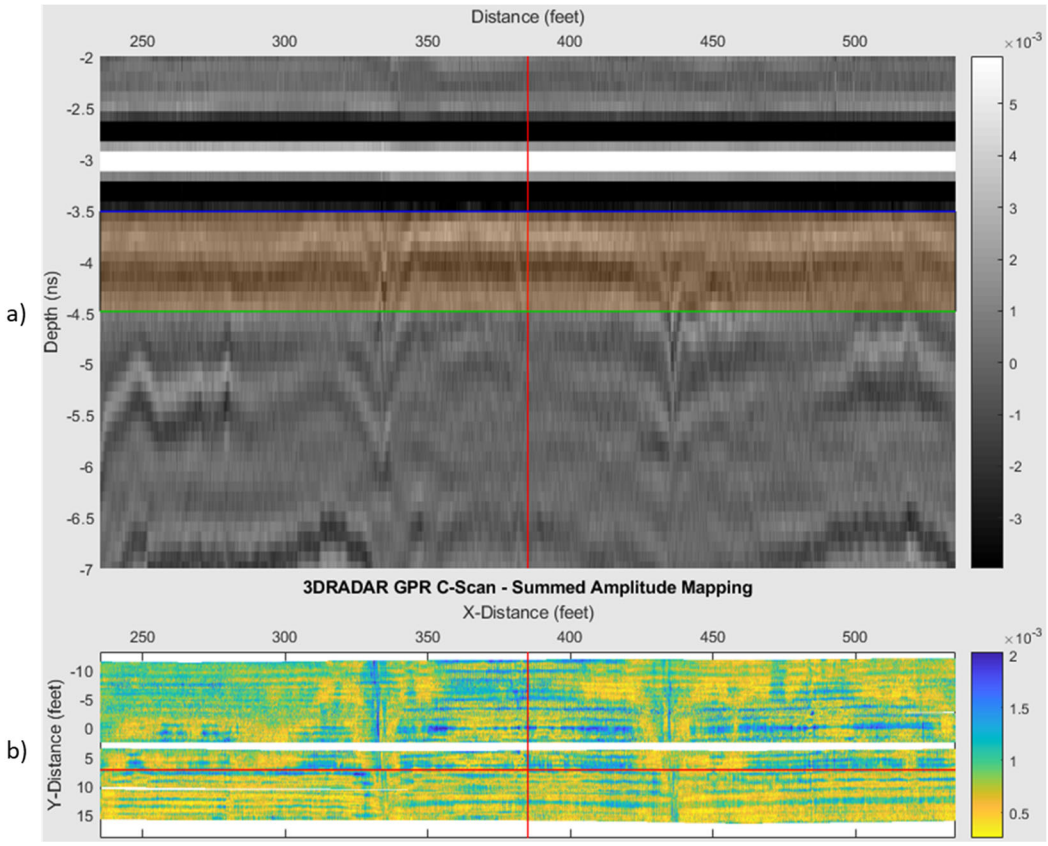

Figure 119: ExploreGPR interface showing the activity analysis performed on interval of 3.5-4.5 ns for stitched files collected over the eastbound lane: a) b-scan; b) color-coded reflection activity plot for the window specified in a).

Representative results for Blue Heron bridge are shown in Figure 120 and Figure 121 that show the spatial distribution of increased reflection activity within the defined depth interval using a thresholded contour plots for westbound and eastbound lanes, respectively. Areas shown are those where the reflection activity levels exceed a threshold value, manifesting the deviations of dielectric properties and presence of internal reflectors at variable depths which are not normally seen within intact materials and can be indicative of delamination and/or deterioration. The color scale indicates the degree to which the threshold is exceeded, which represents the severity. Shades of pink color represent areas where moderate levels of reflection activity were observed, shades of blue color delineate areas associated with minor activity levels. Presented maps are not to scale on Y-axis; stretched to be informative and fit the screen well without compromising the visual data representation.

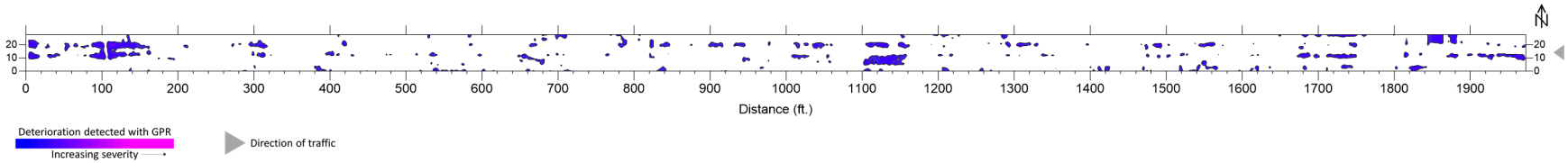

Figure 120: Reflection activity map, generated from the results of analysis of 3D GPR data collected over the westbound lane.

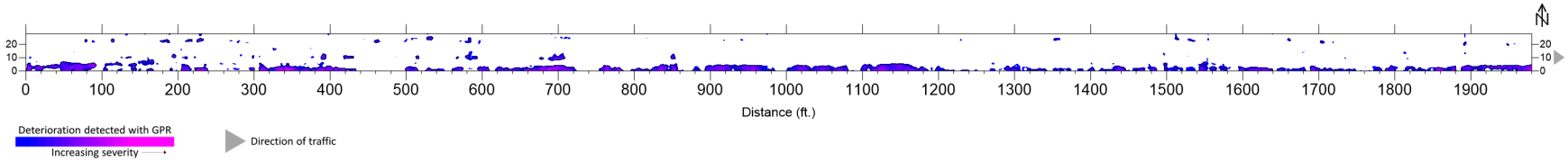

Figure 121: Reflection activity map, generated from the results of analysis of 3D GPR data collected over the eastbound lane.

Bridge #940045 (St. Lucie). The 3D-Radar survey was carried out on November 14, 2017. Six lines of data were collected, three each in the westbound and eastbound with intent to map the deterioration development. Rebars reflections appear as a layer reflector in the 3D-Radar data as it is shown in Figure 122. Reflection activity analysis approach was utilized to perform bridge deck condition evaluation.

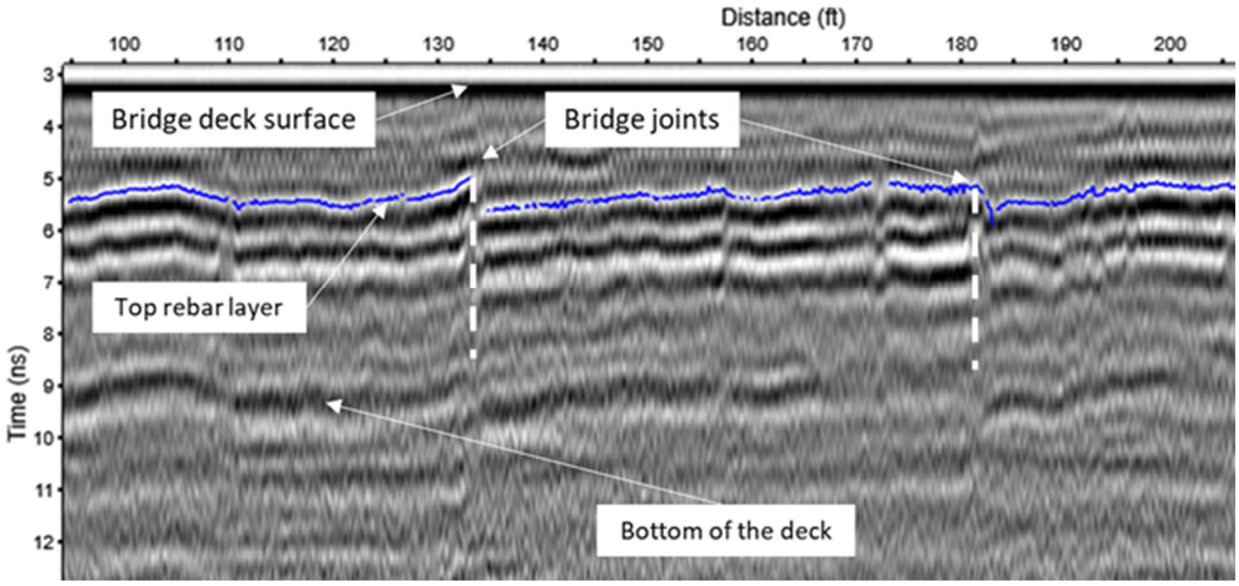

Figure 122: Vertical slice of 3D-Radar data with visible bridge deck elements.

Analysis was carried out similar to that described for bridge 930269. The interval of 7.5 ns (from 3.5 to 11) was selected to represent the activity within the bridge deck. It should be noted that using these limits, the proposed analysis method provides information about the reflection activity within the entire thickness of the deck. Figure 123 displays the reflection activity mode of ExploreGPR software showing the segment of 3D-Radar data, collected over the westbound lane of the bridge.

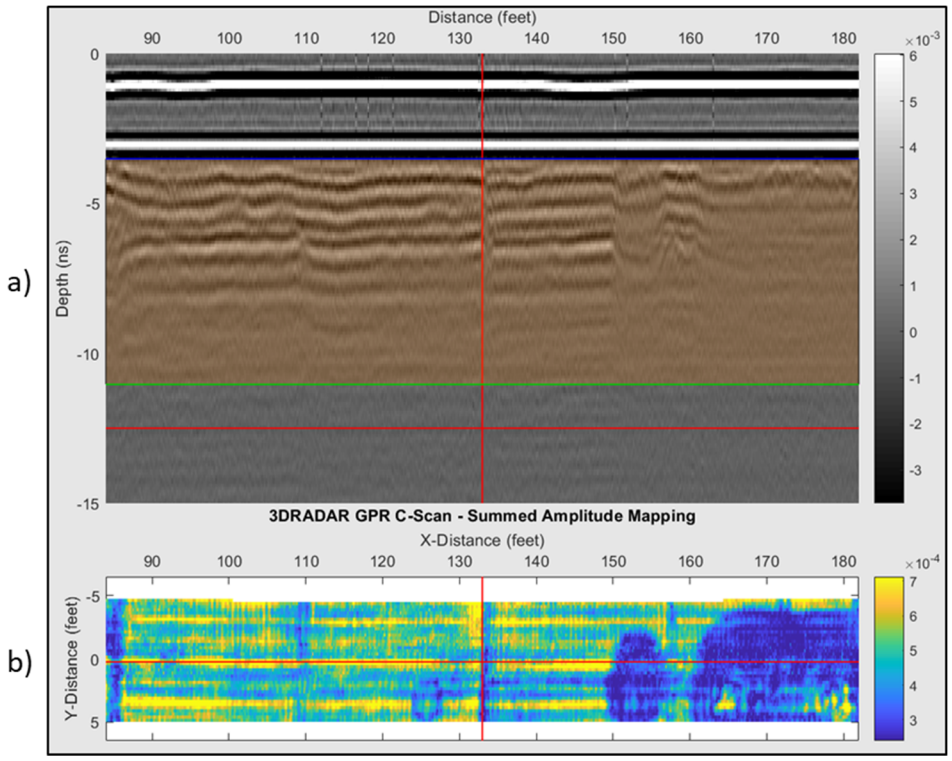

Figure 123: ExploreGPR interface showing the activity analysis performed on interval of 3.5-11 ns for stitched files: a) b-scan; b) color-coded reflection activity plot for the window specified in a).

Representative results for St. Lucie bridge are shown in Figures below. Figure 124 and Figure 125 show the spatial distribution of increased reflection activity within the defined depth interval using a thresholded contour plots for westbound and eastbound lanes, respectively. The rationale of data analysis is the same as in previous section (Blue Heron Bridge). Presented maps are not to scale on Y-axis; stretched to be informative and fit the screen well without compromising the visual data representation.

In summary, two approaches to analyze bridge deck evaluation distribution were made using 3D GPR system. In first case, survey results were used to generate contour plots showing the estimated deterioration extent based on the amplitude analyses. Another approach used increased reflection activity index as an evidence of deterioration development within the bridge deck.

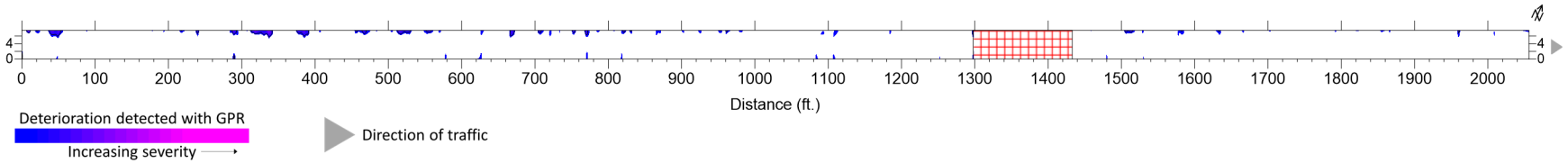

Figure 124: Reflection activity map, generated from the results of analysis of 3D-Radar data collected over the westbound lane. Red frame represents the fortified rebar mesh segment (bascule span).

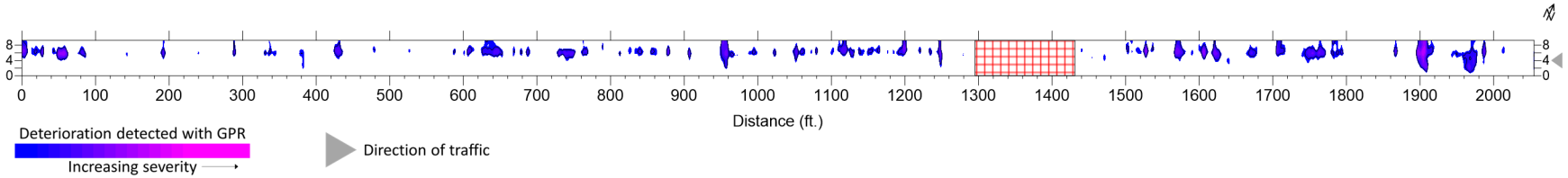

Figure 125: Reflection activity map, generated from the results of analysis of 3D-Radar data collected over the eastbound lane. Red frame represents the fortified rebar mesh segment (bascule span).

5. 3D GPR Return on Investment (ROI) Analysis

A benefit/cost analysis has been carried out to determine the return on investment (ROI) of using 3D-Radar for planning pavement and bridge rehabilitation projects. Factors considered included the 3D-Radar operating arrangements, number of full time staff required to maintain continuity in 3D-Radar data collection and processing, and quality and quantity of data available as compared to traditional GPR and non-GPR data collection and analysis approaches.

The following 3D-Radar applications were addressed in this analysis:

1. Pavement substructure evaluation (concrete base, dowels, subsidence)
2. Pavement stripping evaluation
3. Bridge deck condition surveys.
4. Evaluation of density of new asphalt pavement

The analysis period was selected to be 10 years. The direct benefits of using 3D-Radar were estimated based on the value of acquiring certain data that are only available using 3D-Radar technology or are otherwise available in limited quantities or at greater cost from traditional approaches. The estimates for using 3D-Radar have taken into consideration the complexity and cost of the 3D-Radar technology as well as the training and expertise required for processing data.

It is assumed in this study that FDOT owns and operates the 3D-Radar equipment and will interpret the 3D-Radar data. Other options exist, such as contracting out data analysis, but these have not been considered at this time.

A key issue is the level of agency commitment required to ensure the availability and continuity of qualified staff to conduct 3D-Radar surveys and analyze the 3D-Radar data that is collected. State agencies have typically found that one or two full time staff members are required to provide continuity of capabilities with equipment systems of a complexity similar to that of 3D Radar.

5.1 Computation of Cost

Costs were determined for 3D-Radar technology for each of the following:

1. Capital cost (initial purchase of equipment and software)
2. Personnel Training and Equipment Maintenance
3. Recurring expenses, including equipment maintenance, and operating expenses (personnel, travel and vehicle operation)

Cost estimates were developed for each major element associated with 3D-Radar data collection and analysis.

5.1.1 Capital Costs

In order to collect 3D-Radar data, it is necessary to purchase 3D-Radar equipment, mount it on an appropriate survey vehicle equipped with a distance measuring instrument (DMI) and high-resolution global positioning system (GPS), and purchase suitable software for the data collection and analysis. The typical cost of equipment and software for 3D-Radar is shown in Table 3.

Table 3 – Costs of Equipment and Software

	Item	Cost	*Total Cost*
1	MkIV GeoScope 3GHz GPR (incl. cables, transport container)	$159,600	
1	Model DX 1821 Air Coupled Antenna Array	$44,900	
1	Model DXG 1821 Air Coupled Antenna Array	$44,900	
1	DMI and GPS	$5,000	
	Antenna Mounting Hardware	$2,000	
	Power Supply and Miscellaneou8	$4,000	
	Total Equipment Cost		**$263,400**
Examiner Software for 3D-Radar Data Analysis			
	First year	0	
	Subsequent years	$8,000/yr.	

5.1.2 Initial Personnel Training

3D-Radar data collection and analysis is a specialized activity that requires training of agency personnel. Typically, the 3D-Radar vendor provides a three – or four-day on-site training course for the equipment operators. It is reasonable to assume that two-person weeks of field data collection experience is required to achieve full productivity. In addition, four-person weeks of in-office experience with the data analysis software is required to achieve proficiency in analysis. Maintenance and repair of the equipment includes minor vehicle repairs and maintenance (oil changes, tire rotation, etc.) and small repairs to the 3D-Radar data collection equipment. Expected costs for training and equipment maintenance are provided in Table 4. It is assumed that the equipment and data collection training costs would be paid to the vendor. FDOT labor cost have included direct salary and overhead (see discussion later).

Table 4 – Cost of Training, Maintenance, and Repair

Training					
	Equipment, Data Collection, and Analysis Training				
		4	days 3D Radar @	$1,890	$7,560
	FDOT Personnel Time (training and Ramp up)				
	Equipment & Data Collection	80	hours @	$20	$1,600
	Process	160	hours @	$20	$3,200
	overhead	0.9		$4,800	$4,300
	Total Training Cost				**$16,680**

5.1.3 Equipment Operating Expenses

Equipment operating expenses includes the personnel to operate the 3D-Radar data collection equipment and to analyze the data, and equipment maintenance. Field expenses include travel costs to operate the vehicle (fuel, insurance, etc.) and per diem expenses for the operator. The analysis has been completed for a number of scenarios. The complete assumptions used in the analysis are as follows:

1. Two field personnel are required to collect the data
2. At least one office person is required to analyze the data
3. Each day of data collection requires 5 days of data analysis
4. For one month (22 days) of data collection per year, one full time equivalent (FTE) is required for both data collection and analysis
5. Based on the productivity of the 3D Radar system, we can assume 2 projects are surveyed per field day.
6. Employee rate of pay is $25 per hour

Table 5 summarizes the annual cost of owning and operating the 3D Radar equipment over a 5-year period based on the assumptions described above.

Table 5 – Annual Cost of owning and operating 3D Radar equipment

Expenses			
	Fuel, etc.	2000 miles @ $0.60 per mile	$1,200
	Per Diem	2 persons @ $80 per day	$3,520
Total Hours for 1 FTE			2,000
Labor Cost with Overhead			$76,000
		Total	**$82,720/yr.**

5.2 Benefit Scenarios

Three scenarios were used to provide the basis for determining the cost/benefit relationship for using 3D-Radar technology. These were:

1. General evaluation of pavement substructure (concrete base, dowels, subsidence)
2. Pavement stripping evaluation for rehab design
3. Bridge deck condition surveys.
4. Evaluation of thickness and density of new asphalt pavement

5.2.1 General Evaluation of Pavement Substructure

An example of this type of work was carried out on SR 5 (US 1) in St. Johns County. In 2016 a consultant surveyed the area using a ground-coupled GPR system with two separate antennas, an 800 MHz antenna and a 1600 MHz antenna. The roadway was 2 lanes in each direction, the total length of the section was about 3.25 miles, and 7 lines of GPR data were collected in each direction, 2 lines in each lane and additional lines in the shoulders. The objective was to identify pavement substructure and subsidence conditions that might have an impact on utilities and on rehabilitation design. Although not clearly stated in the report, it is assumed that this type of survey would have been a walking speed survey requiring traffic control and would have taken about 3 days to complete. The cost of project, including data collection, traffic control, and data analysis of the two separate channels of data is estimated at $25,000 if carried out by a consultant. If the project were carried out internally, the estimated cost is about $12,500. Since such projects are sometimes done internally and sometimes by consultants, we will assume a 50/50 ratio and calculate the assumed cost savings to by the average of the two, which comes out to $18,750.

The same site was surveyed with 3D Radar on February 15, 2017. The survey focused on the low speed lane, which covered with two passes of the 3D Radar system in each direction, one on the right side of the lane and the other on the left. The data collection was carried out at normal driving speed and took about 1 hour to complete. Adding the 1 ½ hour drive to and from Gainesville, the entire process took ½ a day. Data analysis was carried out by one analyst over a 40-hour period. This ratio of collection to analysis fits the 1 FTE personnel requirement assumed in this analysis.

5.2.2 Stripping Evaluation for Rehabilitation Design of Existing Pavement

For this analysis we assume a 5-mile section of roadway, one lane in each direction, which needs rehabilitation. The presence of stripping is suspected, but the location and extent are not clear. Two possible options can be considered:

1. Conventional rehabilitation without consideration of the stripping (option 1)
2. Detailed evaluation of the stripping using 3D Radar, and design of rehabilitation to address repair of stripped areas (option 2)

Option 1 would involve a standard mill and overlay design to achieve an 18-year design life. Option 2 would be similar, except that the milling would be designed to take out the stripped material, so that it might be deeper, and the overlay thicker, in some areas of the project as compared to option 1.

Without doing a detailed structural analysis, it is reasonable to assume that the life of the pavement under option 1 would be considerably less than under option 2, while the cost of option 2 would be higher. It has been assumed, for the sake of this analysis that option 1 will fail prematurely after 12 years of service, while option 2 will last the full 18-year design life. In the analysis below, the savings has been annualized using Equivalent Uniform Annual Costs (EUAC), calculated as

$$EUAC = Initial\ \ Cost \frac{i(1+i)^n}{(1+i)^n - 1} \qquad \text{Equation 1}$$

Where:

i = Discount rate (%/100).
n = Number of years of the analysis period

For this analysis the annual discount rate was selected as 3 percent.

The benefit of conducting this type of survey is calculated as follows:

1. Assume:
   a. Five miles of pavement, 1 lane each direction, = 10 lane miles
   b. Cost of option 1 rehabilitation is $100,000 per lane mile
   c. Cost of option 2 rehabilitation is $120,000 per lane mile.
   d. Actual life of pavement in option 1 is 12 years due to premature failure.
2. Calculate Benefit:
   a. Option 1 - Total cost of rehabilitation = 10 lane miles × $100,000 = $1,000,000
   b. Option 2 - Total cost of rehabilitation = 10 lane miles × $120,000 = $1,200,000
   c. Option 1 Actual life = 12 yrs.; actual EUAC = $100,462
   d. Option 2 Design life = 18 yrs.; EUAC = $87,250
   e. **Benefit** = ($100,462 – $87,250) = **$13,212/year**

5.2.3 Bridge Deck Surveys

Bridge deck delamination is traditionally assessed using the chain drag chain method. Chain dragging involves closing one or more lanes and using the chain to detect by ear the "hollow" sounding areas associated with delamination. Based on the sounds that are heard, the operator marks out the boundaries of each delamination. If repair is to take place at the time of the survey, the markup is used by the contractor to determine the limits of repair. If the survey is to be used for planning and scoping purposes, then the markup needs to be converted into a map showing the location and quantities of delamination.

GPR has demonstrated the capable of evaluating bridge deck condition. The use of GPR for this purpose is based on the fact that the GPR signal attenuates more significantly in the areas of delamination due to the corrosion and chloride contamination.[1] Note that FDOT has a 4-antenna GSSI GPR system that is capable of conducting bridge deck surveys, However, 3D Radar is particularly effective implementation of GPR for bridge decks since it provides higher resolution, and each pass automatically projects the data onto a geospatial plan map of the bridge, so that the results of a 3D Radar analysis are automatically mapped and recorded. In addition, a 3D Radar bridge deck survey provides a map of the depth of rebar. This is important because it indicates the volume or repair, which is not available with a chain drag survey.

The estimated cost of conducting a chain drag survey on a typical 5000 sq. foot deck is shown below in Table 6. It is estimated that sounding the deck and mapping the results would require two lane closures (one for each lane and shoulder) and a crew of 2 persons working for 1 ½ days (including time to setup and take down of each closure). The cost of chain dragging and sounding is estimated at:

Table 6 – Cost for Chain Dragging a 5000 sf. Bridge Deck

	QUANTITY	$/UNIT	$ COST
Mobilization (ea.)	1	$500	$500
Survey crew (person-hr.)	24	$38	$900
Fixed lane closure (contracted)	1.5	$2,000	$3,000
Total			**$4,400**

In addition to the economic benefit, there is a safety benefit associated with the elimination of the exposure of agency personnel to traffic hazards. Bridge deck surveys using 3D Radar take about 1 hour, the time it takes to drive back and forth over the bridge enough times to cover all of the lanes, so, depending on their location, multiple bridge decks can typically be surveyed in one day.

2.4 Quality Assurance for New Pavement

The final scenario addresses the use of 3D-Radar to determine whether a construction contractor has placed HMA at the prescribed thickness. This scenario assumes that 3D Radar has updated their Examiner software to include the metal plate calibration and the dielectric calculation required for thickness evaluation.

[1] ASTM D6087-08 (2008), "Standard Method for Evaluation Asphalt-Covered Bridge Decks using Ground Penetrating Radar"

The benefit analysis relies on previous work by Deacon, et al[2] for the California Department of Transportation. He developed a relationship between the variation in thickness within a new pavement section and the reduction in pavement life. The reduction in expected pavement life is then used to modify the pay that the paving contractor receives. Figure 1 is taken from Deacon, et al. The horizontal axis in the figure shows the mean thickness deviation for the actual pavement versus the specified pavement. The vertical axis shows the pay factor that will be used for the corresponding mean thickness deviation. The pay factor also is numerically equal to the change in expected pavement life. Figure 126 provides three lots, one for each level of variability of the pavement thickness, as measured by the coefficient of variation (COV).

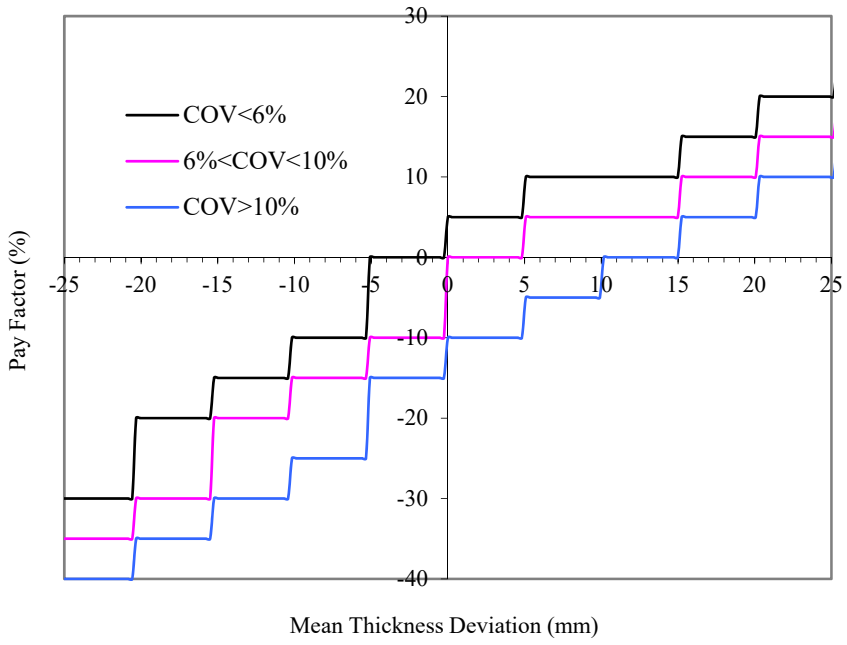

Figure 126 – Pay Factor vs. Thickness Deviation for Different COV's (from Deacon et. al.)

For this scenario, the following assumptions are made:

1. Nominal pavement thickness = 4 inches = 102 mm
2. Mean measured pavement thickness (using GPR) = 3.5 inches = 89 mm

[2] Deacon, J. A., C. L. Monismith, and J. T. Harvey (1997). *Pay Factors for Asphalt-Concrete Construction: Effect of Construction Quality on Agency Costs*. Technical Memorandum, TM-UCB-CAL/APT-97-1, April 1997.

3. Based on Deacon et al (1997), this loss of thickness and the variability in thickness results in loss in pavement life.
4. The design life is 18 years
5. 3D-Radar can measure the mean pavement thickness within +/ – 2.5 mm
6. 3D-Radar can correctly characterize the variability in pavement thickness
7. Project size is 10 lane miles

The mean deviation is computed as:

Mean deviation = actual – specified

The mean deviation is therefore 89 mm – 102 mm = – 13 mm

The COV (coefficient of variation) is a measure of the variability of the pavement thickness. Examining the bottom-left quadrant of Figure 1, the mean deviation value yields the following values for Pay Factor (and reduction in pavement life) from the three thickness variability plots:

COV < 6%	-15%
6% < COV < 10%	-20%
COV > 10%	-30%

When these values are applied to the 18-year design life used for Florida pavements, the values for expected life shown in Table 7 are the result. The reduction in pavement life is the difference between the design pavement life and the expected pavement life.

The benefit of detecting thickness variations is calculated as follows:

1. Assume:
   a. Five miles of pavement at two lanes wide = 10 lane miles
   b. Cost of rehabilitation is $100,000 per lane mile
2. Calculate Benefit:
   a. Total cost of rehabilitation = 10-line miles × $100,000 = $1,000,000
   b. EUAC of rehabilitation for 18-year design life = $72,708 at 3% discount rate
   c. Difference in actual life and design life for COV <6 percent with a pay factor of -15 % = 2.7 yrs.
   d. EUAC of rehabilitation for 15.3-year design life = $82,461 at 3% discount rate
   e. **Benefit** = $82,461 -$72,708 = **$9,753/yr.**

Table 7 – Benefit of Using 3D-Radar to Reduce Thickness Variability

COV	**Pay Factor**	**Expected Life Years**	**Reduction in Pavement Life Years**	**Total Value**
COV < 6%	-15%	15.3	2.7	$149,221
6% < COV < 10%	-20%	14.4	3.6	$199,198
COV > 10%	-30%	12.6	5.4	$299,501

The analysis described above quantifies the loss of remaining life due to deviations from design thickness, but similar losses can also occur due to deviations from design density. For example, it has been shown that every 1% increase in air void above the base design level reduces the pavement life by 10%[3] which, for an 18-year design life is equal to 1.8 years and would cost over $100,000. As described above in relationship to thickness, the ability to detect and correct density deviations s at the time of construction could provide significant savings.

5.3 Summary

Three scenarios have been presented for the evaluation of benefits of using 3D Radar

1. General evaluation of pavement substructure
2. Pavement stripping evaluation
3. Bridge deck condition surveys.
4. Evaluation of thickness (and density) of new asphalt pavement

The results of these analyses can be summarized as shown in Table 6.

The values in Table 8 represent the benefit for each type of project in each year. The number of each type of project carried out per year has been assumed based on FDOT's experience with these types of projects This quantity of projects is well within the cost structure shown in Table 3. Based on this stream of costs and returns, the Net Present Value of the 10-year costs and the 10-year returns have been calculated, to yield the ROI calculation shown below:

ROI = $5,573,480/$1,131,848 = 4.92

[3] Linden, R. N., Mahoney, J., and Jackson, N. (1989)"Effect of Compaction on Asphalt Concrete Performance". *Transportation Research Record No. 1217*, Transportation Research Board

The graph in Figure 127 below shows the relationship between the expenditures to own and operate the 3D Radar system and the return derived from this ownership.

Figure 127 – Cumulative Expense and Return for Owning and Operating a 3D-Radar System

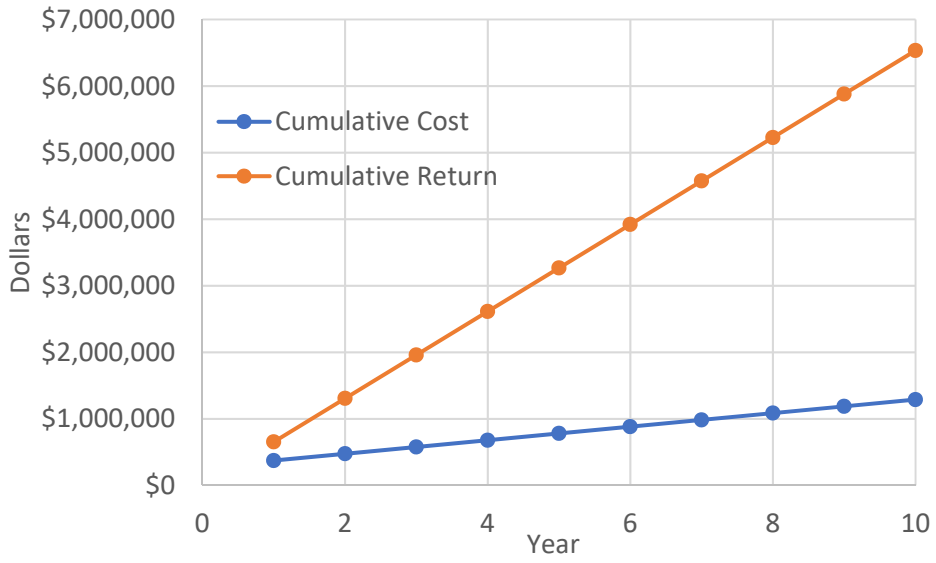

Table 8 – Summary of Costs vs. Return for 3D Radar Equipment Operation over 10-Year Period

	Year									
Cost	1	2	3	4	5	6	7	8	9	10
Purchase	$263,400	$0	$0	$0	$0	$0	$0	$0	$0	$0
Training	$16,680	$0	$0	$0	$0	$0	$0	$0	$0	$0
Software	$0	$8,000	$8,000	$8,000	$8,000	$8,000	$8,000	$8,000	$8,000	$8,000
Operating	$93,720	$93,720	$93,720	$93,720	$93,720	$93,720	$93,720	$93,720	$93,720	$93,720
Total Cost	$373,800	$101,720	$101,720	$101,720	$101,720	$101,720	$101,720	$101,720	$101,720	$101,720

$1,131,848 = NPV of Cost

Benefit by Project Type	projects /yr.	Benefit $/project	1	2	3	4	5	6	7	8	9	10
Pavement Structure Eval	12	$18,750	$225,000	$225,000	$225,000	$225,000	$225,000	$225,000	$225,000	$225,000	$225,000	$225,000
Delamination/Stripping	2	$112,710	$225,419	$225,419	$225,419	$225,419	$225,419	$225,419	$225,419	$225,419	$225,419	$225,419
Bridge Deck	2	$4,400	$8,800	$8,800	$8,800	$8,800	$8,800	$8,800	$8,800	$8,800	$8,800	$8,800
Thickness/Density QA	2	$97,081	$194,163	$194,163	$194,163	$194,163	$194,163	$194,163	$194,163	$194,163	$194,163	$194,163
		Total Return	$653,382	$653,382	$653,382	$653,382	$653,382	$653,382	$653,382	$653,382	$653,382	$653,382

$5,573,480 = NPV of Return

6. Discussion of Results

Final Report represents the results of practical applications of a stepped frequency air-coupled GPR antenna array system (3D-Radar) operating in the range of 300 – 3000 MHz Based on the testing results, the system appears to be capable of identifying moisture damage, stripping, delaminations, bonding segregation, subsidence, density variations in asphalt pavement, thickness variations, “road worms” phenomenon, construction variations in concrete/composite pavement, dowel bar location, damage within the asphalt layer, and bridge deck deterioration. The following list summarizes the results of the reported evaluations:

1. The correlations between the 3D-Radar outputs and built-in imperfections, obtained from qualitative analysis, indicated, that under controlled conditions, 3D-Radar data can precisely reveal delaminations, segregation, and density variations in asphalt pavement;
2. The results confirmed the ability of the 3D-Radar system to locate concrete slabs (installment pattern, dimensions, and reinforcement design) joints, and dowel configuration. The misalignment (horizontal skew and vertical tilt) of dowel bars can be accessed and examined to the limited extent;
3. The results confirmed the 3D-Radar system capacity to monitor the condition of pavement structure with complex composition, where the SSC were installed to mitigate roadway settlement. Details of the pavement structure explaining the strength reduction were successfully revealed;
4. The result confirmed the ability of the 3D-Radar system to map the distribution of bridge deck deterioration, allowing to perform qualitative and quantitative condition evaluation. For the activity analysis approach, the thresholds used to distinguish damaged locations from undamaged are arbitrary and need to be adjusted or calibrated to known conditions for each particular site;
5. Developed post-processing software (ExploreGPR) was tested and evaluated on both pavement and bridge deck data sets.
6. The ability to accurately align and stitch parallel data files is highly dependent on the quality of the GPS data. In the stage 1 testing, the Ag262 GPS unit provided good accuracy, but the received data was occasionally misaligned, possibly due to overhanging trees. In stage 2, the SPS 985 unit provided the ability to track many more satellites and different frequencies, and thus appeared to be less influenced by the survey environment.
7. The quality of the 3D Radar data is affected by the antenna mounting environment. It was found that by mounting the antenna 4 feet away from the vehicle bumper using a low mass mounting arrangement minimized the vehicle interference in the data.

7. References

[1] Ground Penetrating Radar Evaluation of SR 24 in Alachua County (March 2014). Florida Department of Transportation.

[2] GPR evaluation on I-75 Roadway ID: 26260000, Alachua County. Site 1 (MP 14.500 – 17.200) and Site 2 (MP 25.200 – 28.300). State Materials Office, January 2017.

[3] Phase I report of subsurface investigation concrete slab rehabilitation SR 5 (US 1) from SR 207 to city gates St. Johns county, Florida FPID: 436168-1-32-01 & 436169-1-32-01.

[4] Holzschuher, C., NDT. SR 100 Grout Column Evaluation (2010). Florida Department of Transportation.

[5] Nazef, A., Lee, H., Chun, S., Greene, J. (2013). Evaluation of Soil Stabilized Columns Used for flexible embankment support and settlement control. Florida Department of Transportation.

[6] Prakash, B. Final solution for SR 100.

[7] Ground Penetrating Radar Evaluation of Bridge (# 720509) Rebar Cover on SR 202 in Jacksonville, Duval County.

[8] Ground Penetrating Radar Evaluation of SR 24 in Alachua County (March 2014). Florida Department of Transportation.

[9] Ground Penetrating Radar Evaluation of SR 24 (Waldo Road) in Alachua County for Potential Pavement Voids (August 2014). Florida Department of Transportation.

[10] Literature Review for Evaluation of Roadway Worms/Distortions, FDOT/Applied Research Associates, Inc.

[11] T3564 Repair Summary 07132017.